

# vibrational and rotational spectroscopy on surfaces

Thomas Risse

Fritz-Haber-Institut der Max-Planck Gesellschaft,  
Abteilung Chemische Physik  
Faradayweg 4-6  
14195 Berlin

# Outline



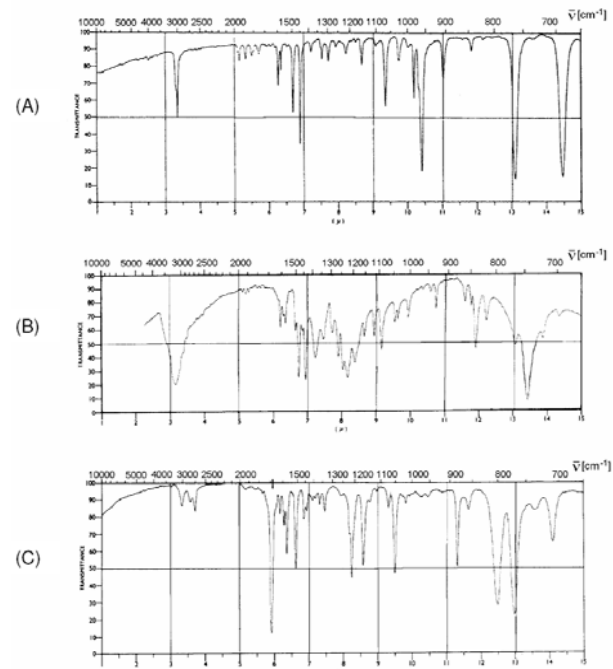
- Introduction
- electron energy loss spectroscopy (EELS)
- infrared spectroscopy
- helium atom scattering (HAS)
- tip enhanced Raman spectroscopy/SERS
- SFG (sum frequency generation)
- electron spin resonance

# Introduction



## chemical perspective

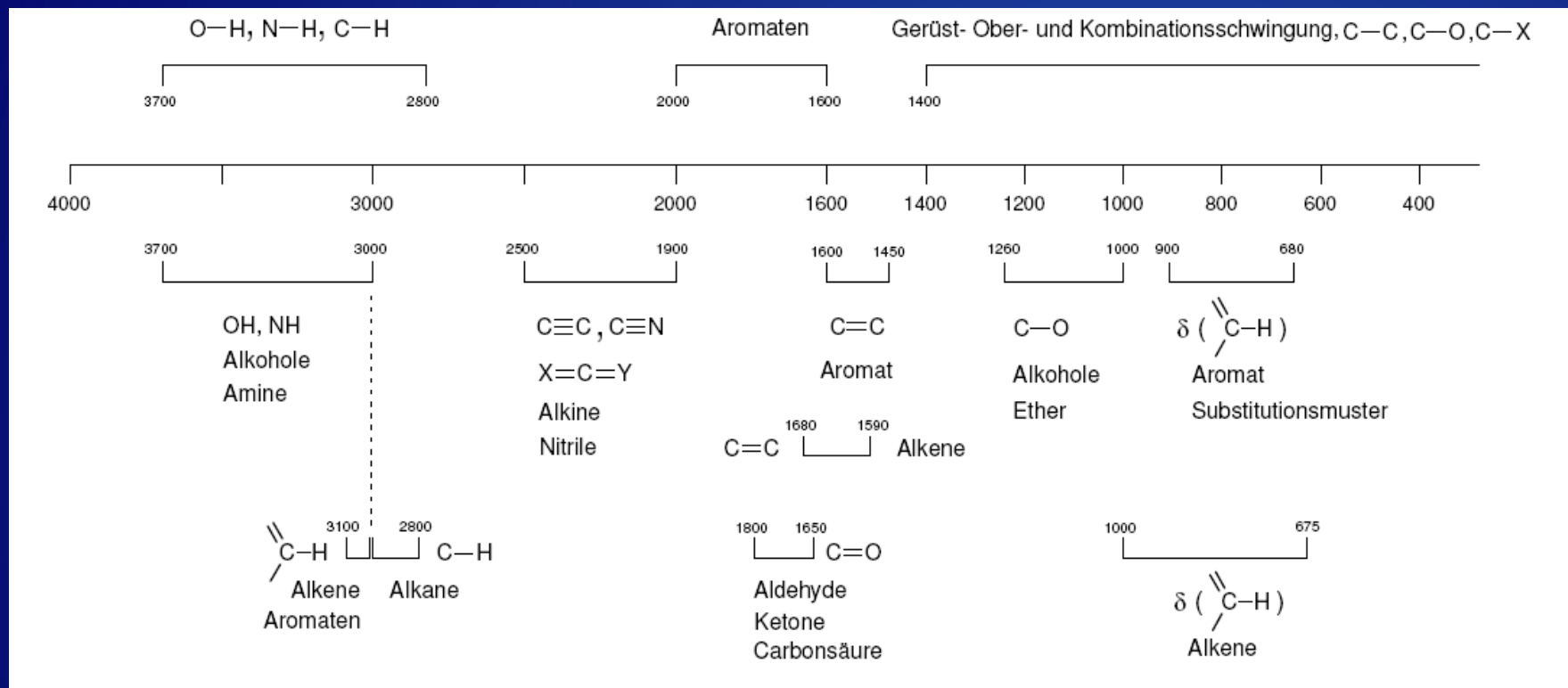
Aufgabe 2: Die dargestellten IR-Spektren können von 1-Naphthaldehyd, E-Zimtaldehyd, trans-Stilben, 2,4,6-Tri-t-butylphenol, 2,2'-Dihydroxybiphenyl und 4,4'-Dihydroxybiphenyl stammen. Welches Spektrum gehört zu welcher Substanz? Ordnen Sie die charakteristischen Banden zu.



# Introduction



## chemical perspective



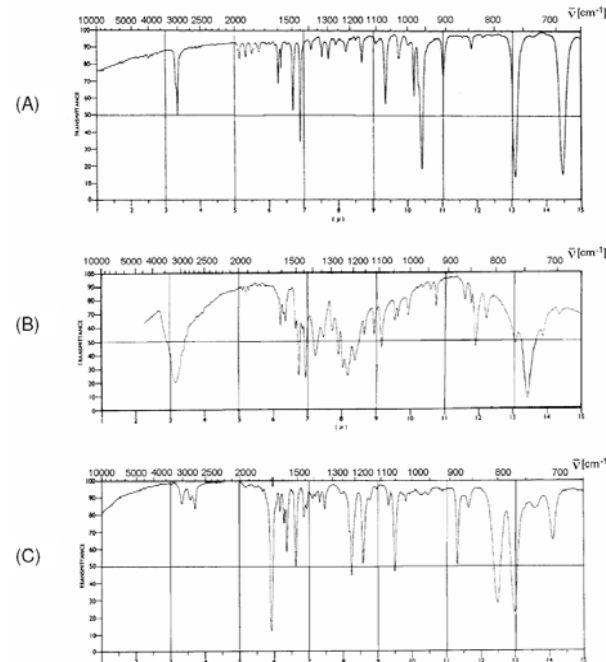
# Introduction



Max-Planck-Gesellschaft

## chemical perspective

Aufgabe 2: Die dargestellten IR-Spektren können von 1-Naphthaldehyd, E-Zimtaldehyd, trans-Stilben, 2,4,6-Tri-t-butylphenol, 2,2'-Dihydroxybiphenyl und 4,4'-Dihydroxybiphenyl stammen. Welches Spektrum gehört zu welcher Substanz? Ordnen Sie die charakteristischen Banden zu.



## physical perspective

PHYSICAL REVIEW B 66, 073414 (2002)

### Anomalous dispersion of adsorbate phonons of Mo(110)-H

Jörg Kröger\*

Institut für Experimentelle und Angewandte Physik, Christian-Albrechts-Universität zu Kiel, D-24098 Kiel, Germany

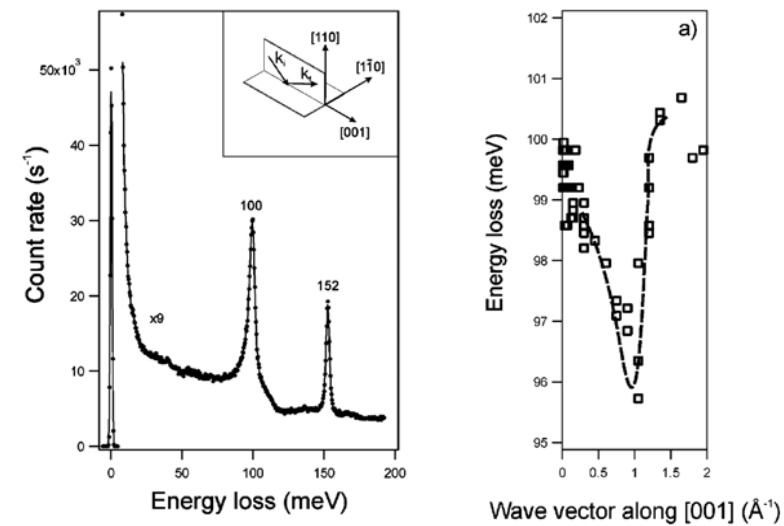
Sieghart Lehwald, Martin Balden, and Harald Ibach  
Institut für Schichten und Grenzen, Forschungszentrum Jülich, D-52425 Jülich, Germany

(Received 8 November 2001; published 21 August 2002)

The dispersion curve of the longitudinal-optical adsorbate phonon on hydrogen-saturated Mo(110) along [001] is found to exhibit an anomalous indentation. The maximum indentation is observed at a wave vector, which coincides within the experimental angular resolution with the wave vector, at which the known giant Kohn anomaly for the transverse- and longitudinal-acoustic substrate surface phonons along [001] occurs.

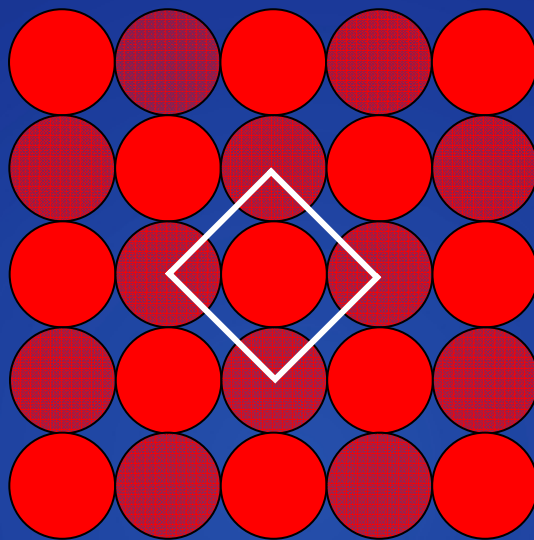
DOI: 10.1103/PhysRevB.66.073414

PACS number(s): 68.35.Ja, 63.20.Kr, 68.43.Pq, 73.20.At



# EELS

H on W(100)



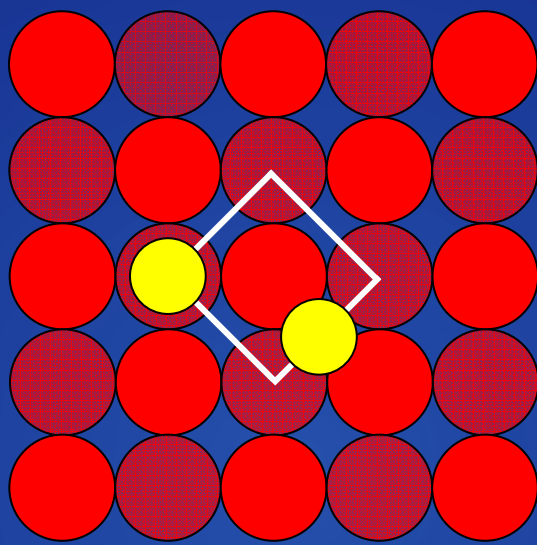
1. layer



2. layer

# EELS

H on W(100)



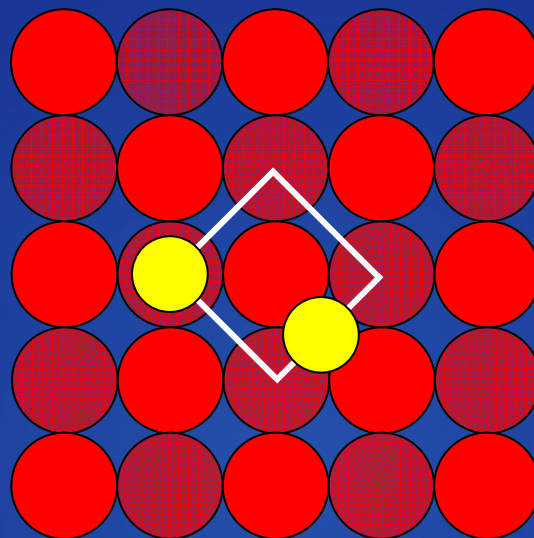
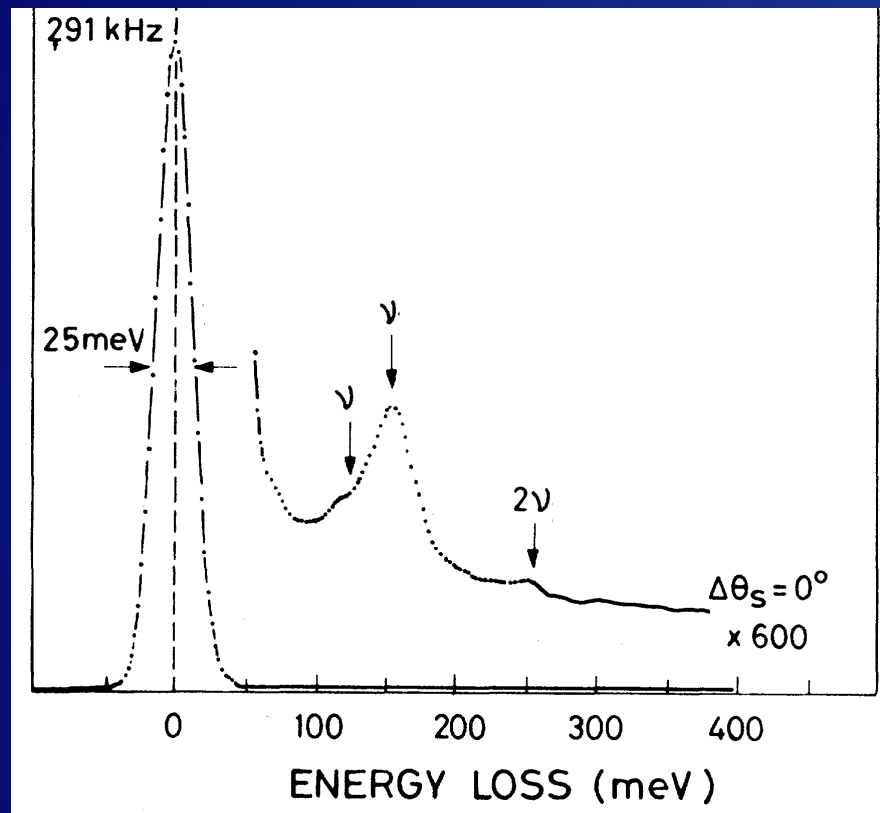
1. layer



2. layer

# EELS

H on W(100)



1. layer

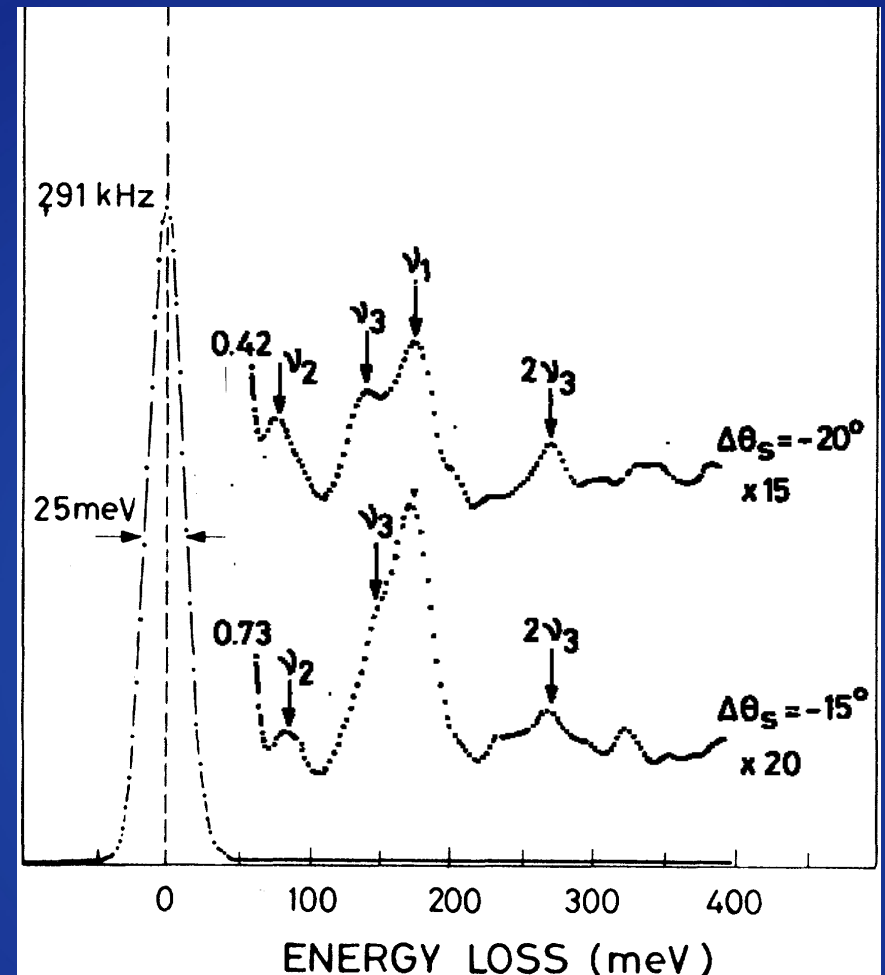
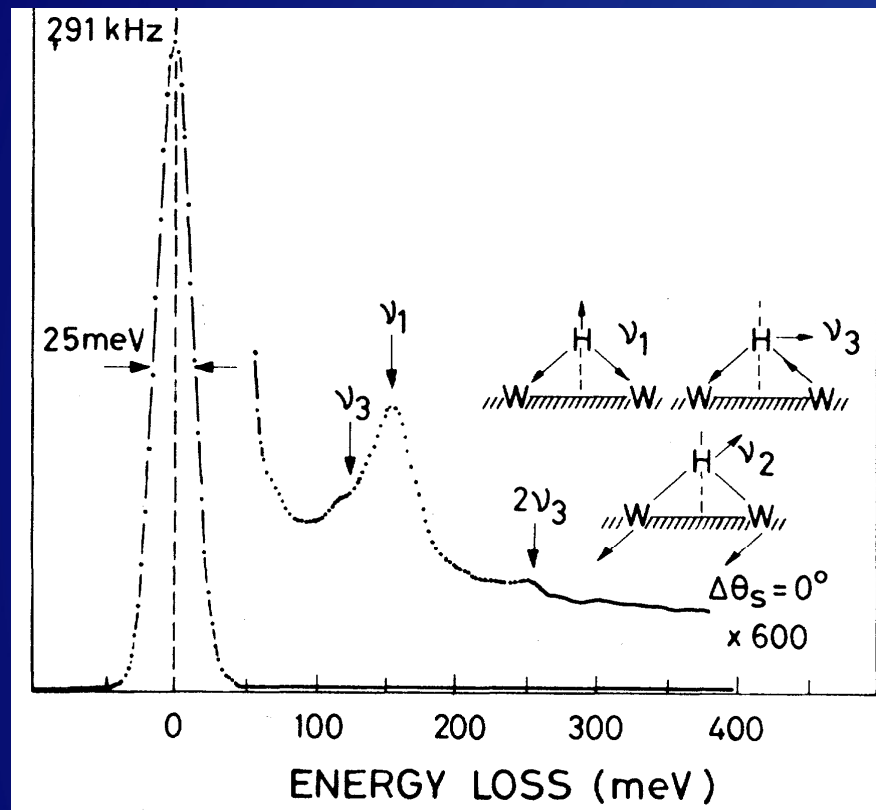


2. layer

W. Ho, R. F. Willis, and E. W. Plummer, Phys. Rev. Lett. 40, 1463 (1978).

# EELS

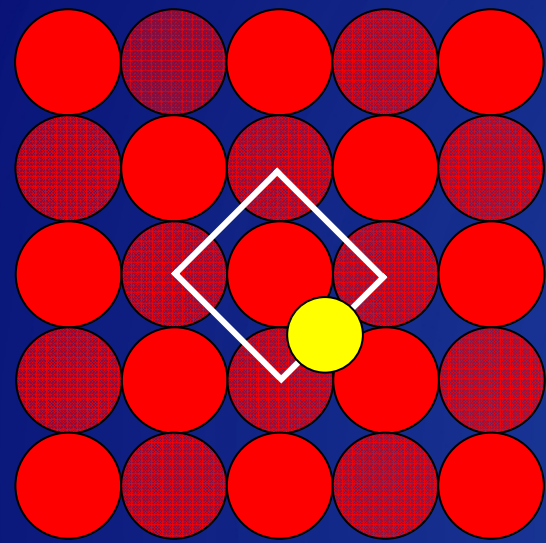
H on W(100)



W. Ho, R. F. Willis, and E. W. Plummer, Phys. Rev. Lett. 40, 1463 (1978).

# EELS

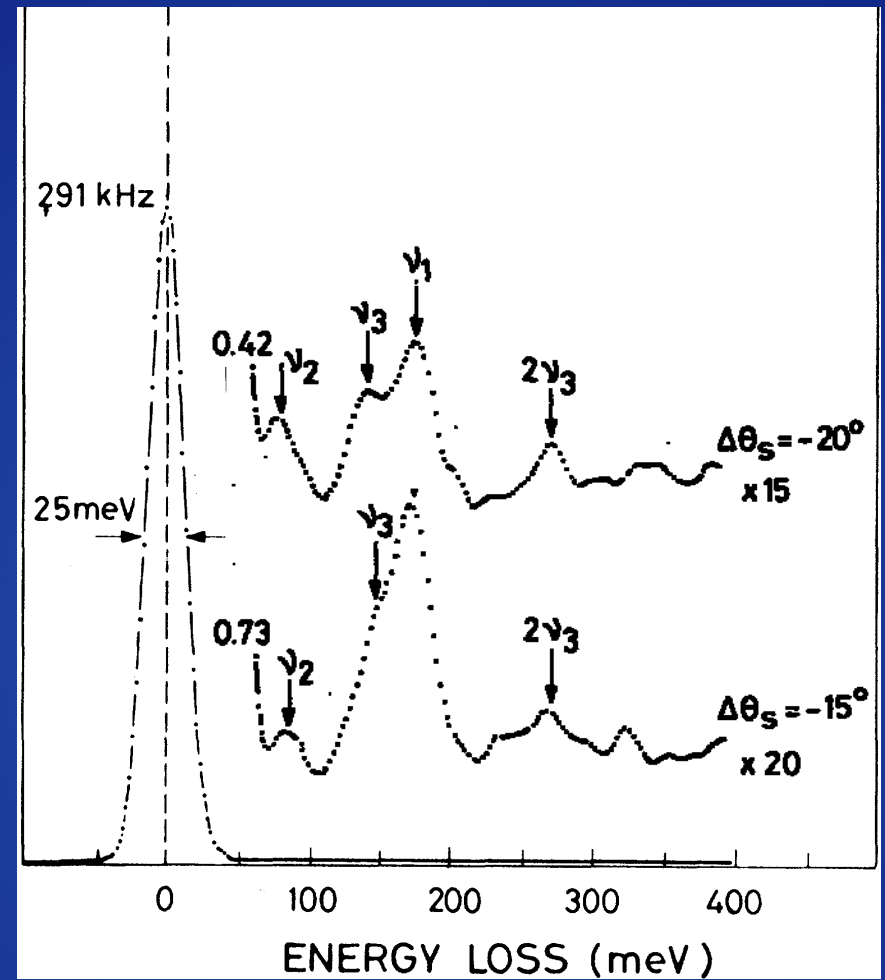
H on W(100)



1. layer

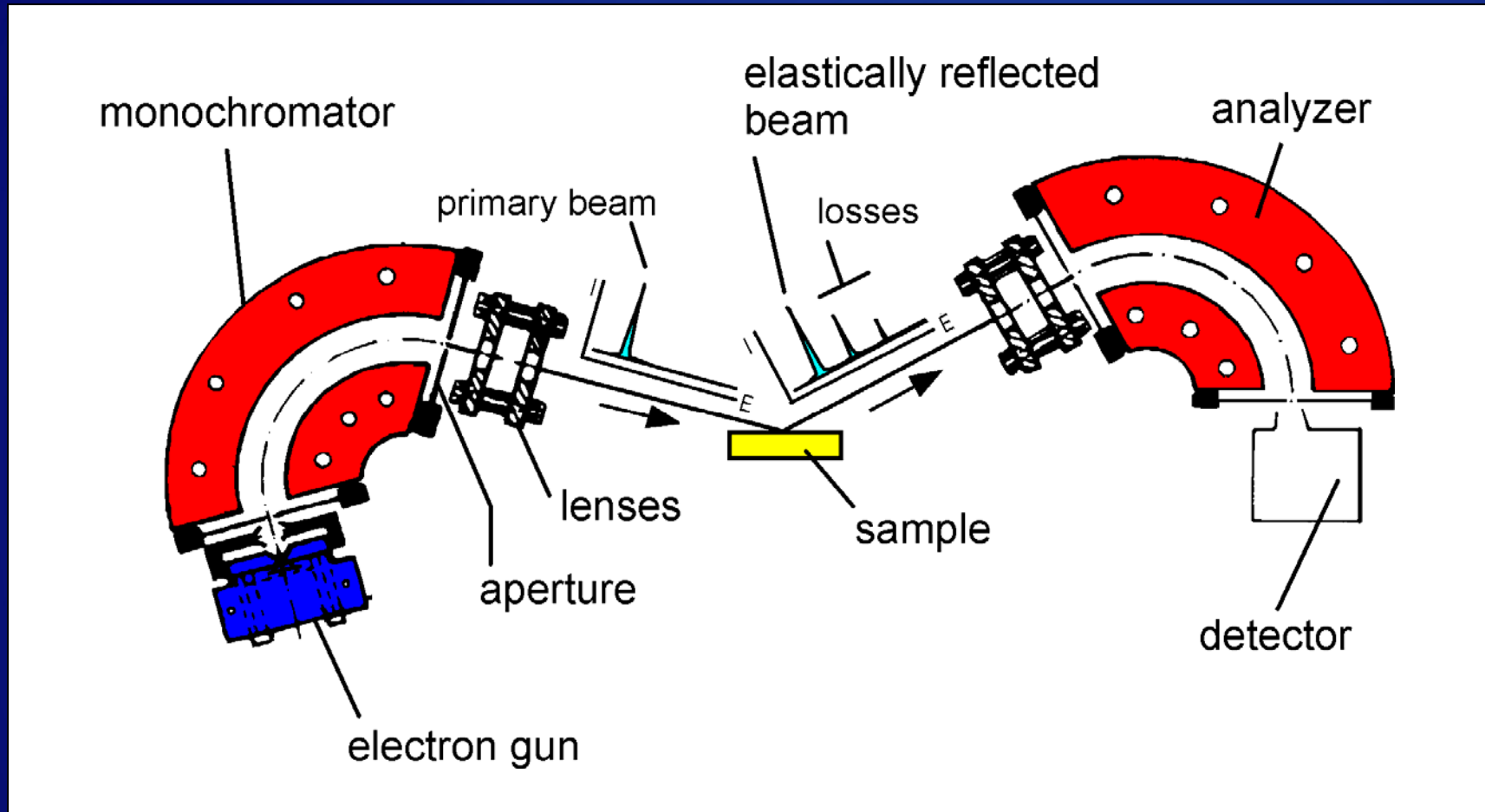


2. layer



# EELS

## principle setup



# EELS principles



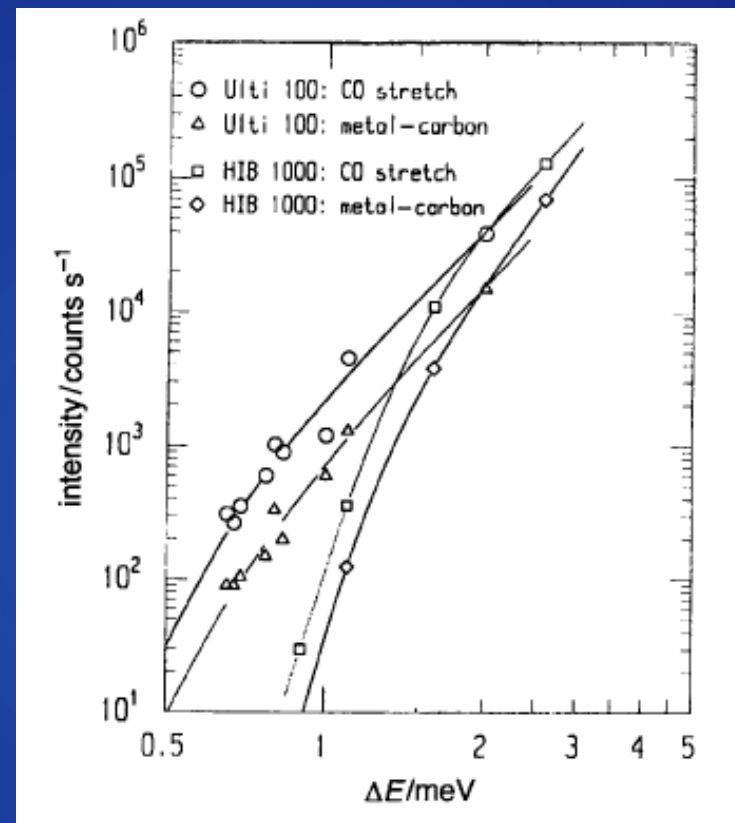
## Why EELS? (pros and cons)

- lower energy vibrations detectable (down to appox.  $100\text{ cm}^{-1}$ )
- dipole selection rule applies only in specular geometry
- off specular geometry allows detection of non IR active modes
- energy resolution to the best  $4\text{ cm}^{-1}$  ( $0.5\text{ meV}$ )
- electron current on the sample decreases with resolution in a power law behavior :  
$$(I \propto (\Delta E - \Delta E_{\min})^{5/2})$$

# EELS principles

## Why EELS? (pros and cons)

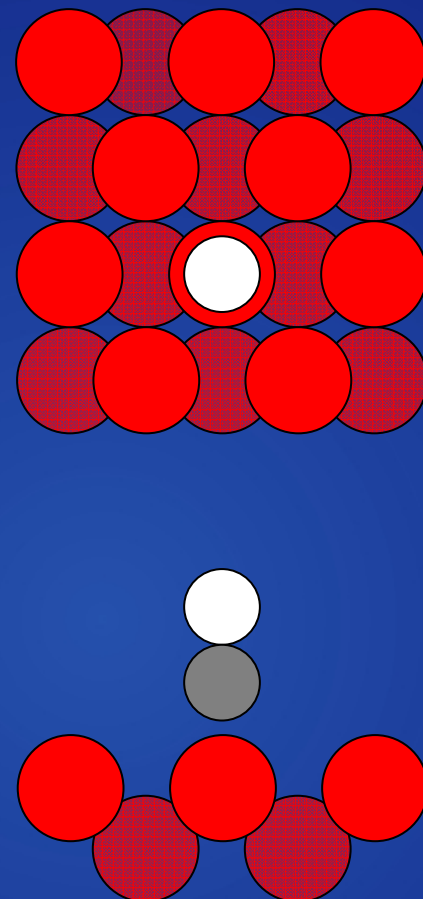
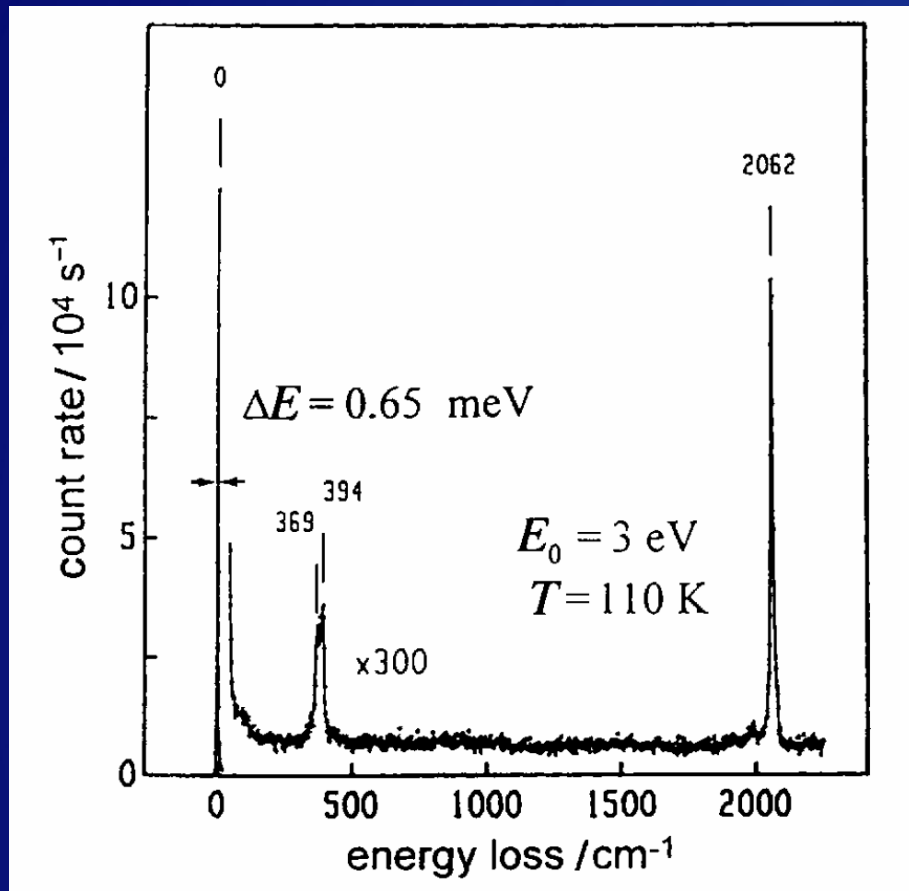
- lower energy vibrations detectable (down to appox.  $100\text{ cm}^{-1}$ )
- dipole selection rule applies only in specular geometry
- off specular geometry allows detection of non IR active modes
- energy resolution to the best  $4\text{ cm}^{-1}$  ( $0.5\text{ meV}$ )
- electron current on the sample decreases with resolution in a power law behavior :  
$$(I \propto (\Delta E - \Delta E_{\min})^{5/2})$$



H. Ibach, M. Balden, S. Lehwald, J. Chem. Soc.-Faraday Trans. **92**, 4771 (1996).

# EELS

## CO/W(110)



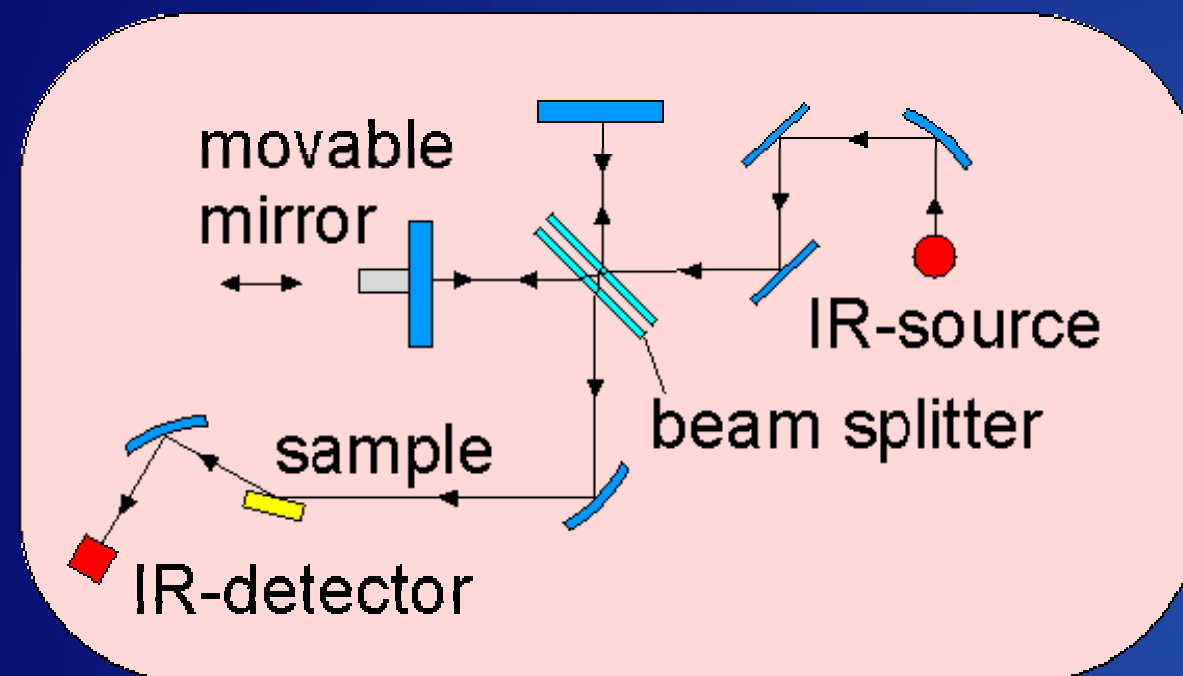
H. Ibach, M. Balden, S. Lehwald, J. Chem. Soc.-Faraday Trans. **92**, 4771 (1996).

# surface vibrations

## IRAS



### principle experimental setup



source (white source)

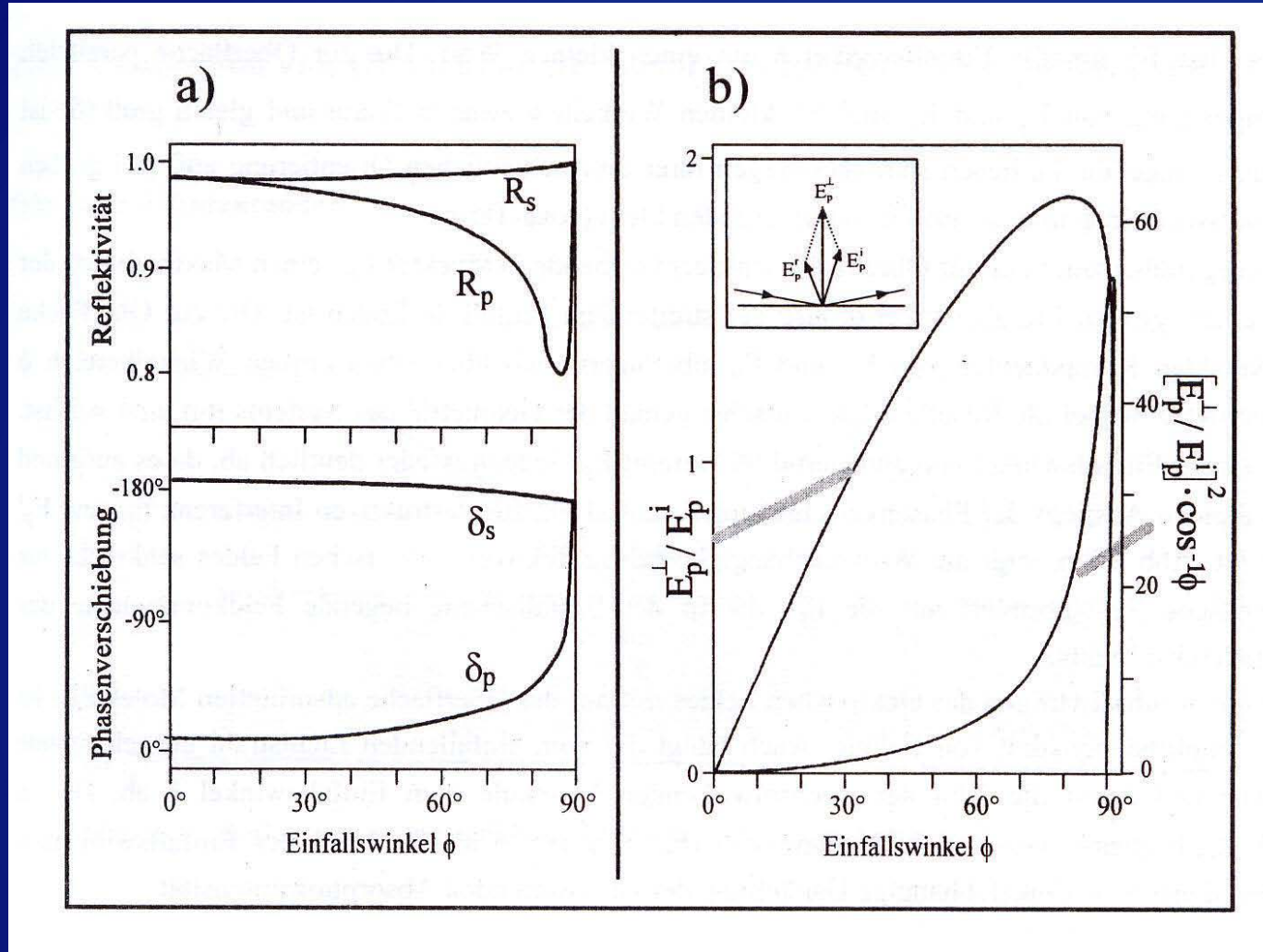
- globar
- Nernst rod

detector

- semiconductor,  
broad band e.g. MCT,  
InSb, GeCu
- bolometer  
(higher sensitivity  
especially for low  
frequencies;  
narrow band)

# surface vibrations

## IRAS

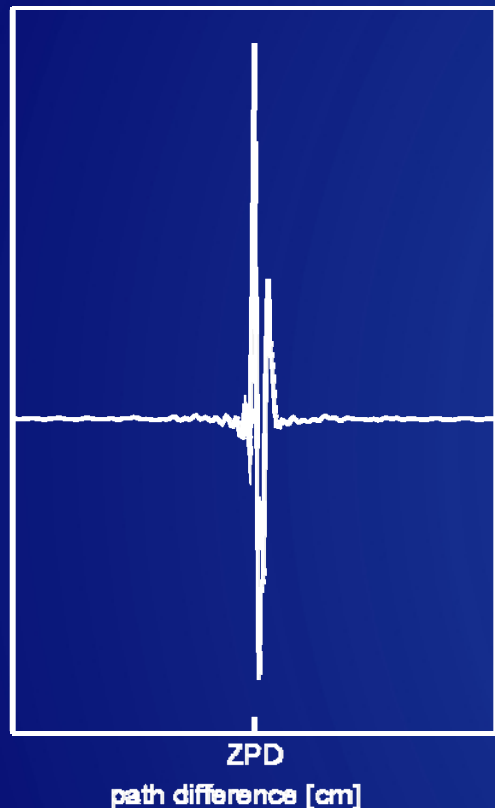


# surface vibrations

## IRAS

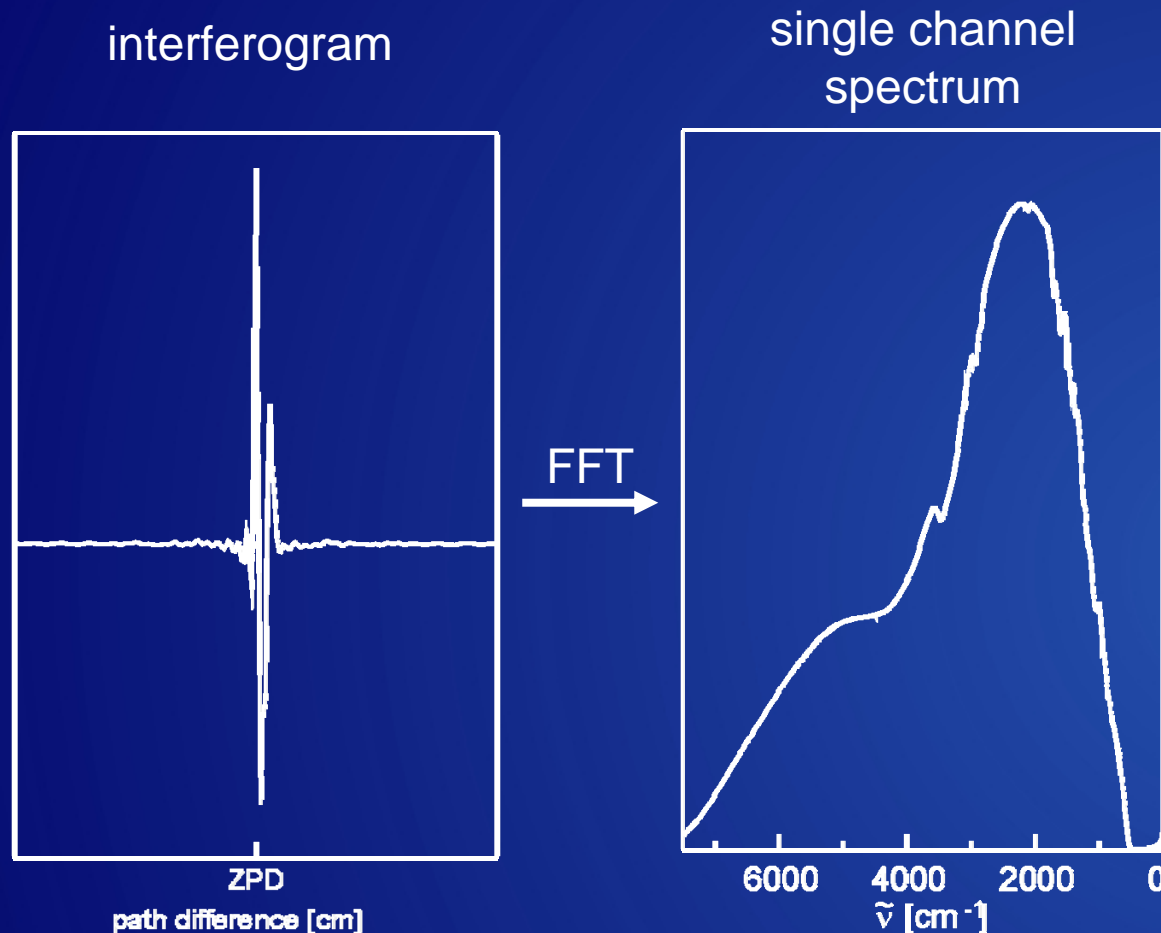


interferogram



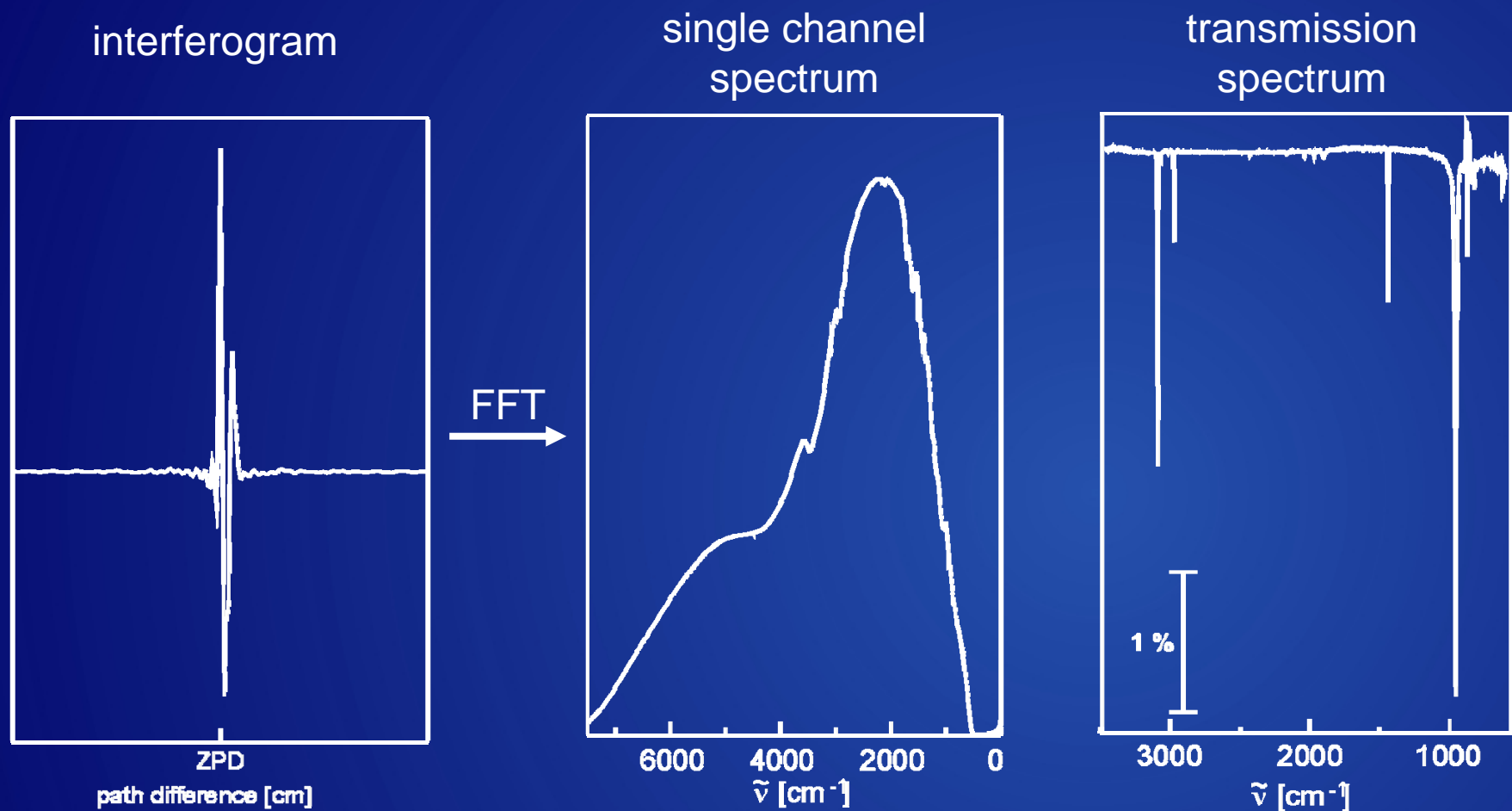
# surface vibrations

## IRAS



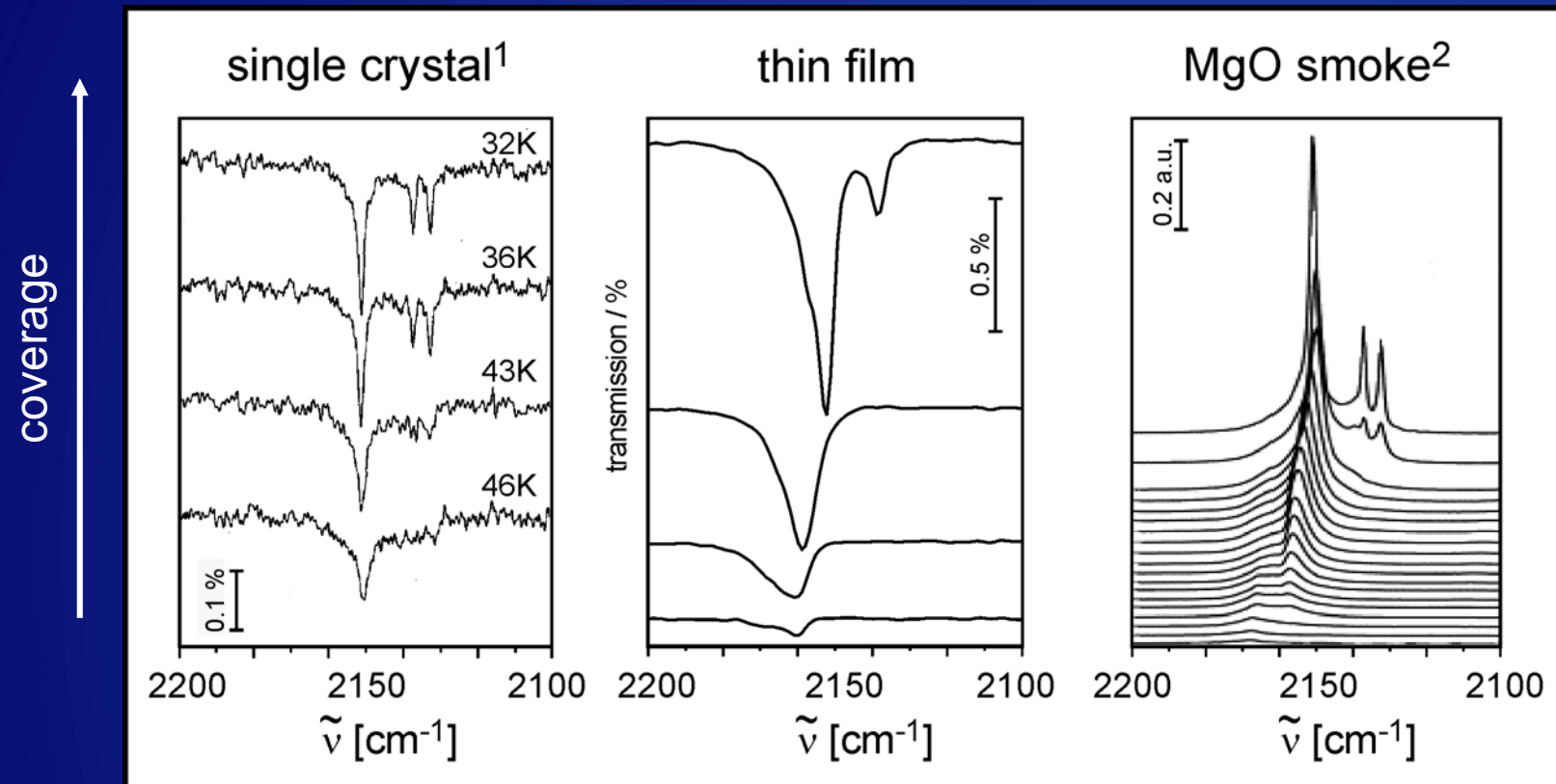
# surface vibrations

## IRAS



# IRAS

## CO on MgO(001)



<sup>1</sup> J. Heidberg et al. *Surf. Sci.* **331-333**, 1467 (1995).

<sup>2</sup> G. Spoto et al. *Prog. Surf. Sci.* **76**, 71, (2004).

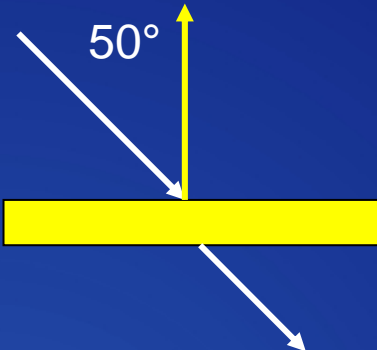
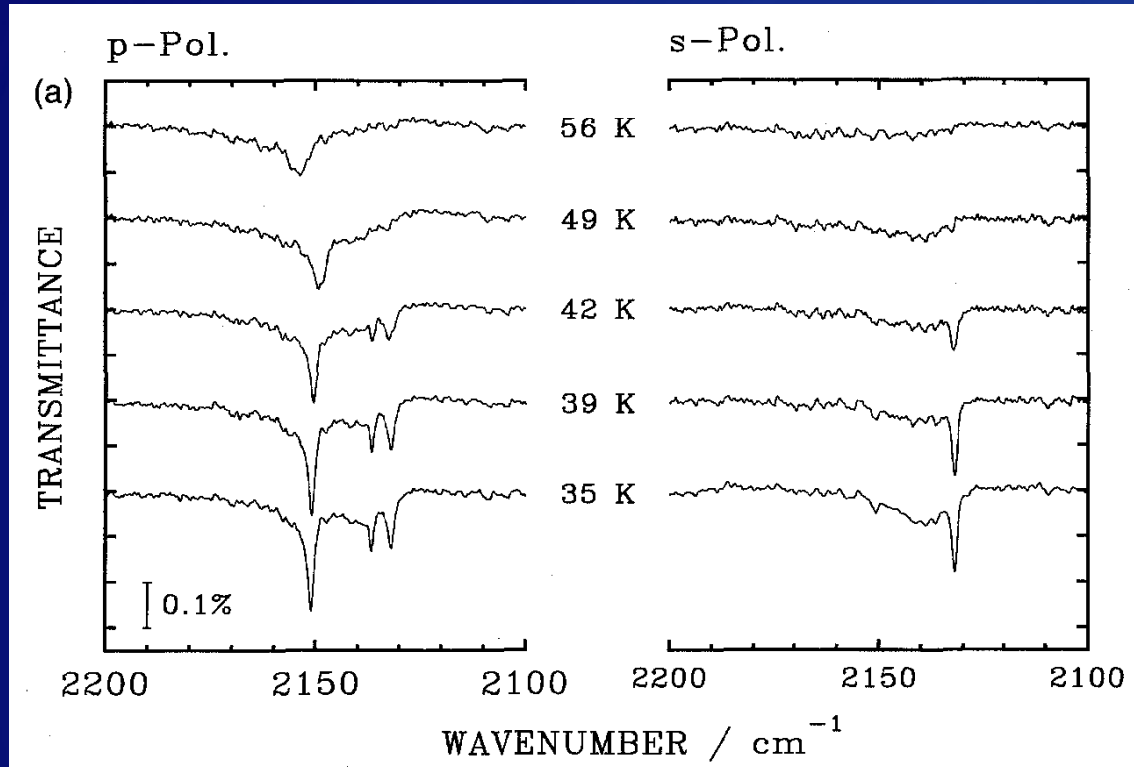
M. Sterrer et al. *Surf. Sci.* **596**, 222 (2005).

# IRAS

## CO on MgO(001)



transmission experiment



- c(4x2) superstructure (LEED)
- 3 molecules in the unit cell (LEED, HAS)
- 1 molecule perpendicular
- 2 molecules tilted

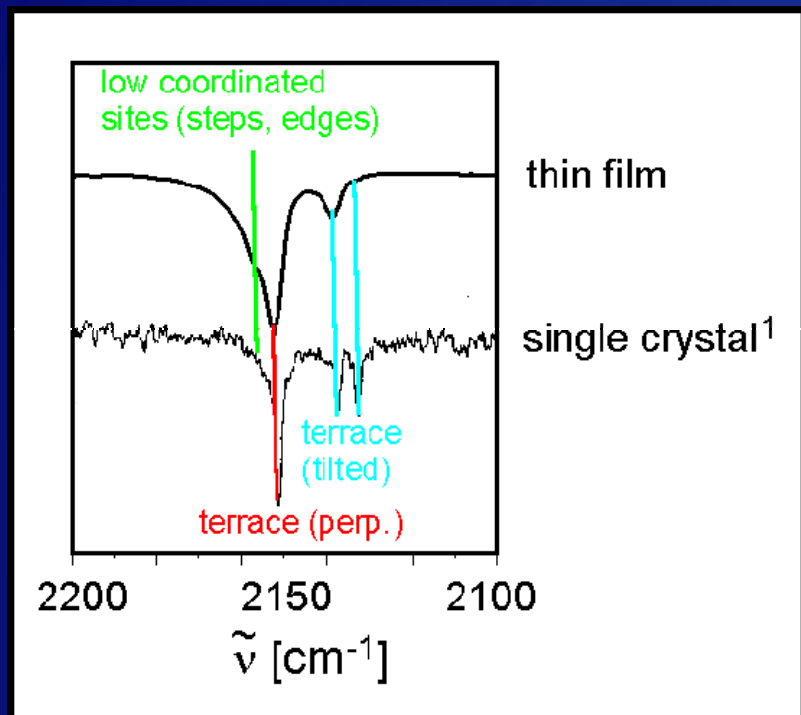
<sup>1</sup> J. Heidberg et al. *Surf. Sci.* **331-333**, 1467 (1995).

# IRAS

## CO on MgO(100)



IR



<sup>1</sup> J. Heidberg et al. *Surf. Sci.* **331-333**, 1467 (1995).

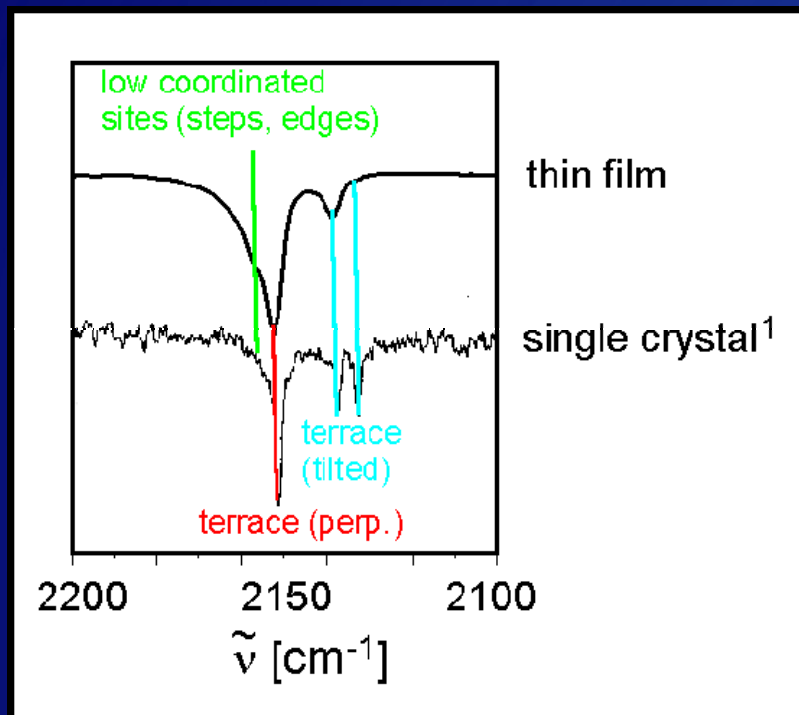
M. Sterrer et al. *Surf. Sci.* **596**, 222 (2005).

# IRAS

## CO on MgO(100)



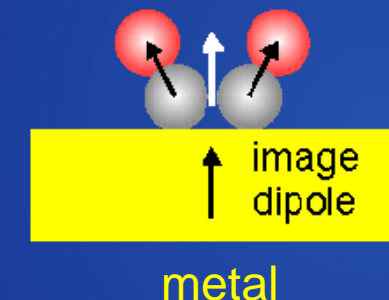
IR



2 tilted molecules

symmetric stretch  
high frequency

**dynamic dipole**



$$\mu_{\text{dyndip}} > 0$$

IR active

asymmetric stretch  
low frequency

**dynamic dipole**



$$\mu_{\text{dyndip}} = 0$$

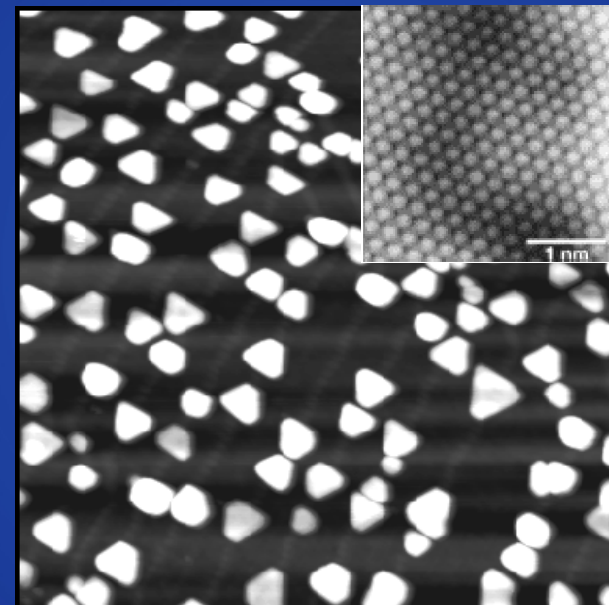
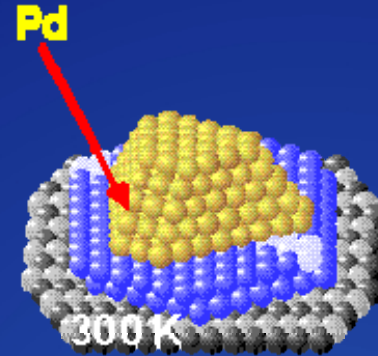
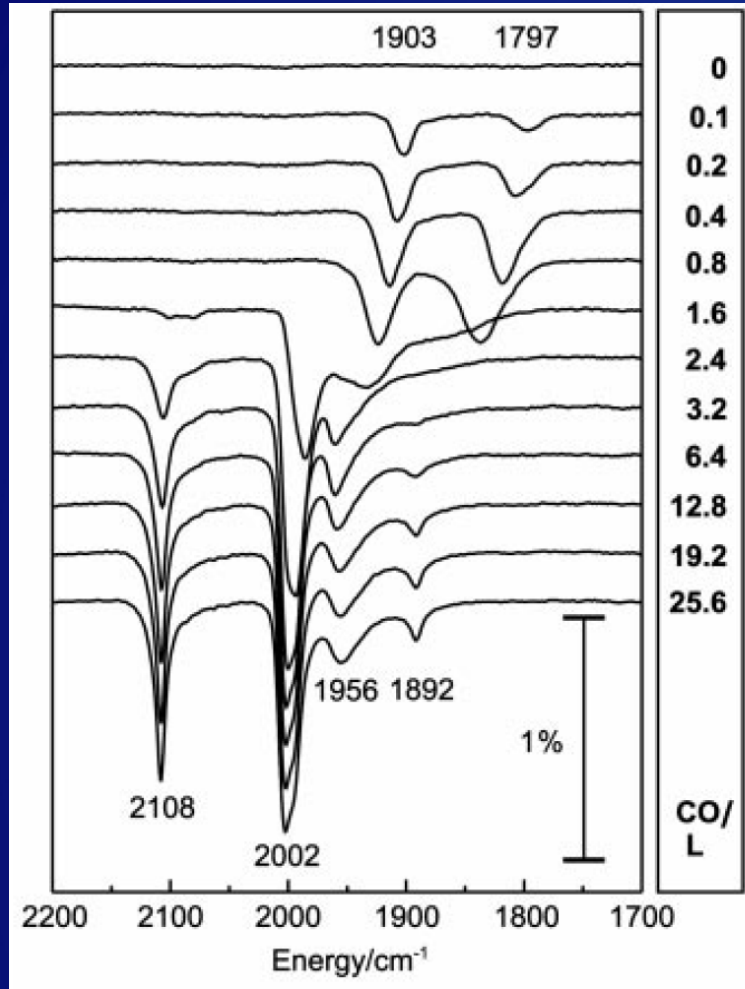
IR inactive

<sup>1</sup> J. Heidberg et al. *Surf. Sci.* **331-333**, 1467 (1995).

M. Sterrer et al. *Surf. Sci.* **596**, 222 (2005).

# Pd particles on thin alumina

## CO IRAS

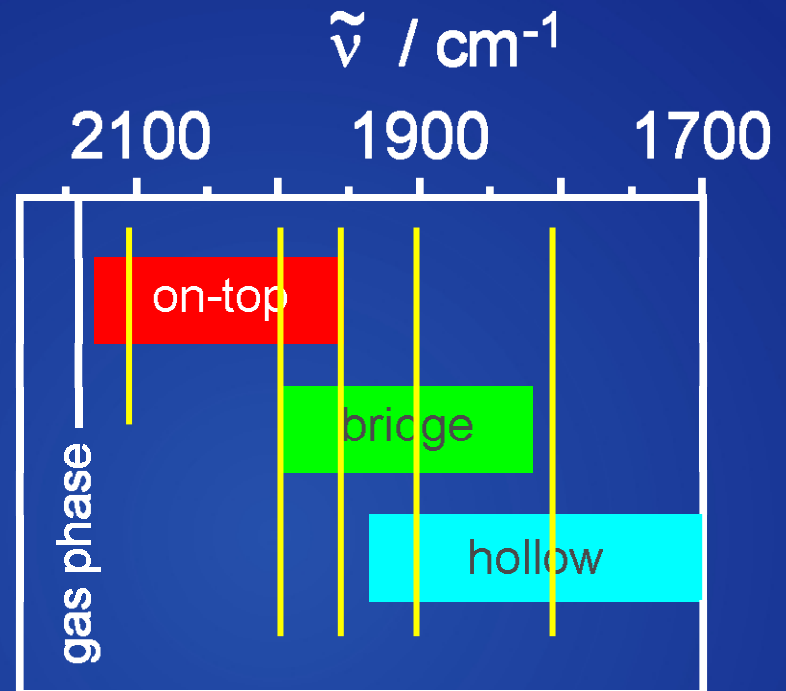
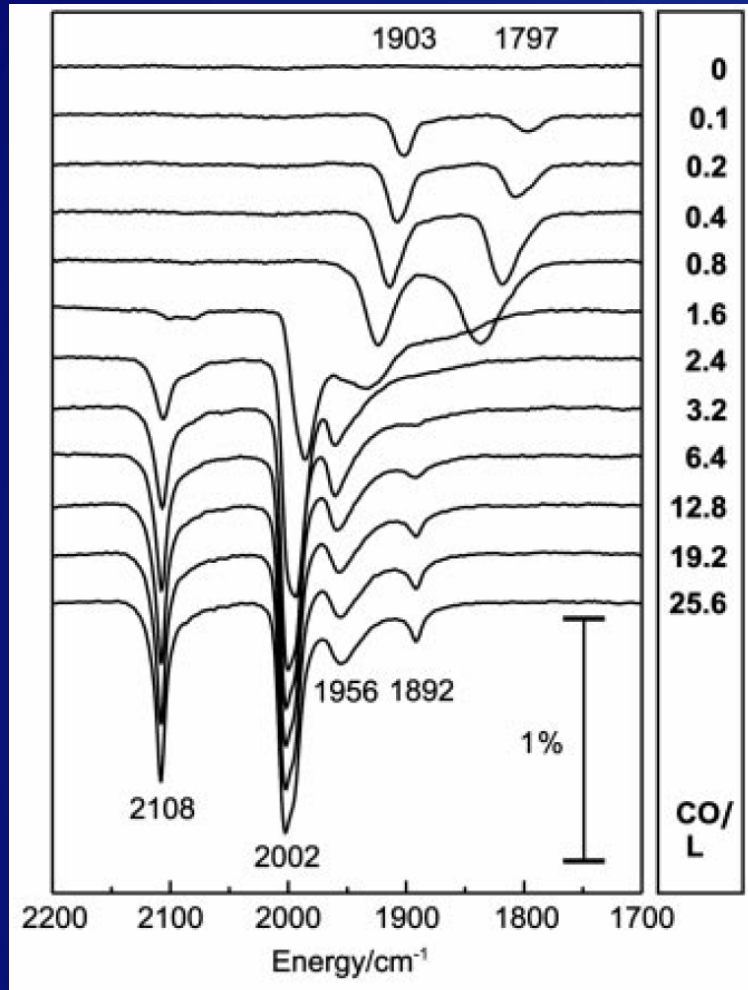


M. Frank and M. Bäumer, PCCP **2**, 3723 (2000).

K. H. Hansen *et al.* Phys. Rev. Lett. **83**, 4120 (1999).

# Pd particles on thin alumina

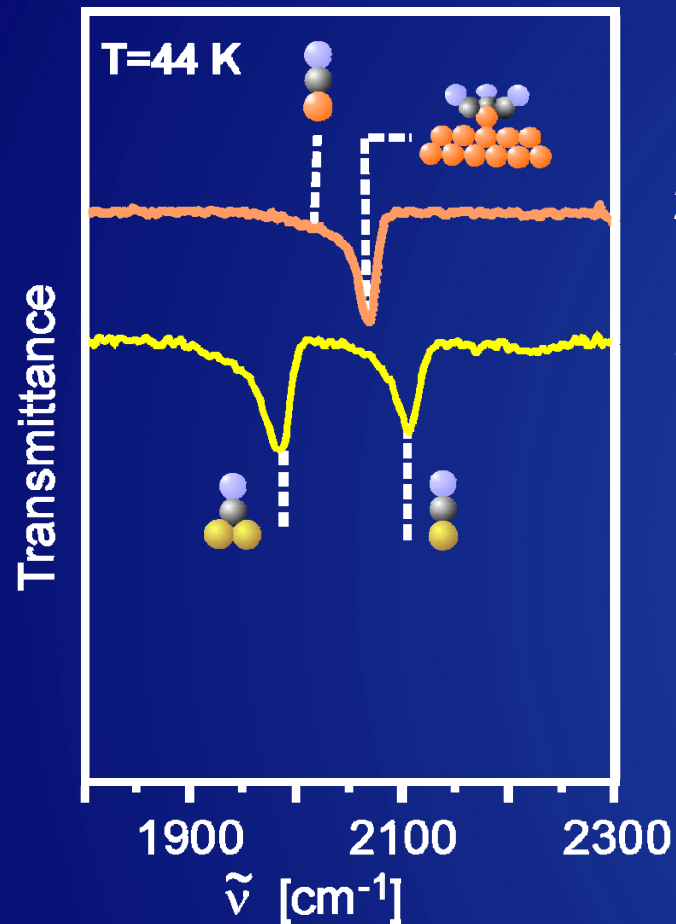
## CO IRAS



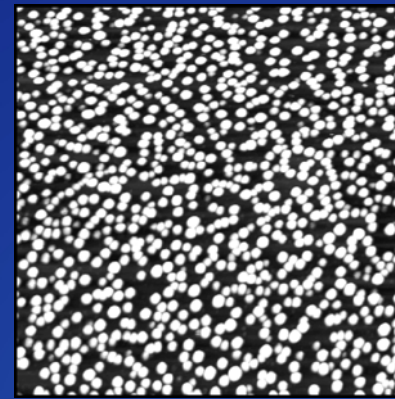
M. Frank and M. Bäumer, PCCP **2**, 3723 (2000).

# Metal particles

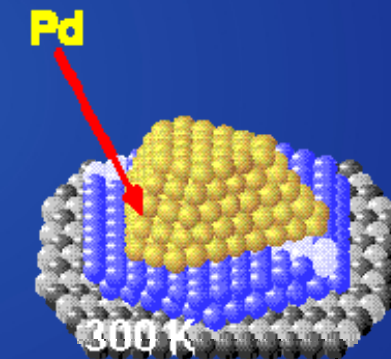
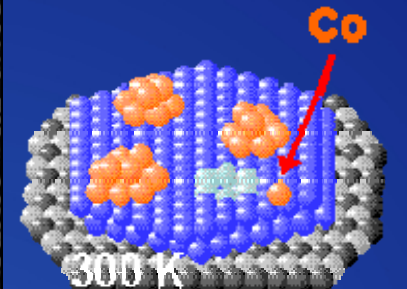
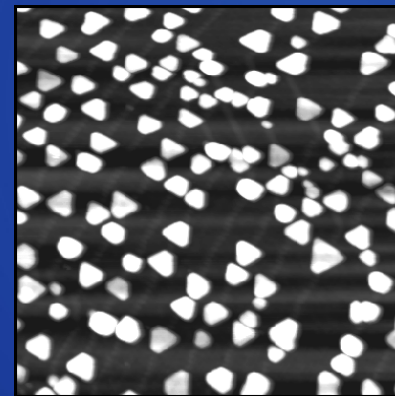
## CO IRAS



$2 \text{ \AA Co}$

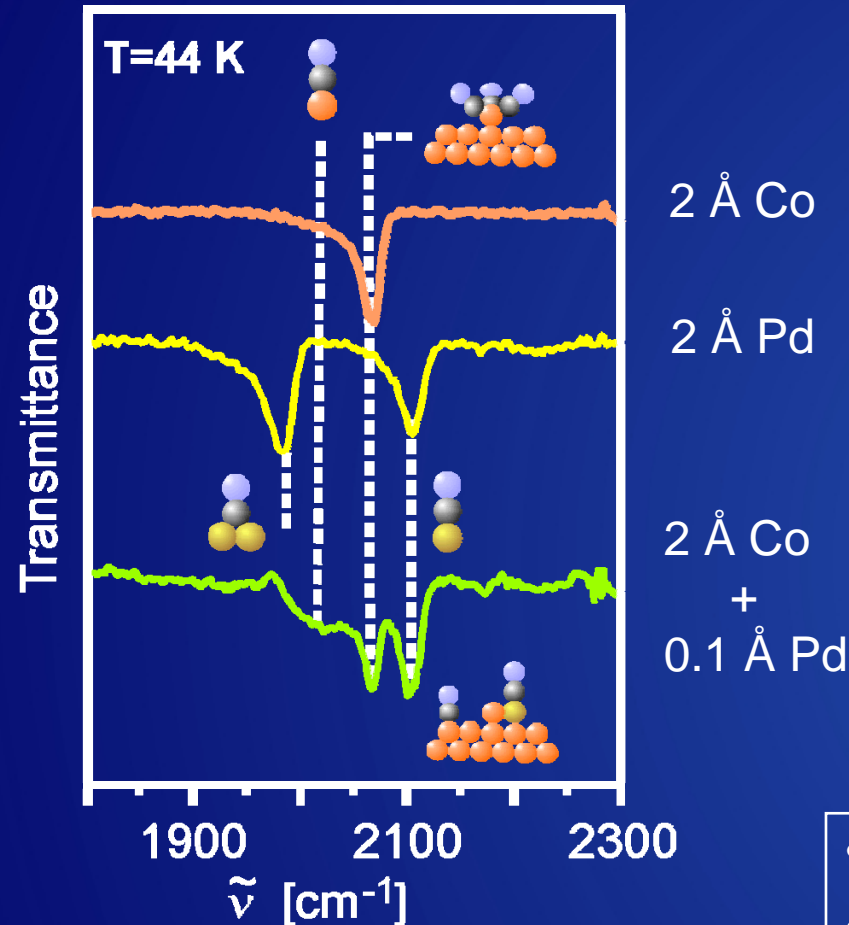


$2 \text{ \AA Pd}$



# Metal particles

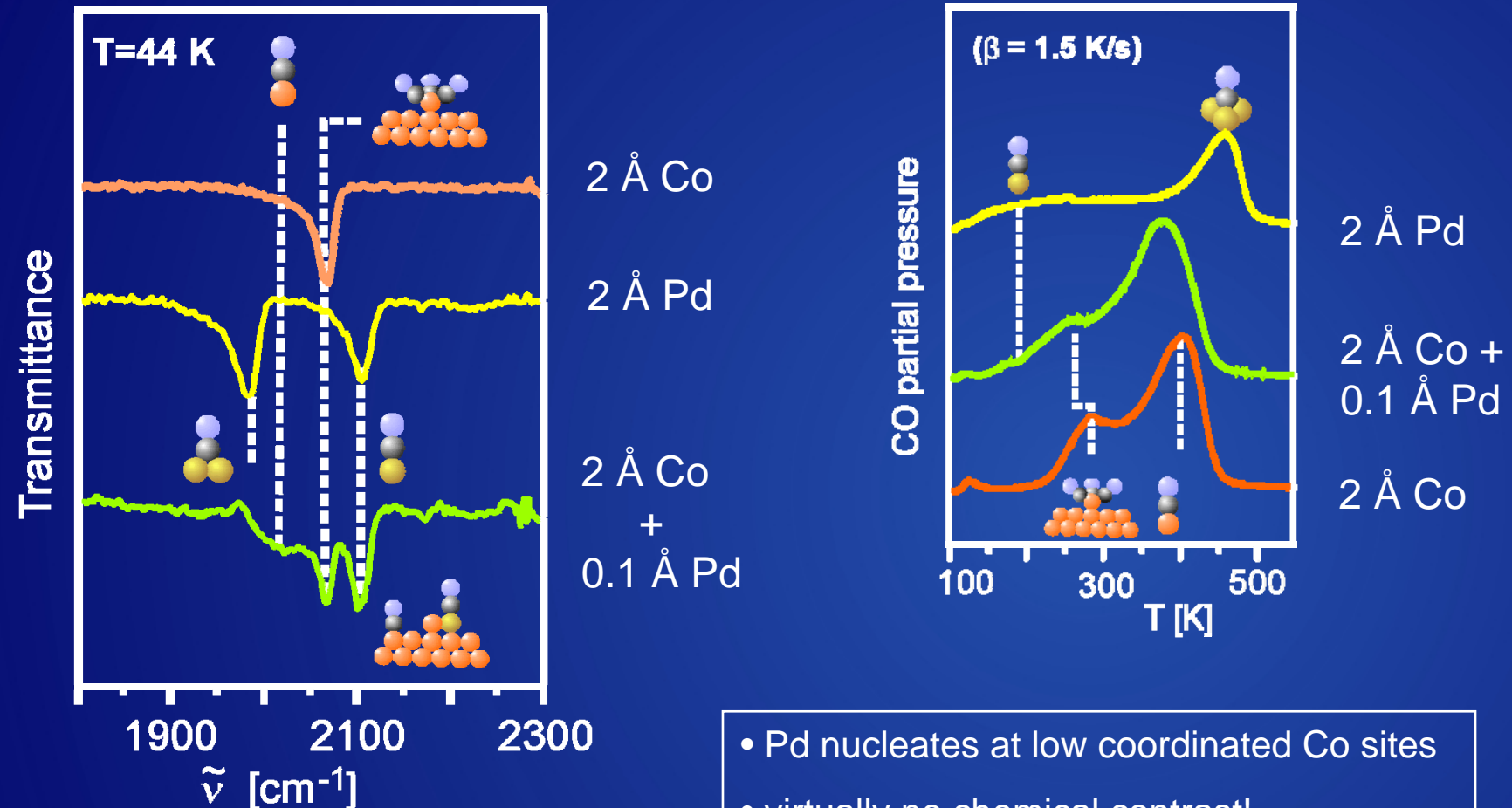
## CO IRAS



- Pd nucleates at low coordinated Co sites
- virtually no chemical contrast!

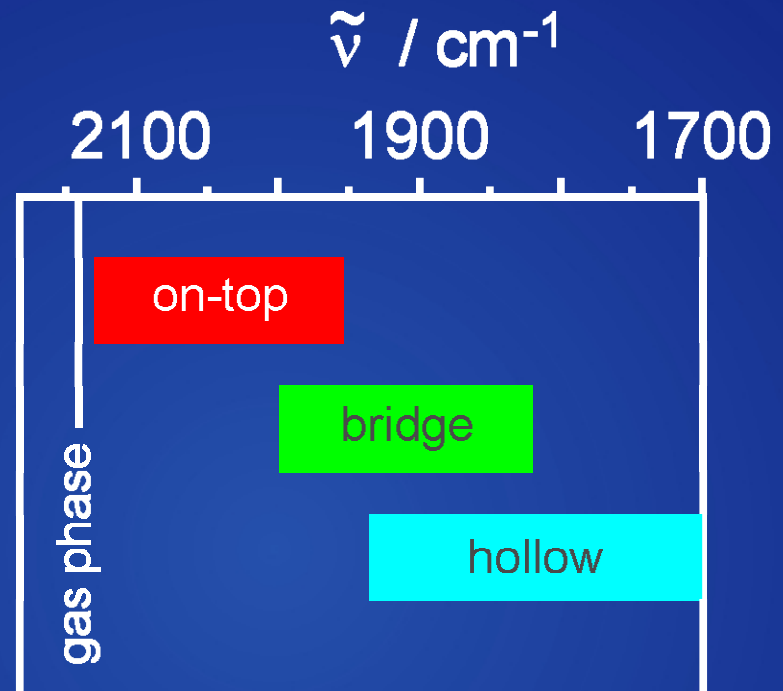
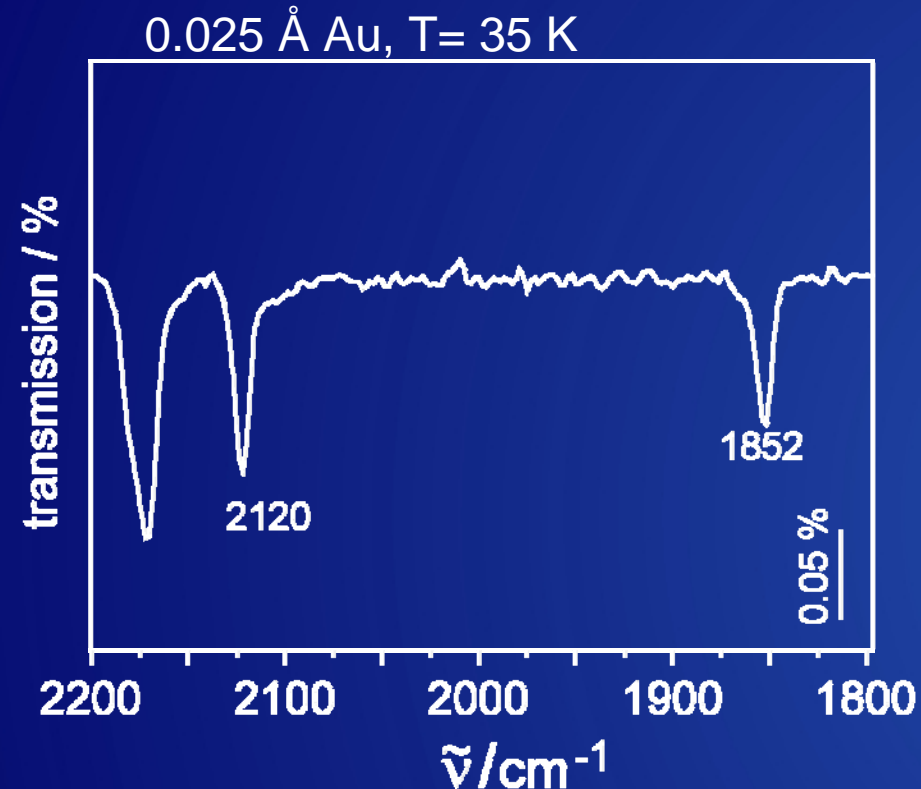
# Metal particles

## CO IRAS



# Au/MgO(001)/Mo(001)

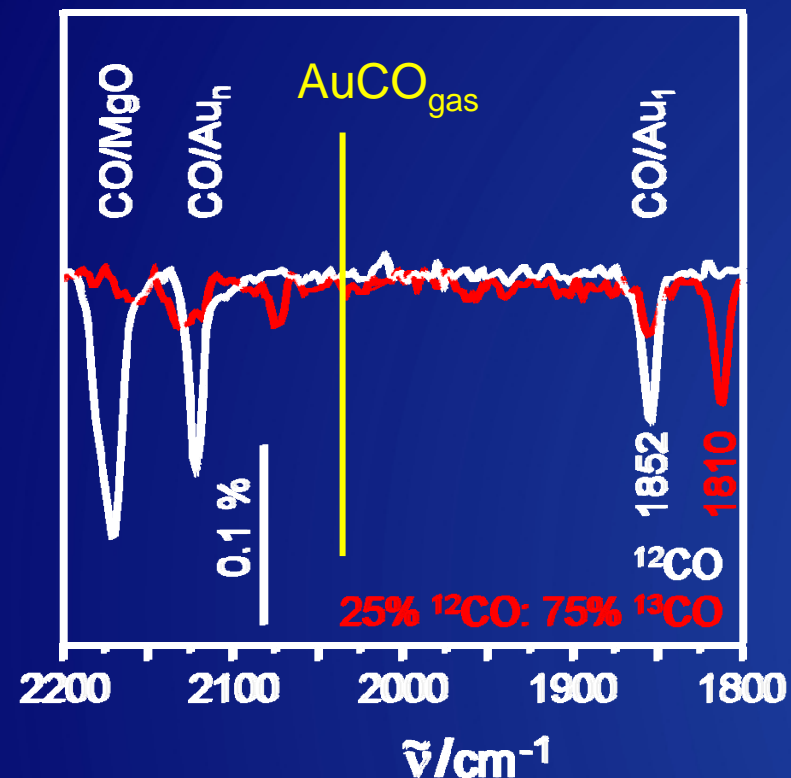
## CO IRAS



M. Sterrer et al. Angew. Chem. Int. Ed. **45**, 2633 (2006)

# Au/MgO(001)/Mo(001)

## CO IRAS

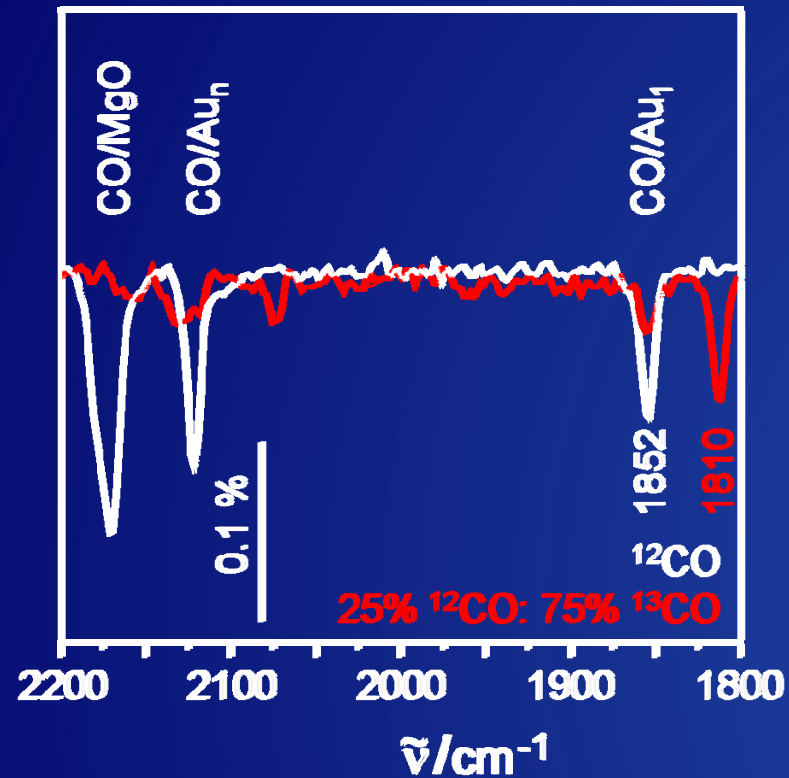


red-shift of CO stretching frequency by  $187 \text{ cm}^{-1}$   
with respect to gas phase AuCO carbonyl

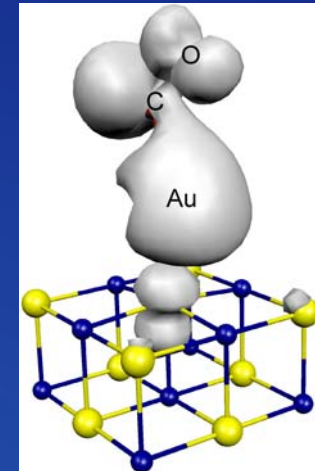
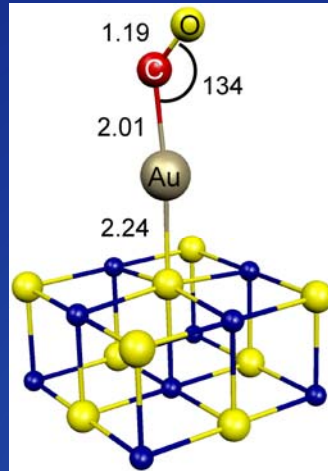
M. Sterrer et al. Angew. Chem. Int. Ed. **45**, 2633 (2006)

# MgO(001)/Mo(001)

## IR of Au atoms



red-shift of CO stretching frequency by  $291 \text{ cm}^{-1}$  with respect to gas phase



Theory prediction:

- red-shift of  $286 \text{ cm}^{-1}$  to gas phase
- large electron transfer to Au/CO complex

=> CO induces the charge transfer

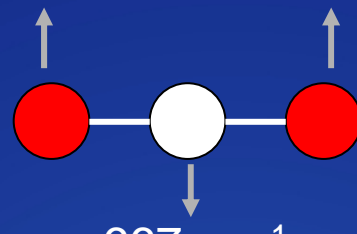
M. Sterrer et al. Angew. Chem. Int. Ed. **45**, 2633 (2006)

# IRAS

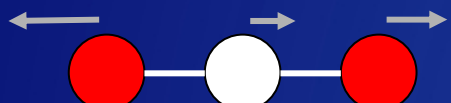
## $\text{CO}_2$ on $\text{NaCl}(001)$



$1288 \text{ cm}^{-1}$



$667 \text{ cm}^{-1}$



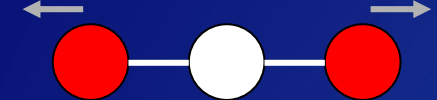
$2349 \text{ cm}^{-1}$



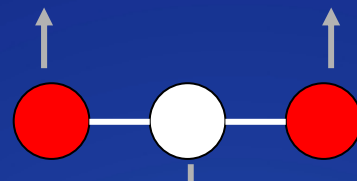
$667 \text{ cm}^{-1}$

# IRAS

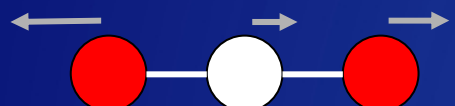
## $\text{CO}_2$ on $\text{NaCl}(001)$



$1288 \text{ cm}^{-1}$



$667 \text{ cm}^{-1}$

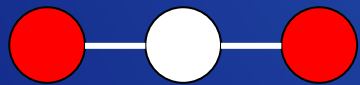


$2349 \text{ cm}^{-1}$



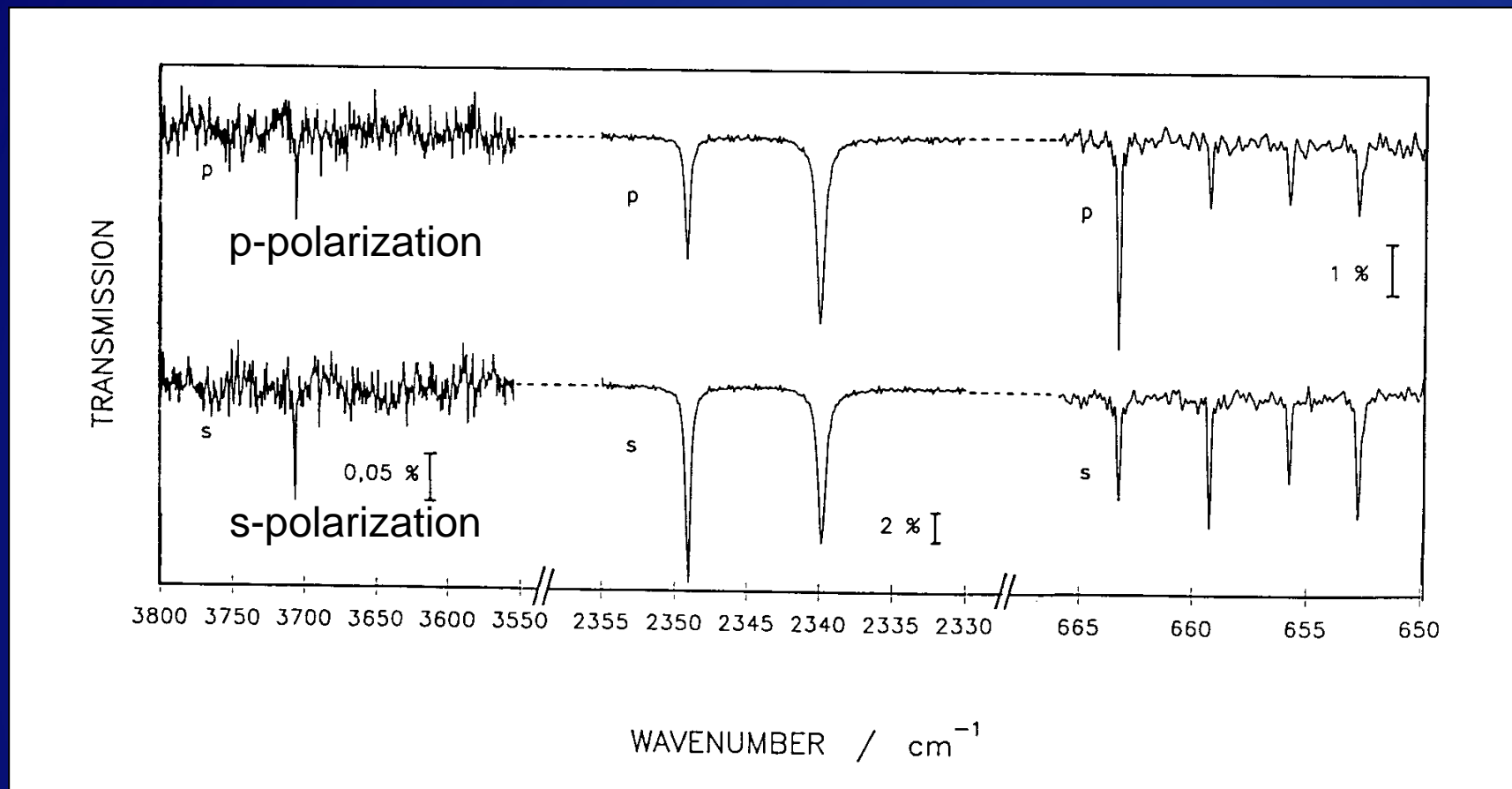
$667 \text{ cm}^{-1}$

What is expected?



# IRAS

## CO<sub>2</sub> on NaCl(001)



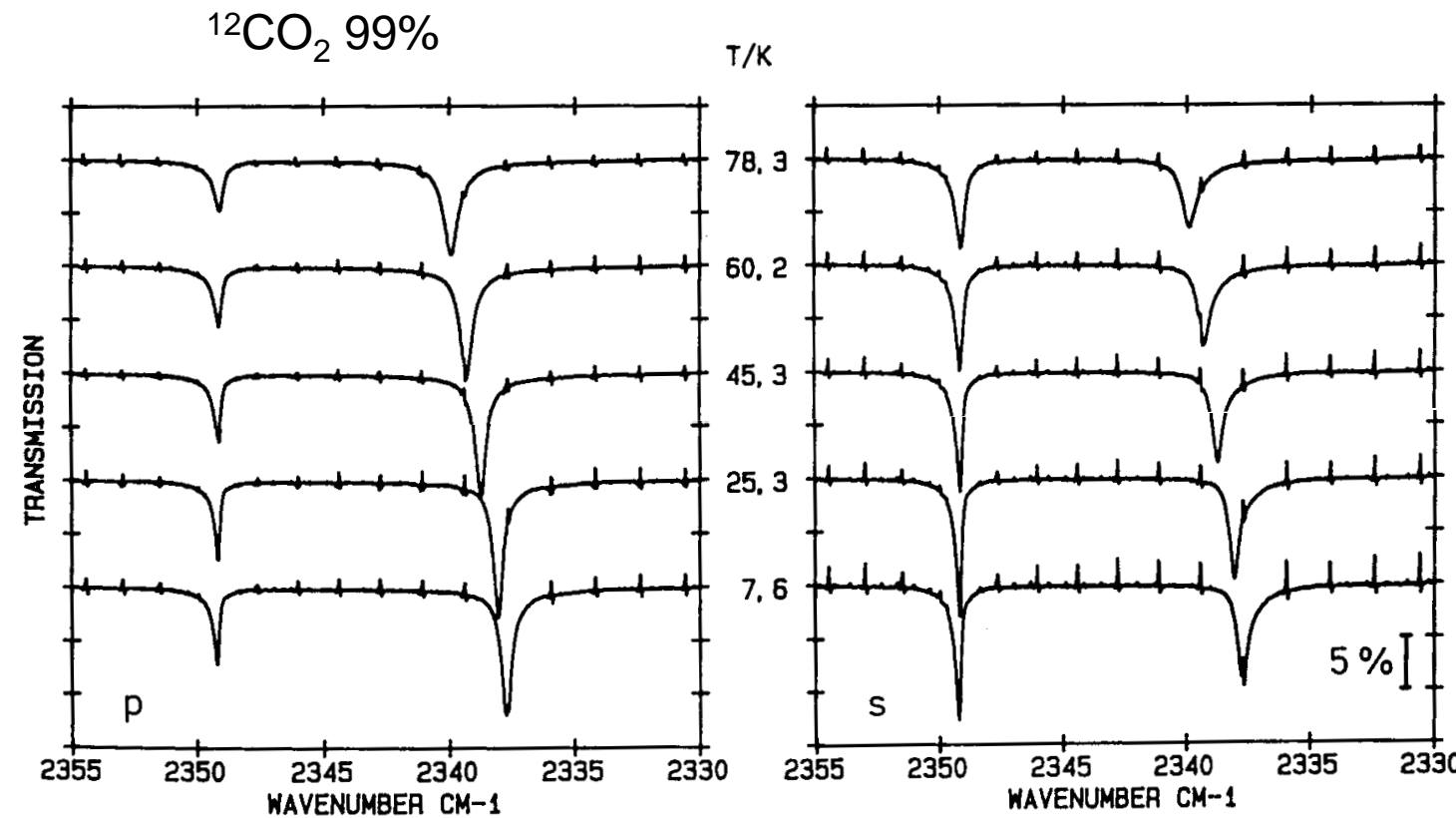
J. Heidberg et al. *J. Electr. Spec. Rel. Phenom.* 64/65, 341 (1993).

Fritz-Haber-Institute, Department of Chemical Physics, Magnetic Resonance Group

T. Risse, 11/21/2007, 34

# IRAS

## $\text{CO}_2$ on NaCl(001)



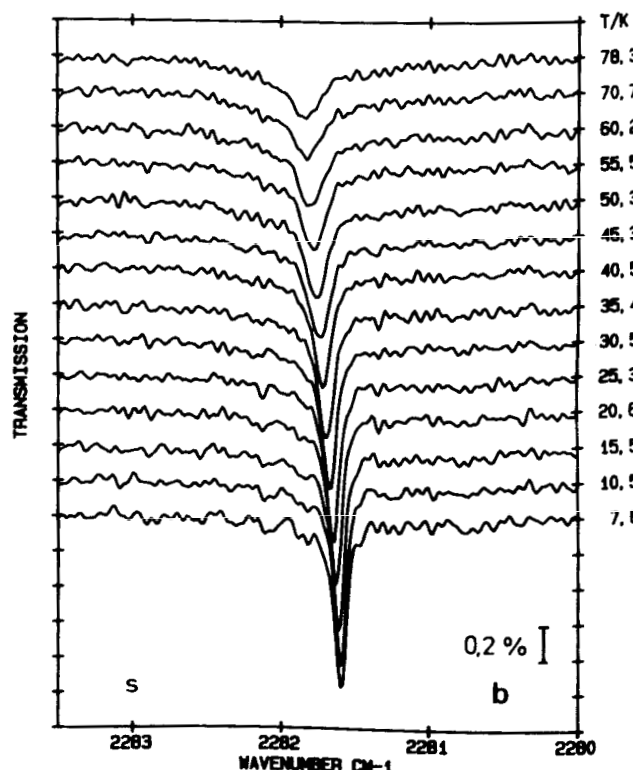
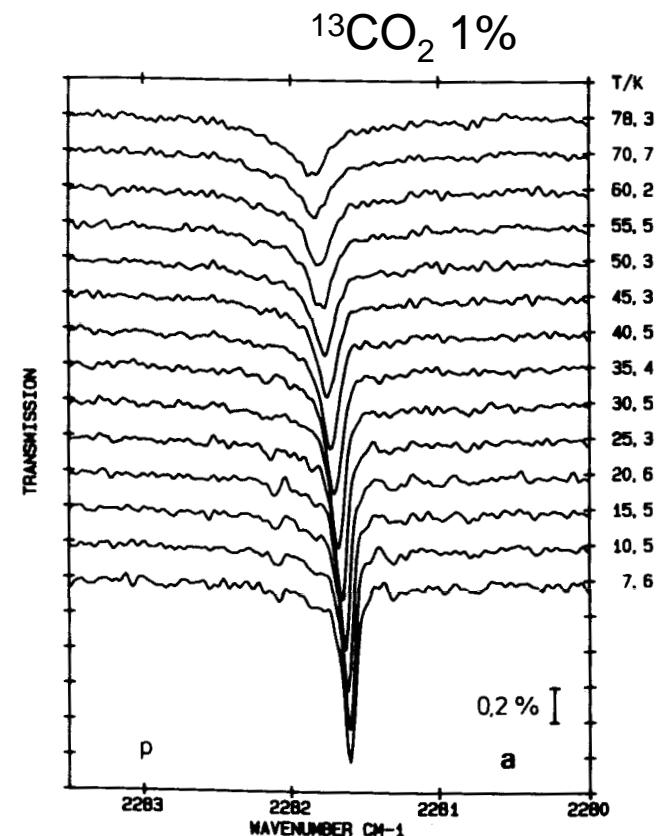
J. Heidberg et al. J. Electr. Spec. Rel. Phenom. 64/65, 341 (1993).

Fritz-Haber-Institute, Department of Chemical Physics, Magnetic Resonance Group

T. Risse, 11/21/2007, 35

# IRAS

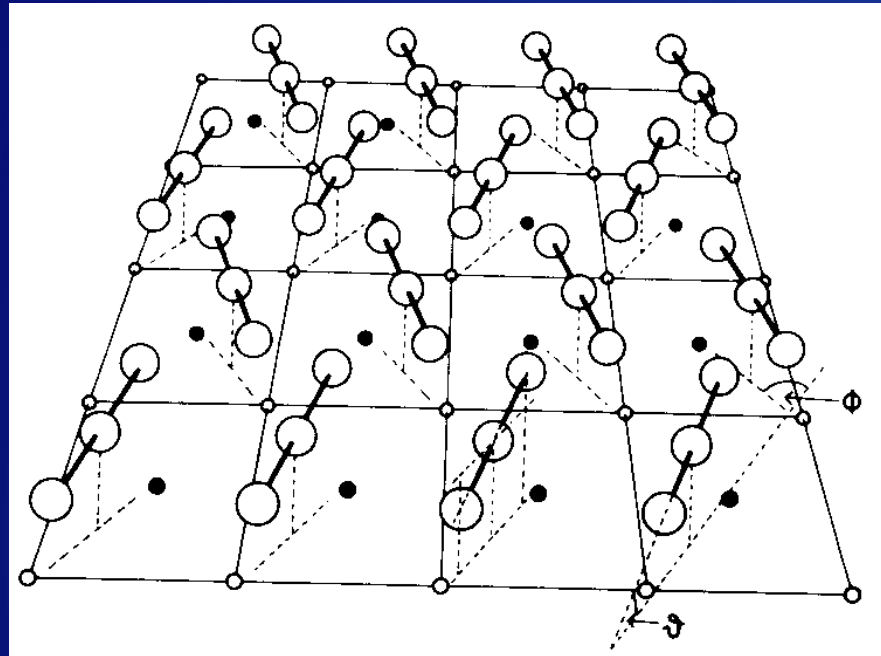
## $\text{CO}_2$ on NaCl(001)



- two lines for  $^{12}\text{CO}_2$ ; one line for highly diluted  $^{13}\text{CO}_2$
- Peak area constant with T
- same shift for s and p polarization

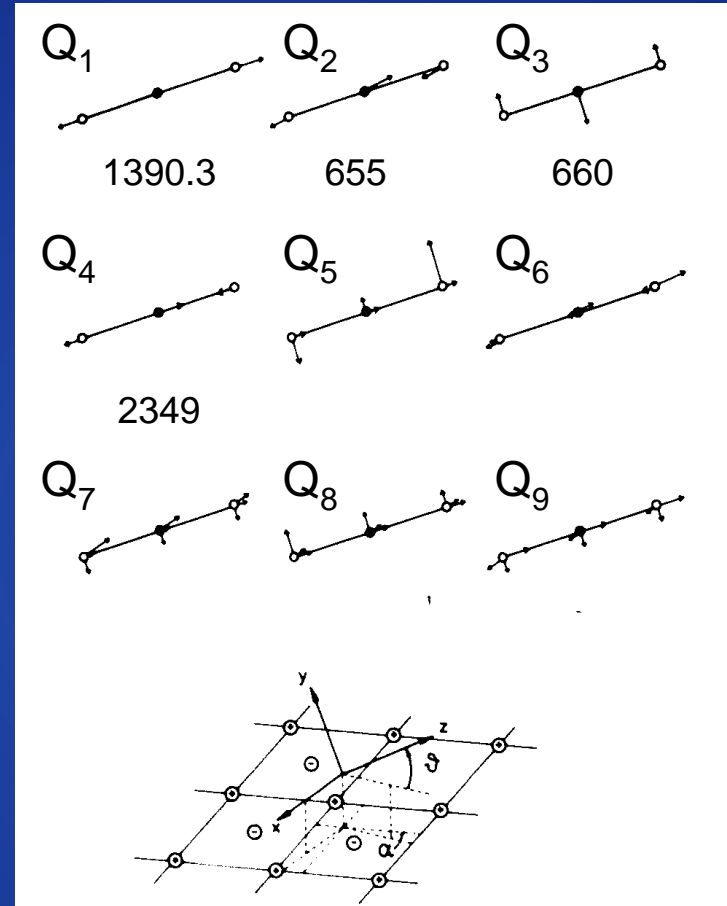
# IRAS

## CO<sub>2</sub> on NaCl(001)

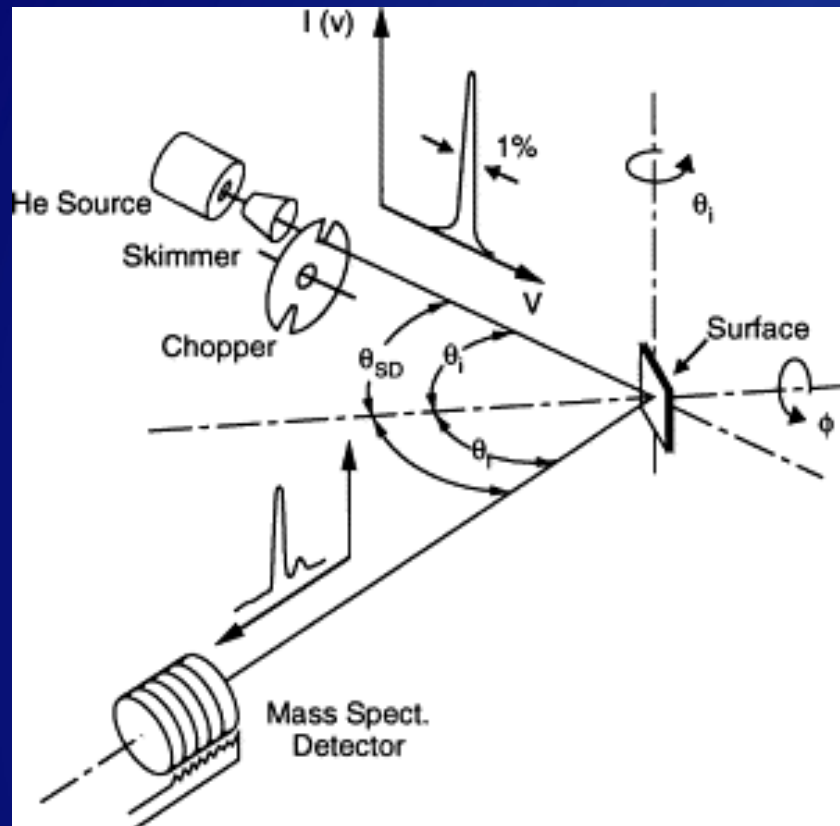


from structural analysis (LEED):

- glide mirror plane (pg symmetry)



# Helium atom scattering (HAS) experimental setup



- energy of the primary beam is ca. 10-40 meV
- inelastic losses by means of a TOF analysis
- Energy resolution: approx 100  $\mu\text{eV}$
- There is also momentum transfer

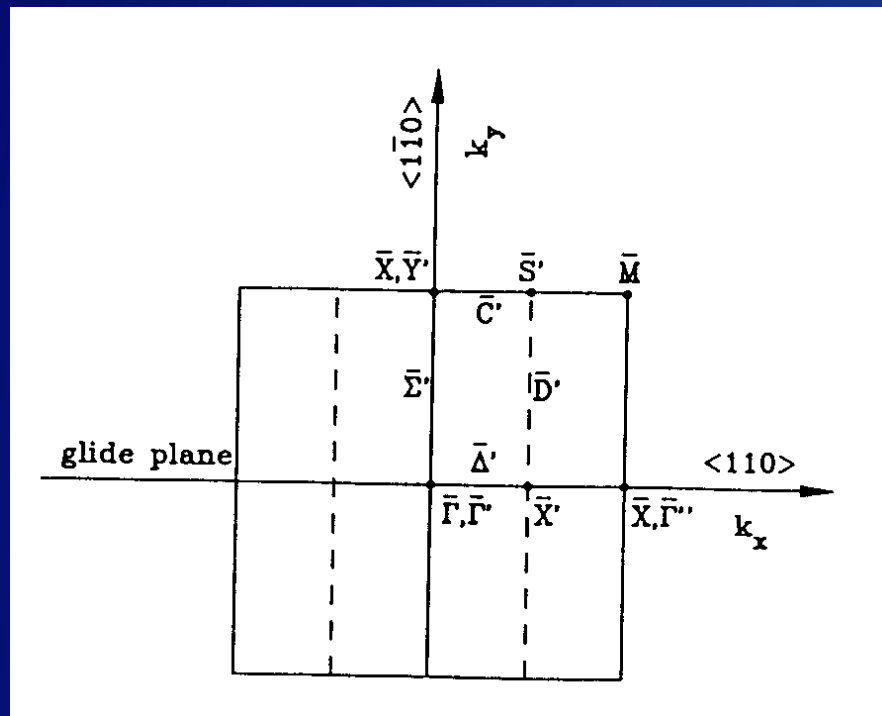
For fixed scattering angle of  $90^\circ$ :

$$\Delta E/E_i = \frac{(\sin(\theta_i) + \Delta k/k_i)^2}{\cos^2(\theta_i)} - 1$$

A. Graham *Surf. Sci. Rep.* 49, 115 (2003).

# HAS

## $\text{CO}_2$ on $\text{NaCl}(001)$



How many “external” modes to expect?

- two molecules in the unit cell, each five external modes

⇒ 10 modes

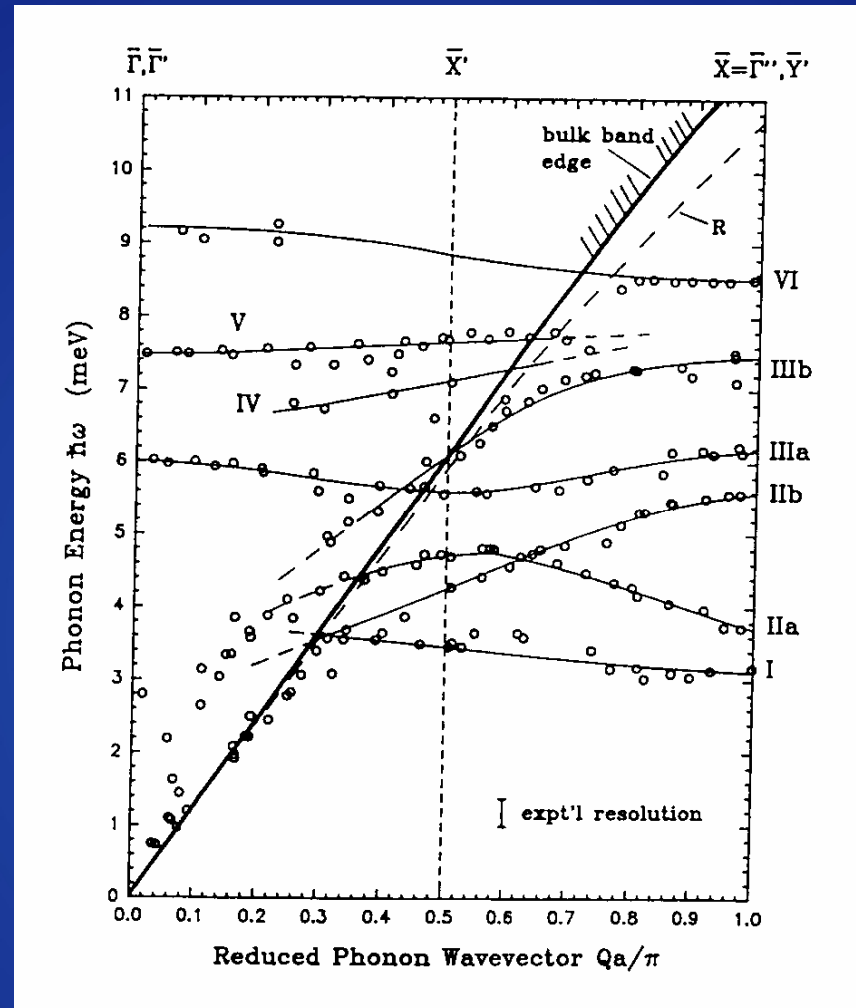
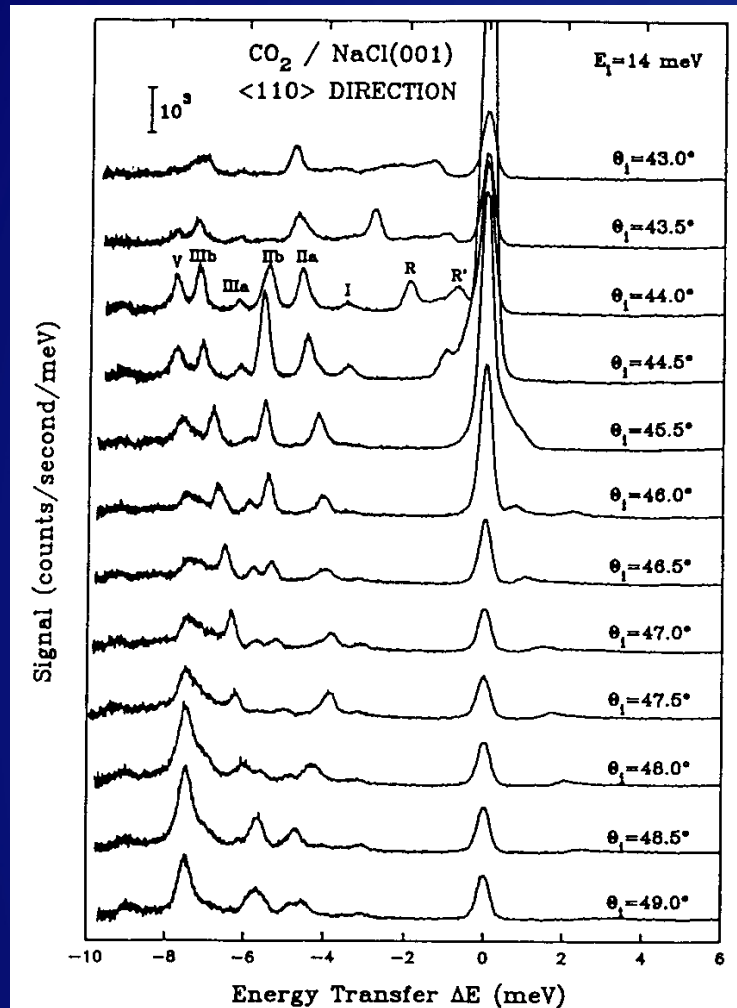
additionally: symmetry equivalent islands (along  $\Delta'$  and  $\Sigma'$ )

along  $\Delta'$  (glide plane) symmetry applies: only five modes

=> 15 modes in total

# HAS

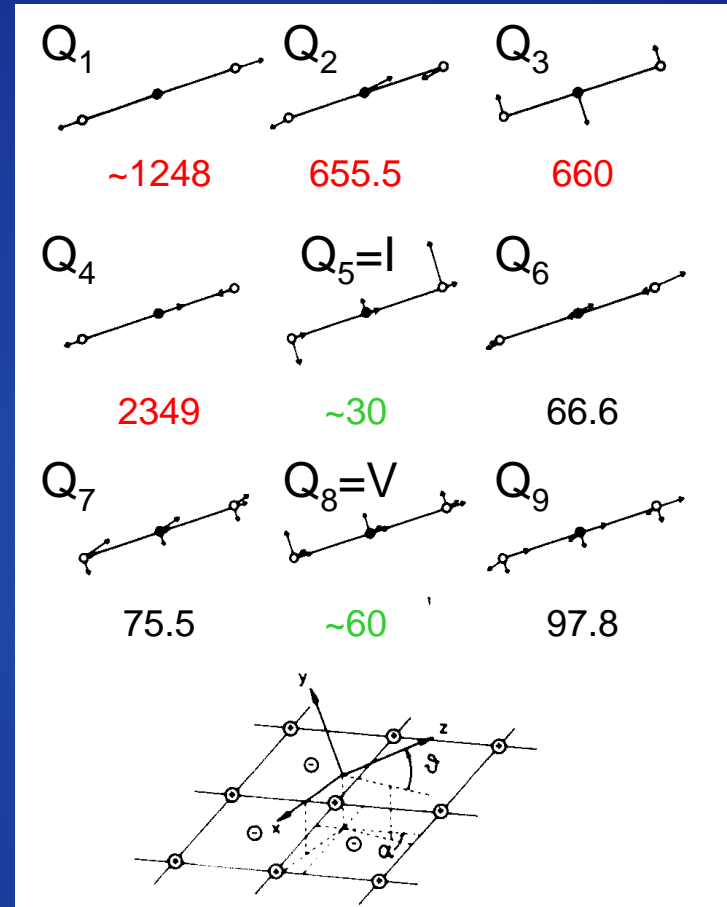
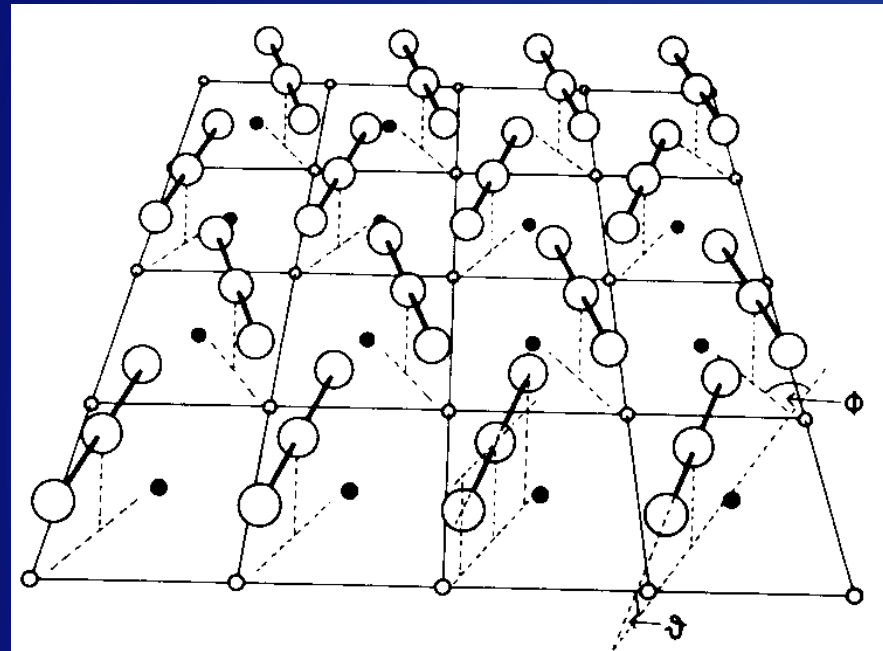
## $\text{CO}_2$ on $\text{NaCl}(001)$



J. Heidberg et al. J. Electr. Spec. Rel. Phenom. 64/65, 341 (1993).

# IRAS

## CO<sub>2</sub> on NaCl(001)



J. Heidberg et al. *Surf. Sci.* 269/270, 120 (1992).

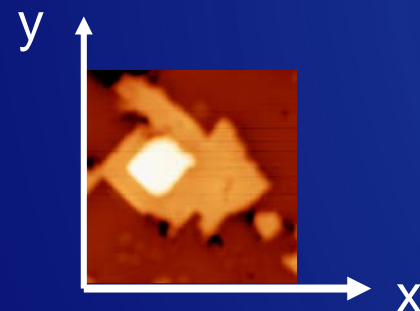
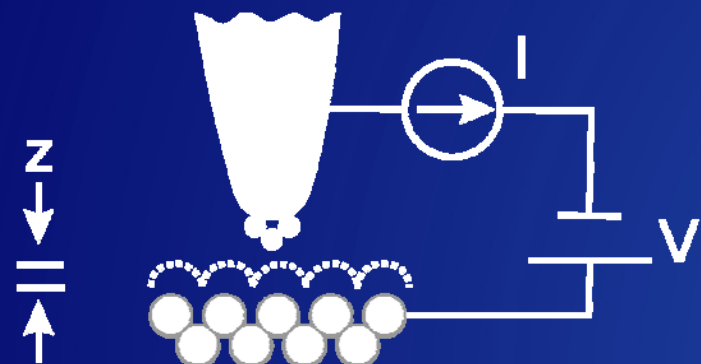
# Single molecule vibrations

## STM/STS



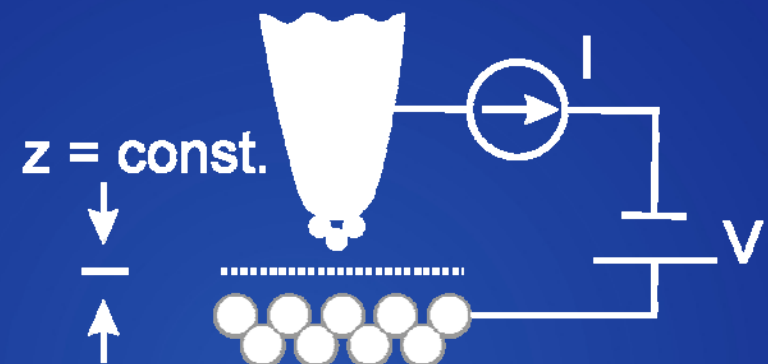
STM

constant current mode

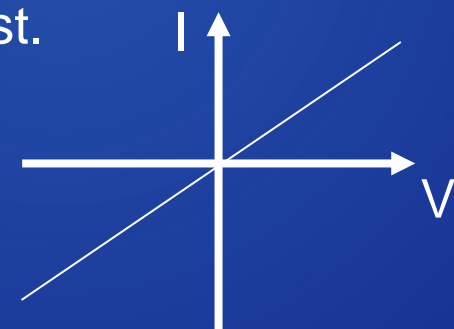


STS

constant height mode



x, y = const.

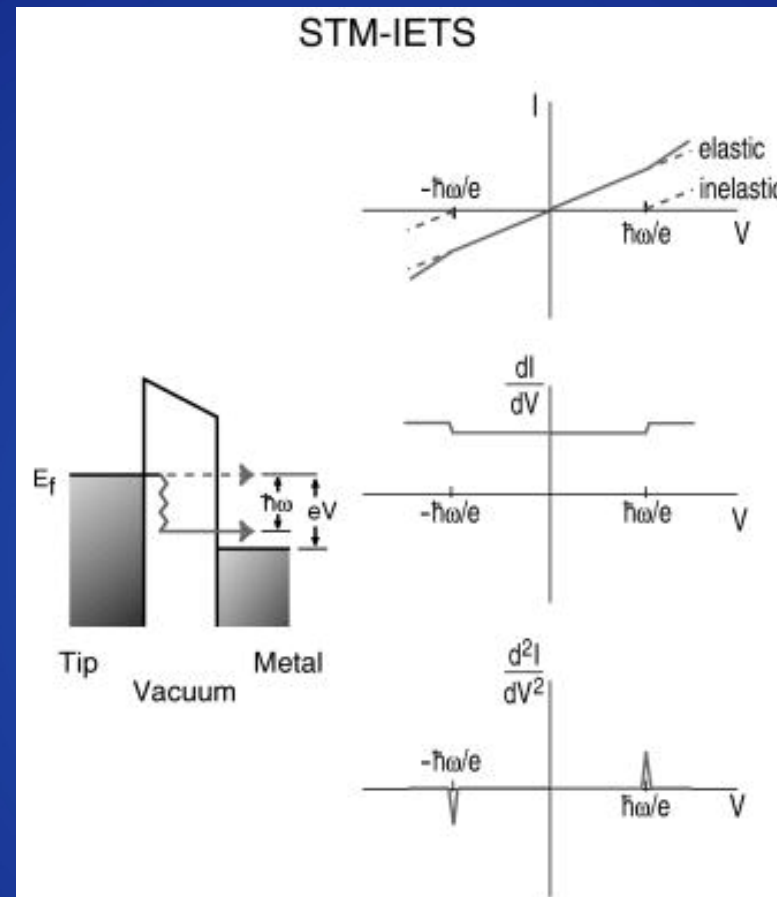


# Single molecule vibrations

## STM-IETS



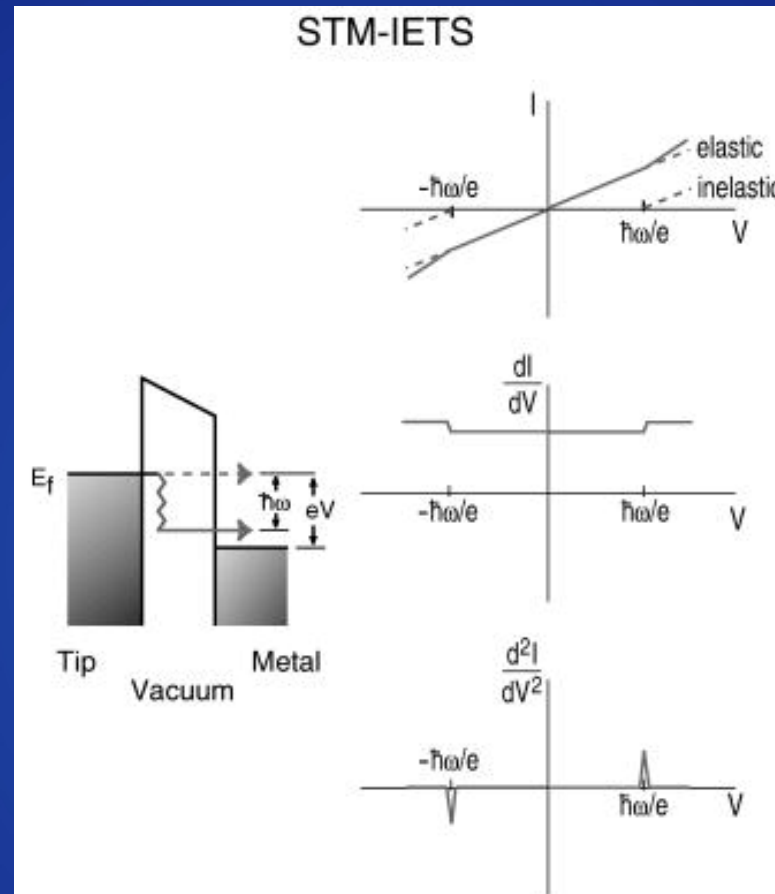
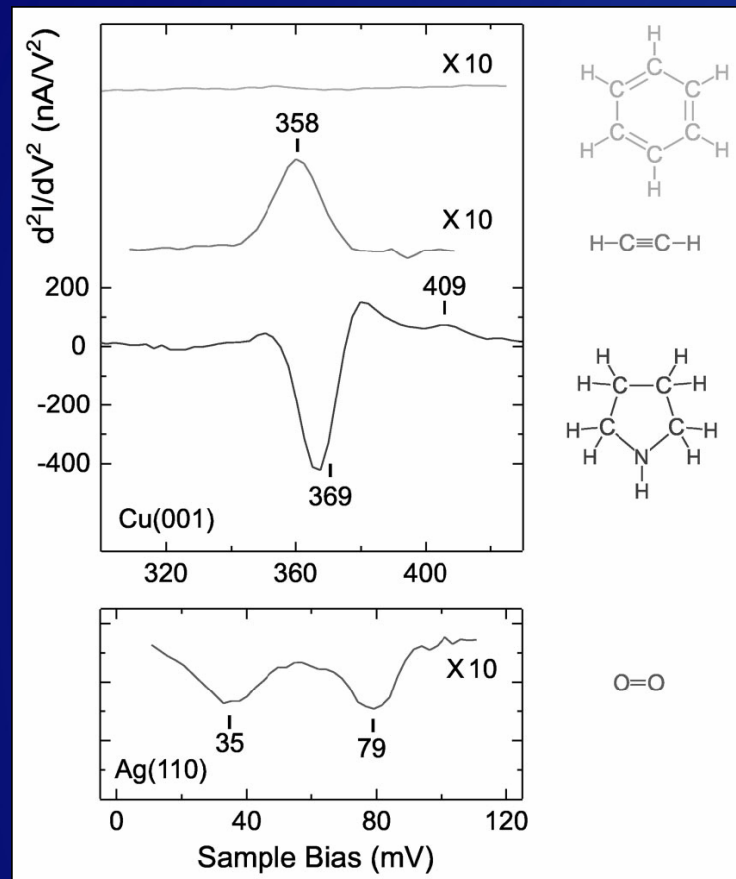
threshold spectroscopy



W. Ho J. Chem. Phys. 117, 11033 (2003).

# Single molecule vibrations

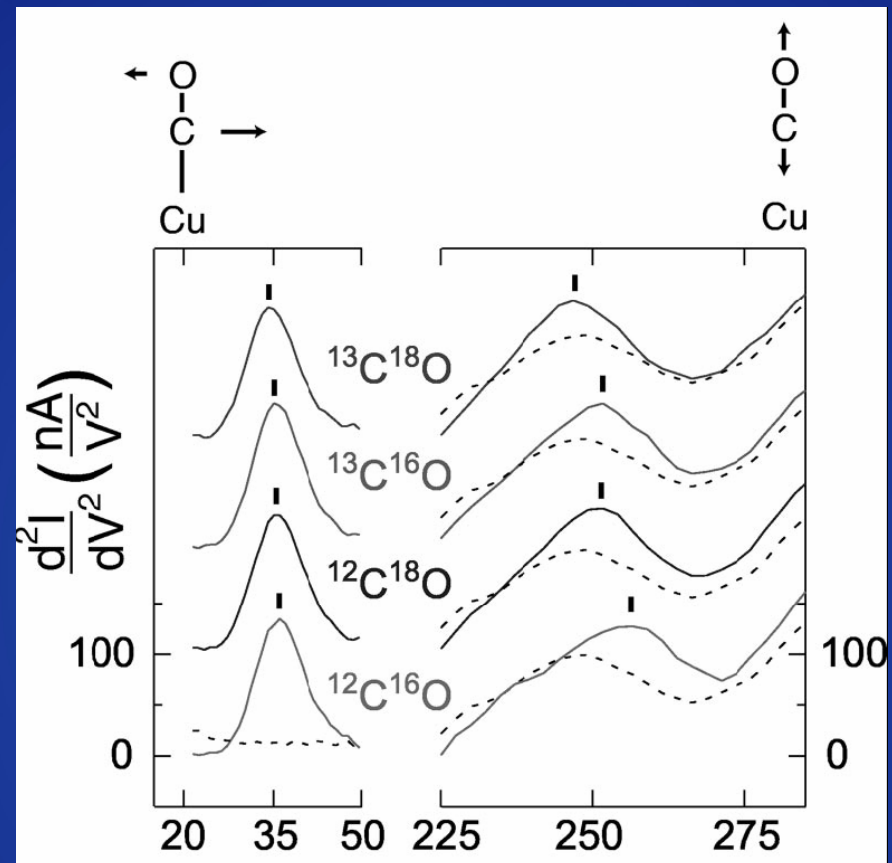
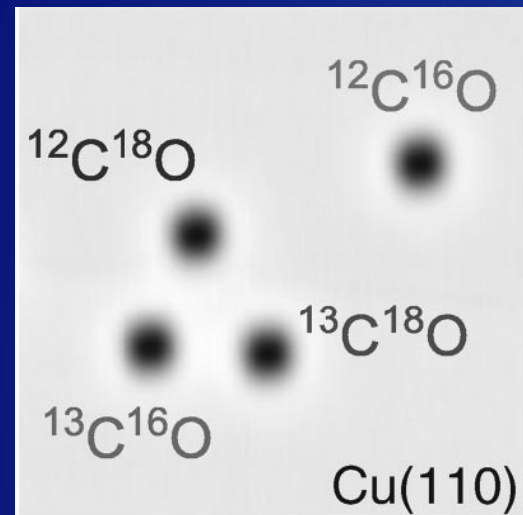
## STM-IETS



W. Ho J. Chem. Phys. 117, 11033 (2003).

# Single molecule vibrations

## STM-IETS



W. Ho J. Chem. Phys. 117, 11033 (2003).

# vibrational and rotational dynamics of adsorbates on surfaces

## Part II

Thomas Risse

Fritz-Haber-Institut der Max-Planck Gesellschaft,  
Abteilung Chemische Physik  
Faradayweg 4-6  
14195 Berlin

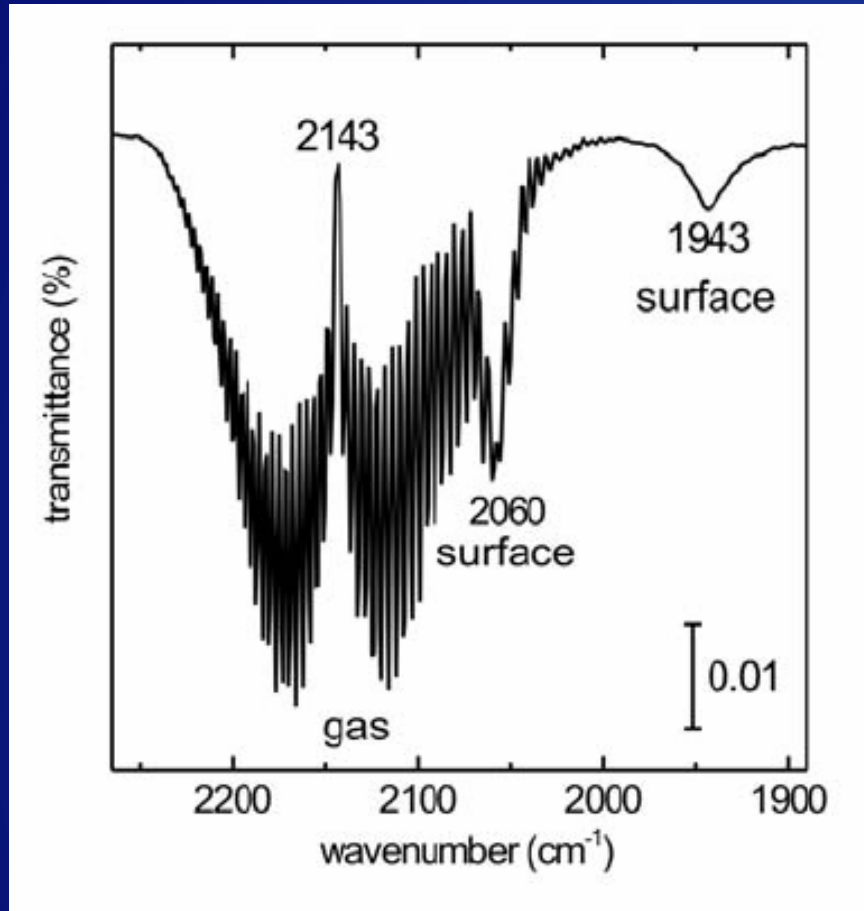
# Outline



- Introduction
  - electron energy loss spectroscopy (EELS)
  - infrared spectroscopy
  - helium atom scattering (HAS)
  - PMIRAS
  - SFG
  - Raman
  - scanning tunneling spectroscopy
  - electron spin resonance

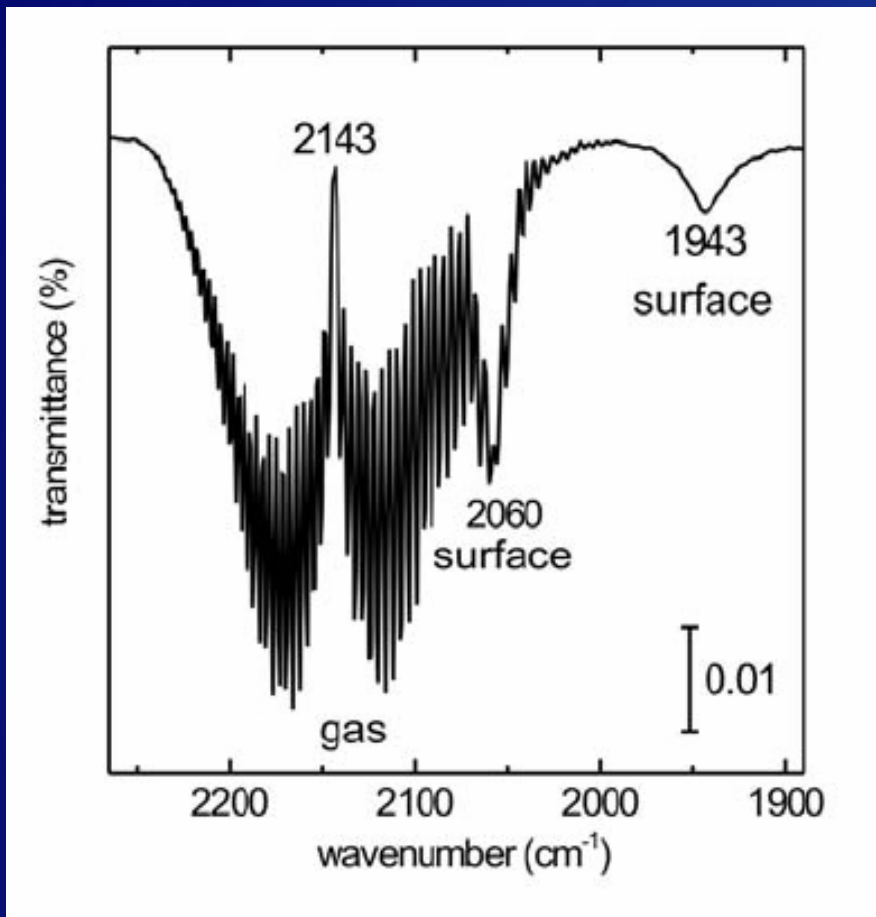
# IRAS

## Ambient pressures



50 mbar CO on  
Pd(111) at 300 K

M. Borasio, PhD-thesis, FU-Berlin (2006)



dynamic dipole



image  
dipole

metal

$$\mu_{\text{dyndip}} > 0$$

IR active

dynamic dipole



image  
dipole

metal

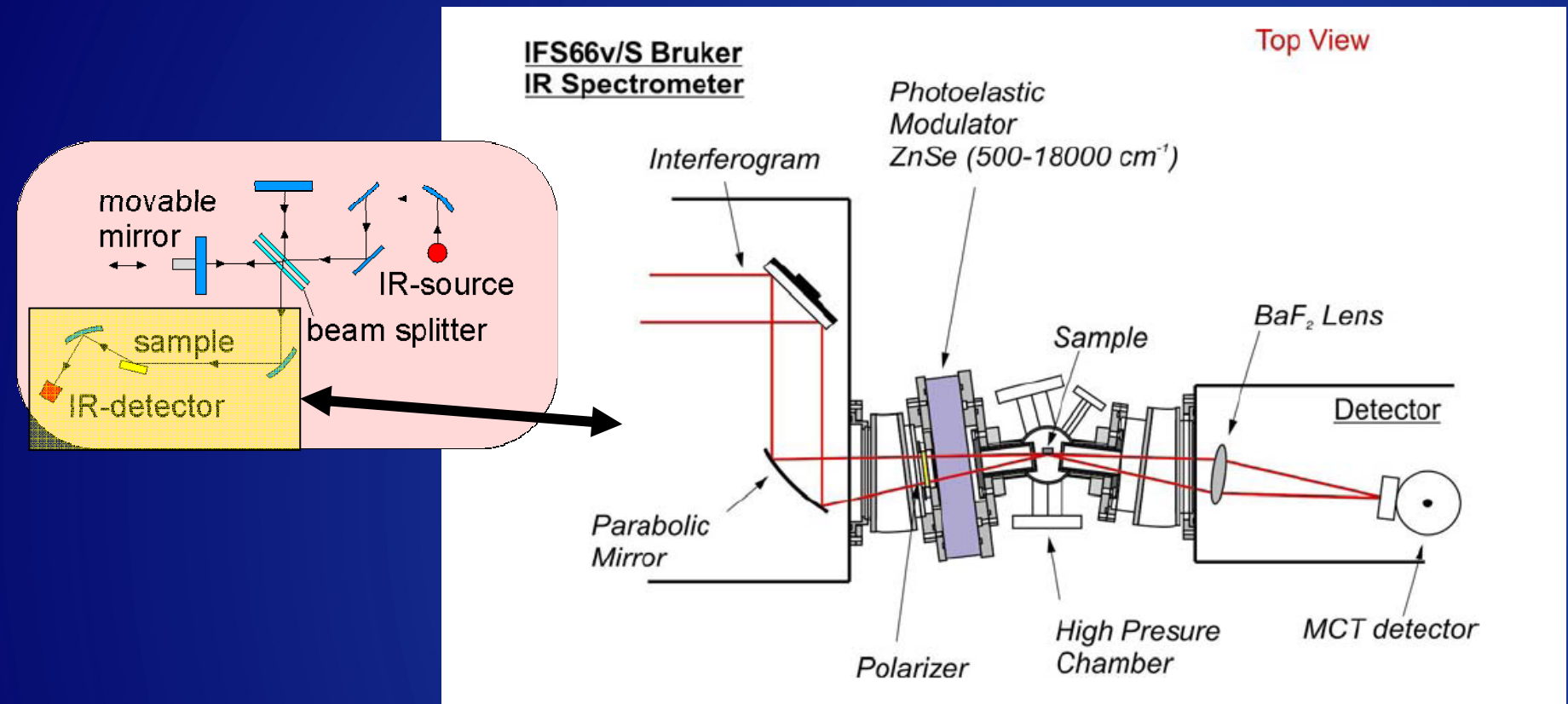
$$\mu_{\text{dyndip}} = 0$$

IR inactive

M. Borasio, PhD-thesis, FU-Berlin (2006)

# IRAS

## PMIRAS

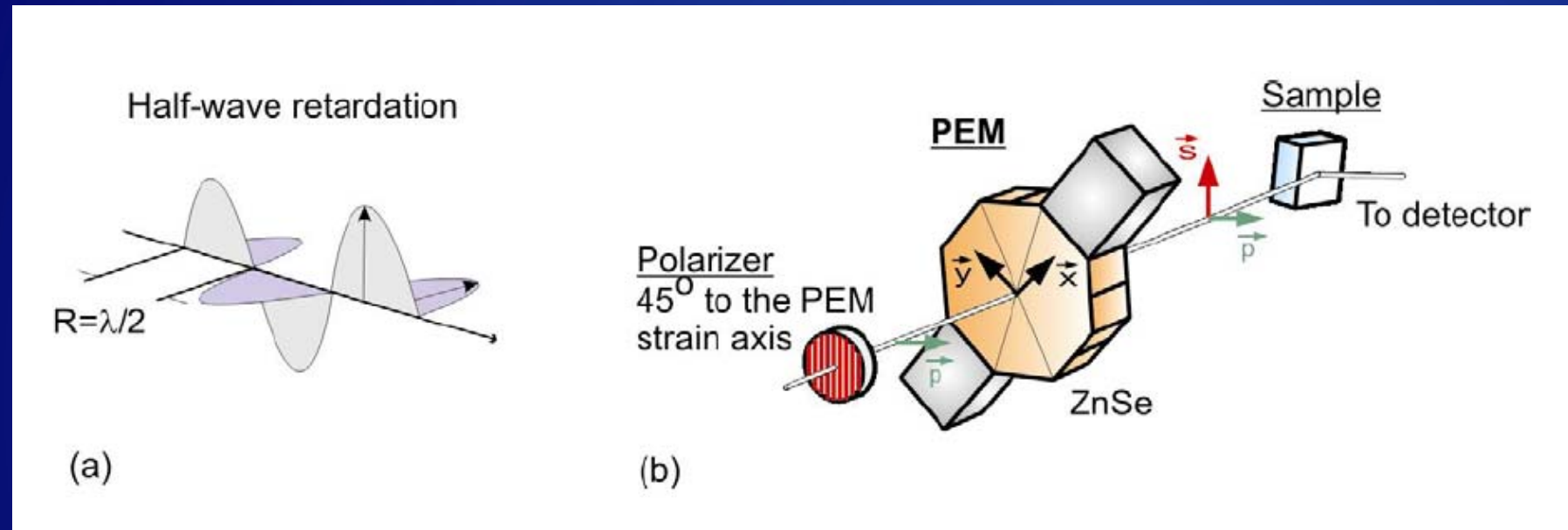


M. Borasio, PhD-thesis, FU-Berlin (2006)

# IRAS PMIRAS



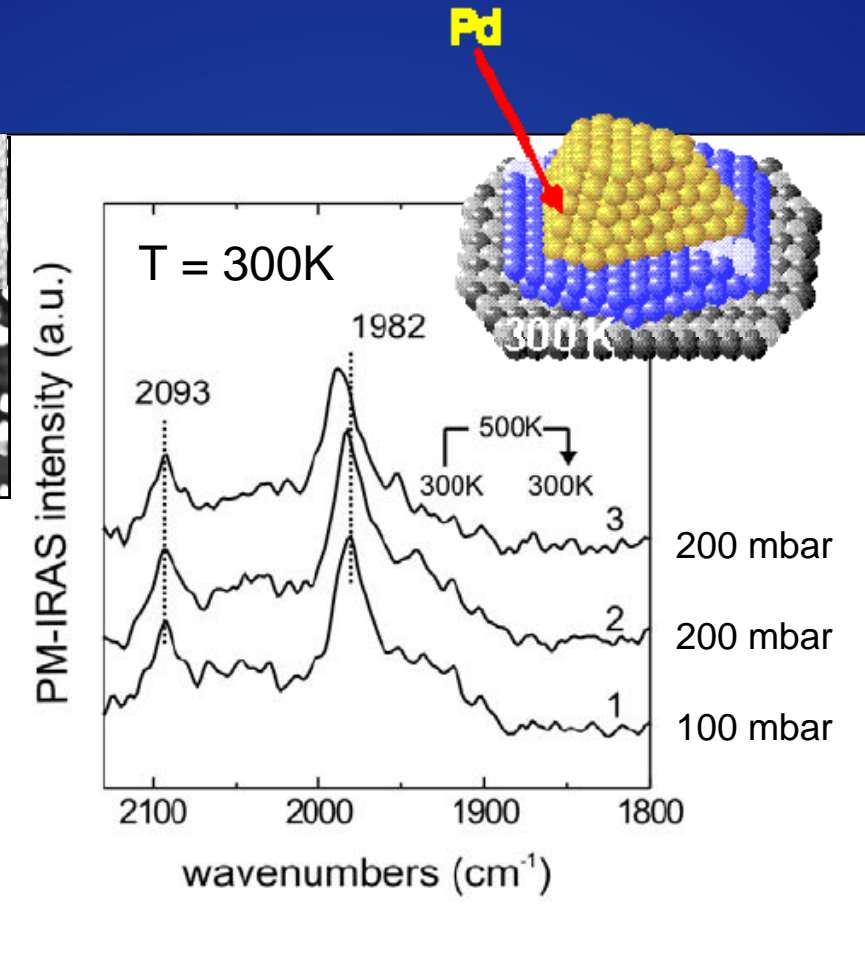
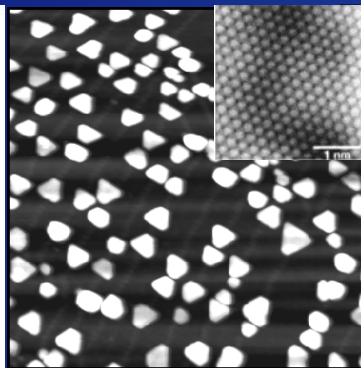
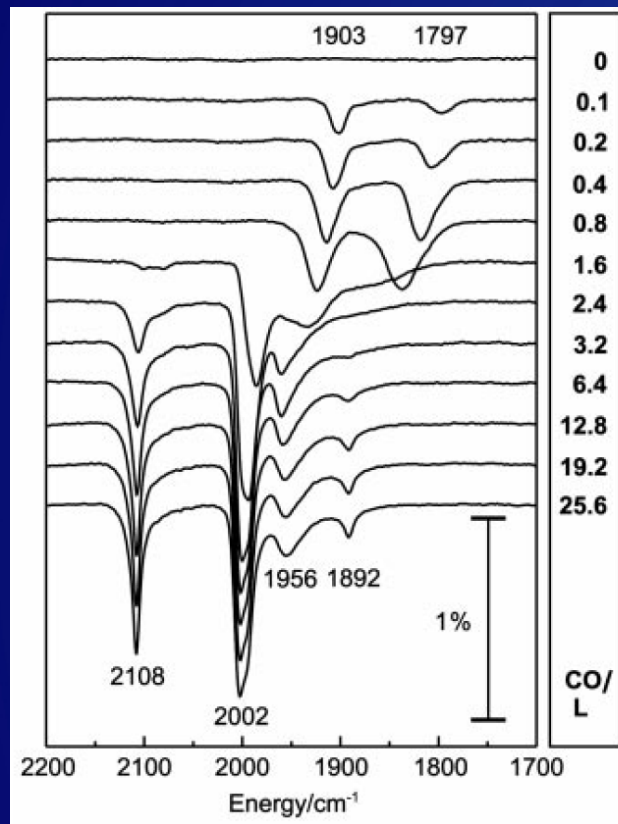
central part: photoacoustic modulator



M. Borasio, PhD-thesis, FU-Berlin (2006)

# PMIRAS

## CO/Pd/ $\text{Al}_2\text{O}_3$ /NiAl(110)

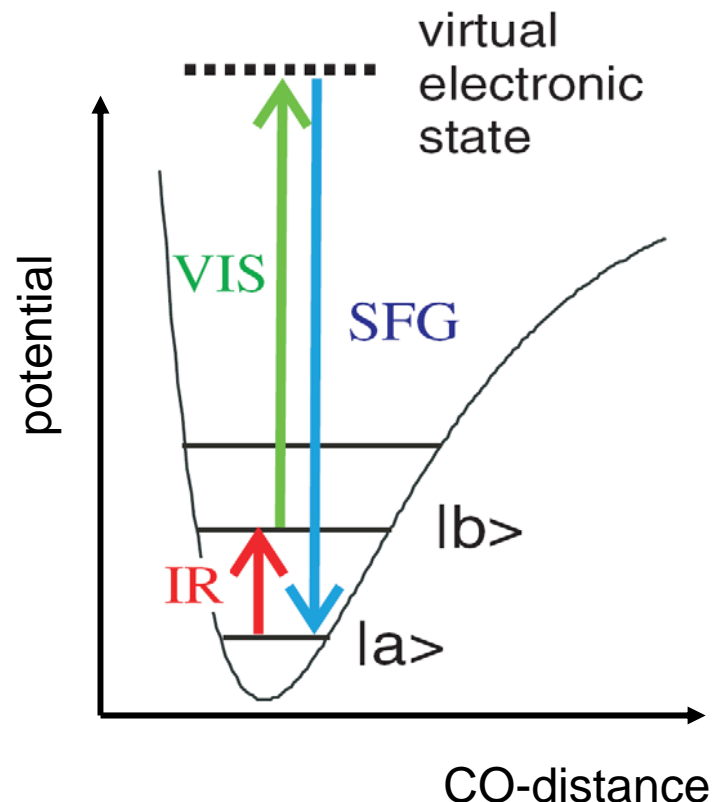


M. Frank and M. Bäumer, PCCP **2**, 3723 (2000).

M. Borasio, PhD-thesis, FU-Berlin (2006)

# Vibrational spectroscopy

## Sum frequency generation



Second order non optical  
linear process

$$\mathbf{P}_{\omega_{\text{SFG}}}^{(2)} = \chi_{\omega_{\text{SFG}}}^{(2)} \mathbf{E}_{\omega_{\text{IR}}} \mathbf{E}_{\omega_{\text{VIS}}}$$

**Surface sensitive method**

SFG is symmetry forbidden  
in isotropic (bulk) media  
(dipole approximation)

# Vibrational spectroscopy

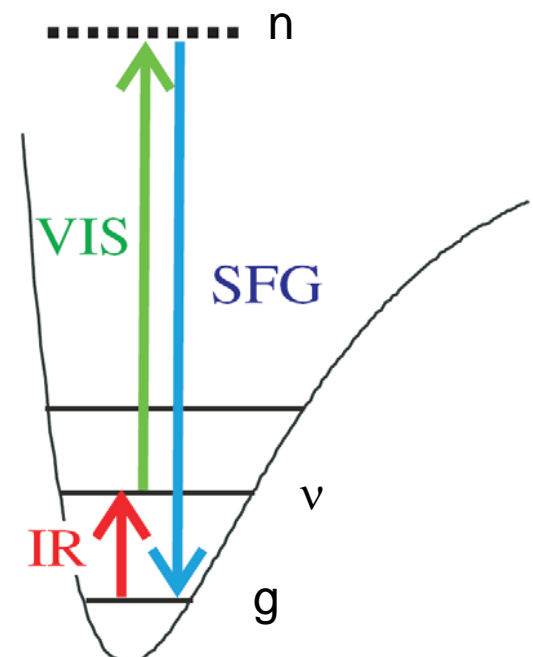
## Sum frequency generation



$$\mathbf{P}_{\omega_{SFG}}^{(2)} = \chi_{\omega_{SFG}}^{(2)} \mathbf{E}_{\omega_{IR}} \mathbf{E}_{\omega_{VIS}}$$

$$\begin{aligned} \chi_{ijk}^{(2)}(-\omega_{SF}; \omega_{vis}, \omega_{IR}) &= \frac{N}{2\varepsilon_0 \hbar^2} \sum_n \rho_{gg}^0 \\ &\times \left\{ \frac{\mu_{gn}^i \mu_{n\nu}^j \mu_{\nu g}^k}{[(\omega_{ng} - \omega_{SF}) - i\gamma_{ng}][( \omega_{\nu g} - \omega_{IR}) - i\gamma_{\nu g}]} \right. \\ &\left. + \frac{\mu_{gn}^j \mu_{n\nu}^i \mu_{\nu g}^k}{[(\omega_{n\nu} + \omega_{SF}) + i\gamma_{n\nu}][( \omega_{\nu g} - \omega_{IR}) - i\gamma_{\nu g}]} \right\} \end{aligned}$$

- molecules in the vibronic ground state g
- IR light in resonance with a vibration



R.W. Boyd *Nonlinear Optics*, Academic Press, New York, 1992.

# Vibrational spectroscopy

## Sum frequency generation



$$\mathbf{P}_{\omega_{SFG}}^{(2)} = \chi_{\omega_{SFG}}^{(2)} \mathbf{E}_{\omega_{IR}} \mathbf{E}_{\omega_{VIS}}$$

$$\begin{aligned} \chi_{ijk}^{(2)}(-\omega_{SF}; \omega_{vis}, \omega_{IR}) &= \frac{N\rho_{gg}^0}{2\varepsilon_0\hbar^2} \frac{\mu_{\nu g}^k}{[(\omega_{\nu g} - \omega_{IR}) - i\gamma_{\nu g}]} \\ &\quad \times \sum_n \left\{ \frac{\mu_{gn}^i \mu_{n\nu}^j}{[(\omega_{ng} - \omega_{SF}) - i\gamma_{ng}]} + \frac{\mu_{gn}^j \mu_{n\nu}^i}{[(\omega_{n\nu} + \omega_{SF}) + i\gamma_{n\nu}]} \right\}. \end{aligned}$$

$$\chi_{ijk}^{(2)}(-\omega_{SF}; \omega_{vis}, \omega_{IR}) = \frac{N\rho_{gg}^0}{2\varepsilon_0\hbar} \frac{\mu_{\nu g}^k}{[(\omega_{\nu g} - \omega_{IR}) - i\gamma_{\nu g}]} \alpha_{g\nu}^{ij}(-\omega_{SF}; \omega_{vis})$$

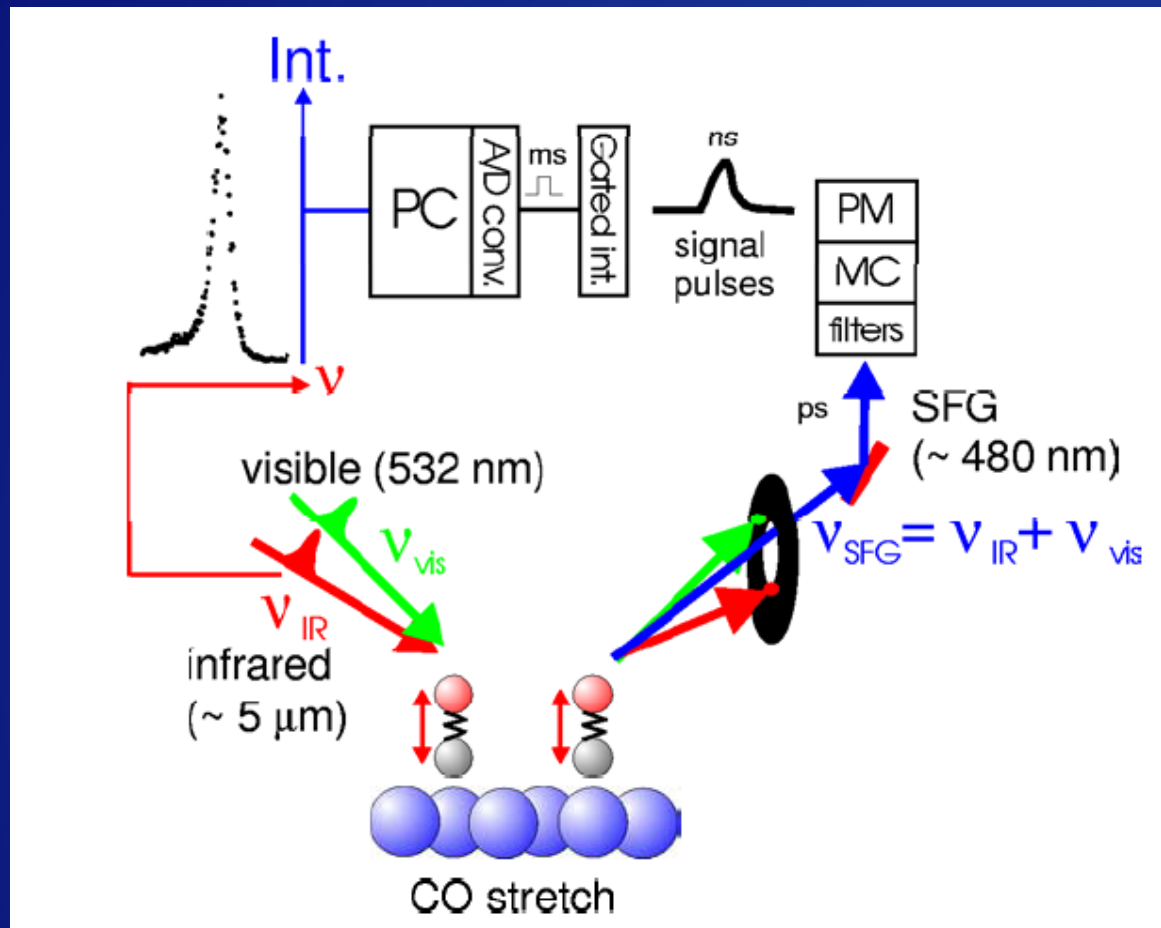
$$\alpha_{g\nu}^{ij}(-\omega_{SF}; \omega_{vis}) = \frac{1}{\hbar} \sum_n \left\{ \frac{\mu_{gn}^i \mu_{n\nu}^j}{(\omega_{ng} - \omega_{SF})} + \frac{\mu_{gn}^j \mu_{n\nu}^i}{(\omega_{ng} + \omega_{vis})} \right\}.$$

$a_{gv}$ : 1. order hyperpolarizability (anti Stokes Raman intensity)

R.W. Boyd *Nonlinear Optics*, Academic Press, New York, 1992.

# Vibrational spectroscopy

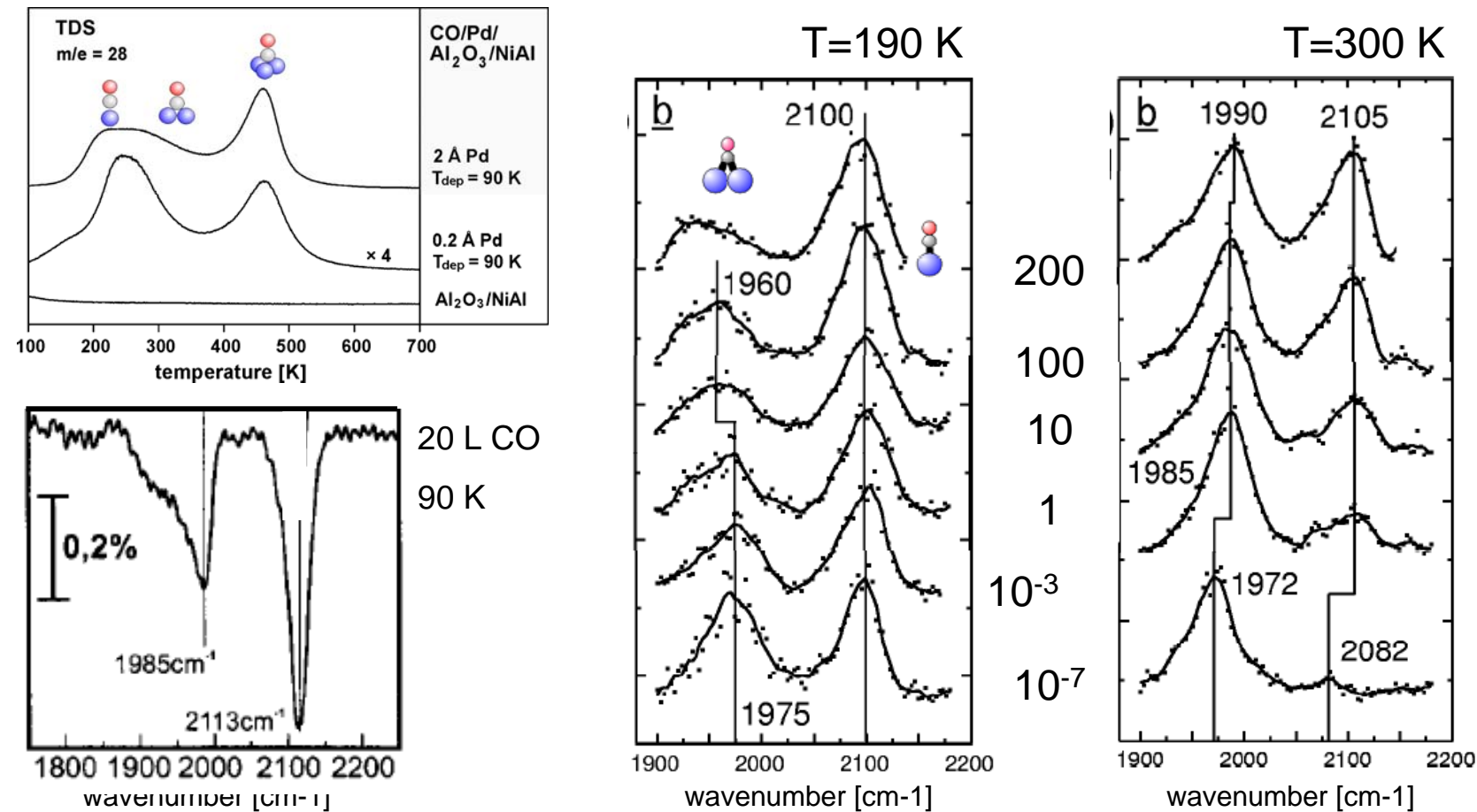
## Sum frequency generation



H. Unterhalt, PhD-thesis, FU-Berlin (2002)

# SFG

CO/Pd/ $\text{Al}_2\text{O}_3$ /NiAl(110)



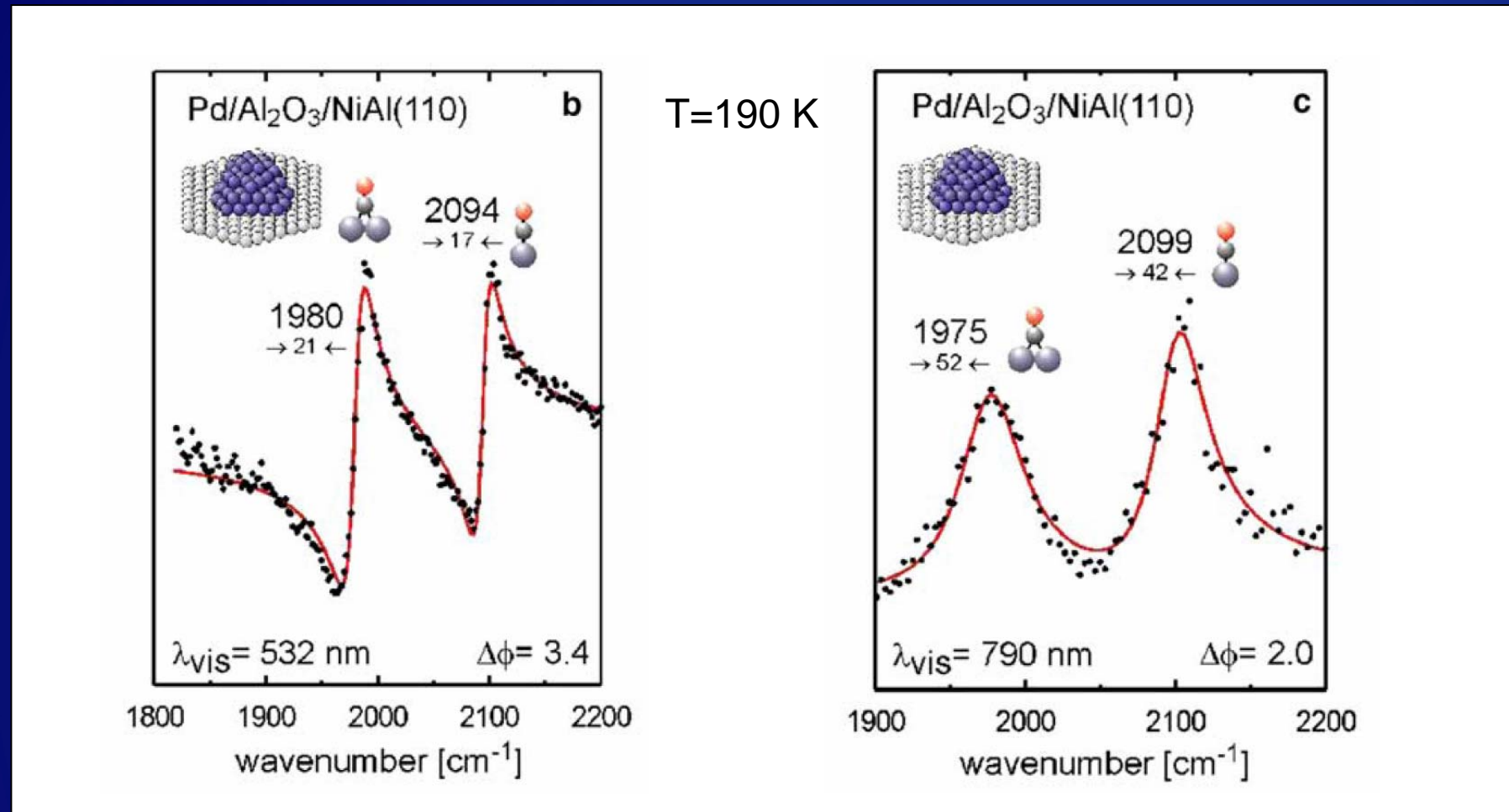
K. Wolter et al. Surf. Sci. **399**, 190 (1998).

H. Unterhalt et al. J. Phys. Chem. B **106**, 356 (2002).

M. Bäumer et al. Ber. Bunsenges. Phys. Chem. **99**, 1381 (1995).

# SFG

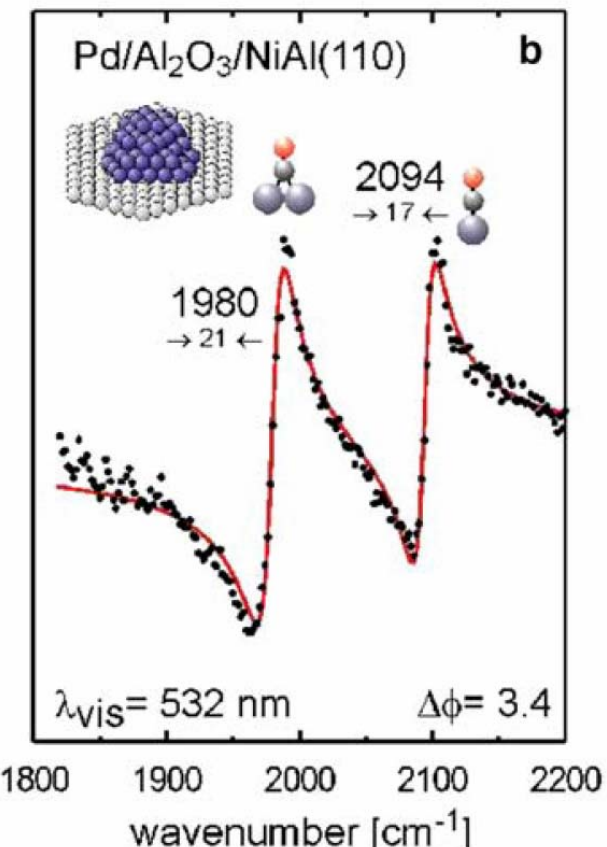
CO/Pd/Al<sub>2</sub>O<sub>3</sub>/NiAl(110)



M. Morkel et al. Surf. Sci. **586**, 146 (2005).

# SFG

CO/Pd/Al<sub>2</sub>O<sub>3</sub>/NiAl(110)



$$\chi_s^{(2)} = \chi_{\text{NR}}^{(2)} + \chi_{\text{R}}^{(2)} = A_{\text{NR}} \cdot e^{i\phi_0} + \sum_q \frac{A_q \cdot e^{i\phi_q}}{(\omega_q - \omega_{\text{IR}}) - i\Gamma_q}$$

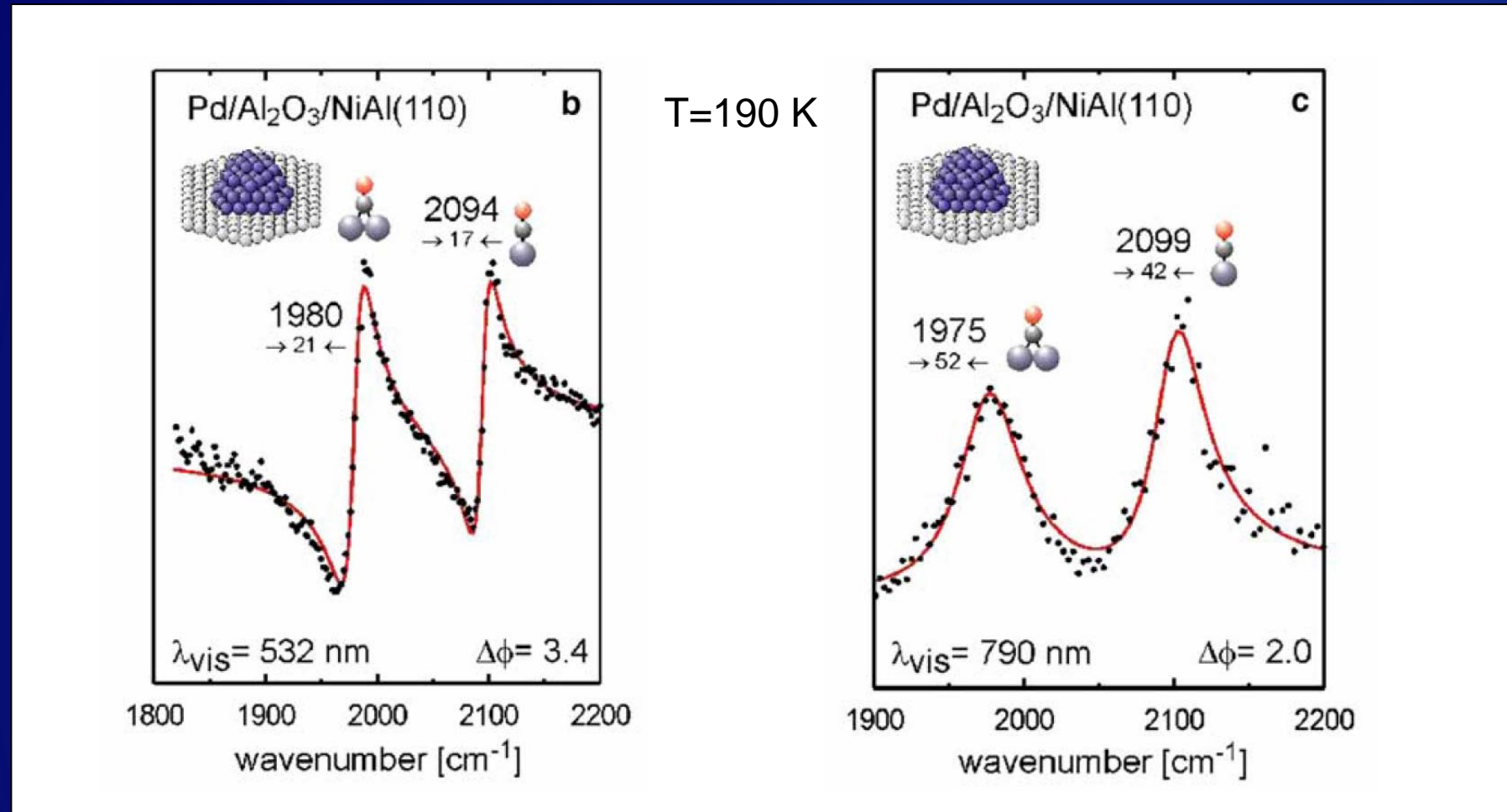
In case the phase of the non resonant background is constant  $I_{\text{SFG}}$  does only depend on the phase difference  $\Delta\phi_{0q}$ :

$$I_{\text{SFG}} \propto \left| A_{\text{NR}} + \sum_q \frac{A_q \cdot e^{i\Delta\phi_{0q}}}{(\omega_q - \omega_{\text{IR}}) - i\Gamma_q} \right|^2 \cdot I_{\text{vis}} \cdot I_{\text{IR}}$$

M. Morkel et al. Surf. Sci. **586**, 146 (2005).

# SFG

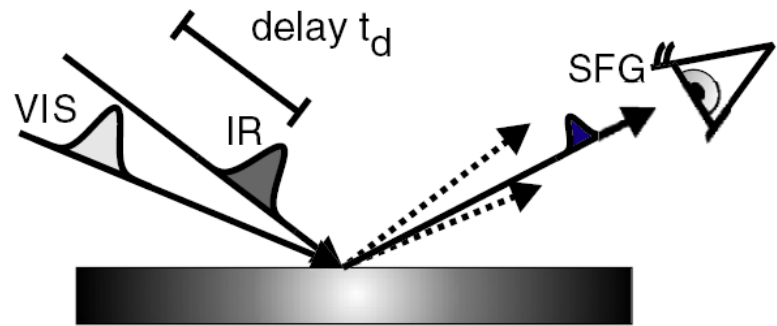
CO/Pd/Al<sub>2</sub>O<sub>3</sub>/NiAl(110)



M. Morkel et al. Surf. Sci. **586**, 146 (2005).

# SFG

## Time resolved measurements

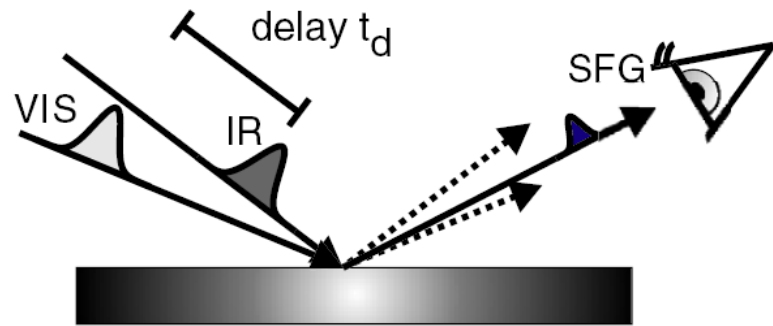


**What happens if both pulses  
are fs in duration?**

M. Bonn *et al.* J. Phys.: Condens. Mat. **17**, S201 (2005).

# SFG

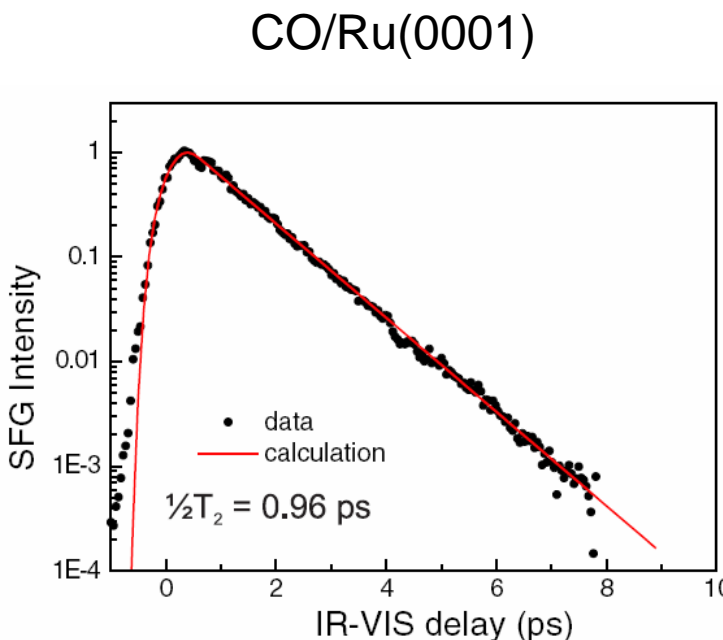
## Time resolved measurements



**What happens if both pulses  
are fs in duration?**

⇒ Loss of spectral resolution!

For 200 fs spectral width:  $165 \text{ cm}^{-1}$



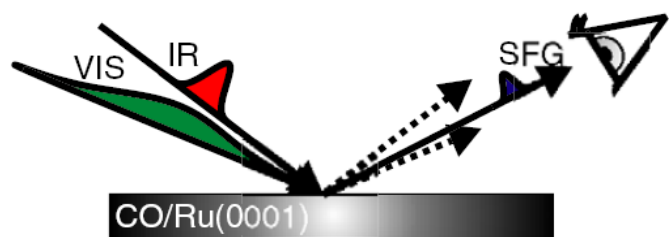
M. Bonn *et al.* J. Phys.: Condens. Mat. **17**, S201 (2005).

# SFG

## Time resolved measurements

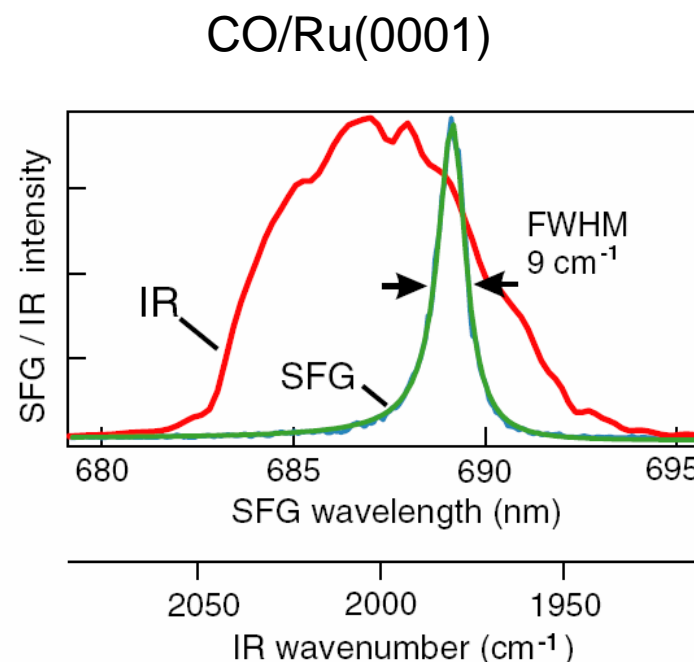


How to measure a frequency domain spectrum?



fs IR pulse: broad spectral width

long VIS pulse (ps; pulse shaper)  
(narrow spectral width appox.  $7 \text{ cm}^{-1}$ )



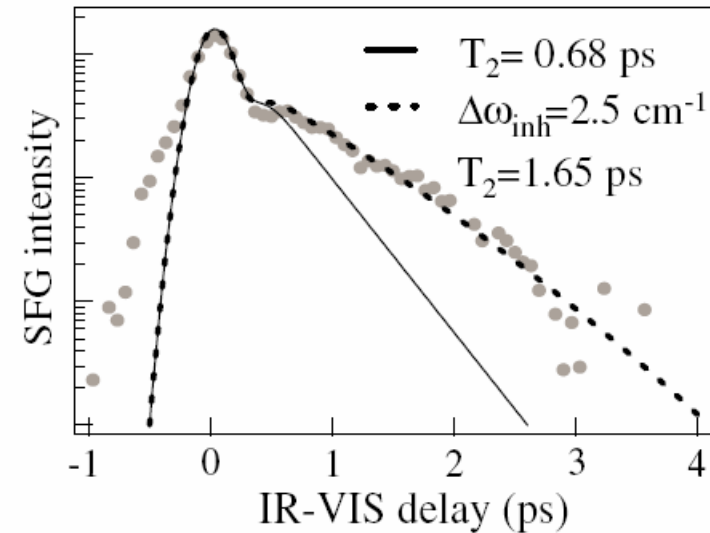
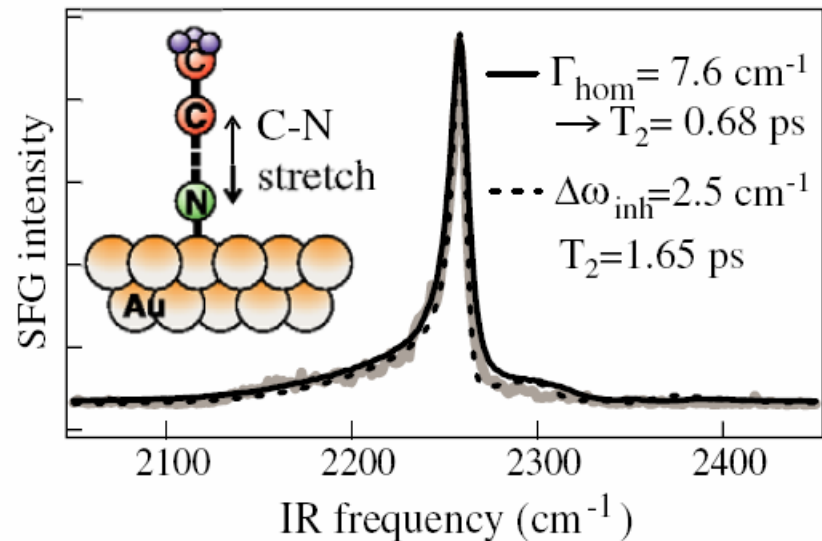
M. Bonn *et al.* J. Phys.: Condens. Mat. **17**, S201 (2005).

# SFG

## Time resolved measurements



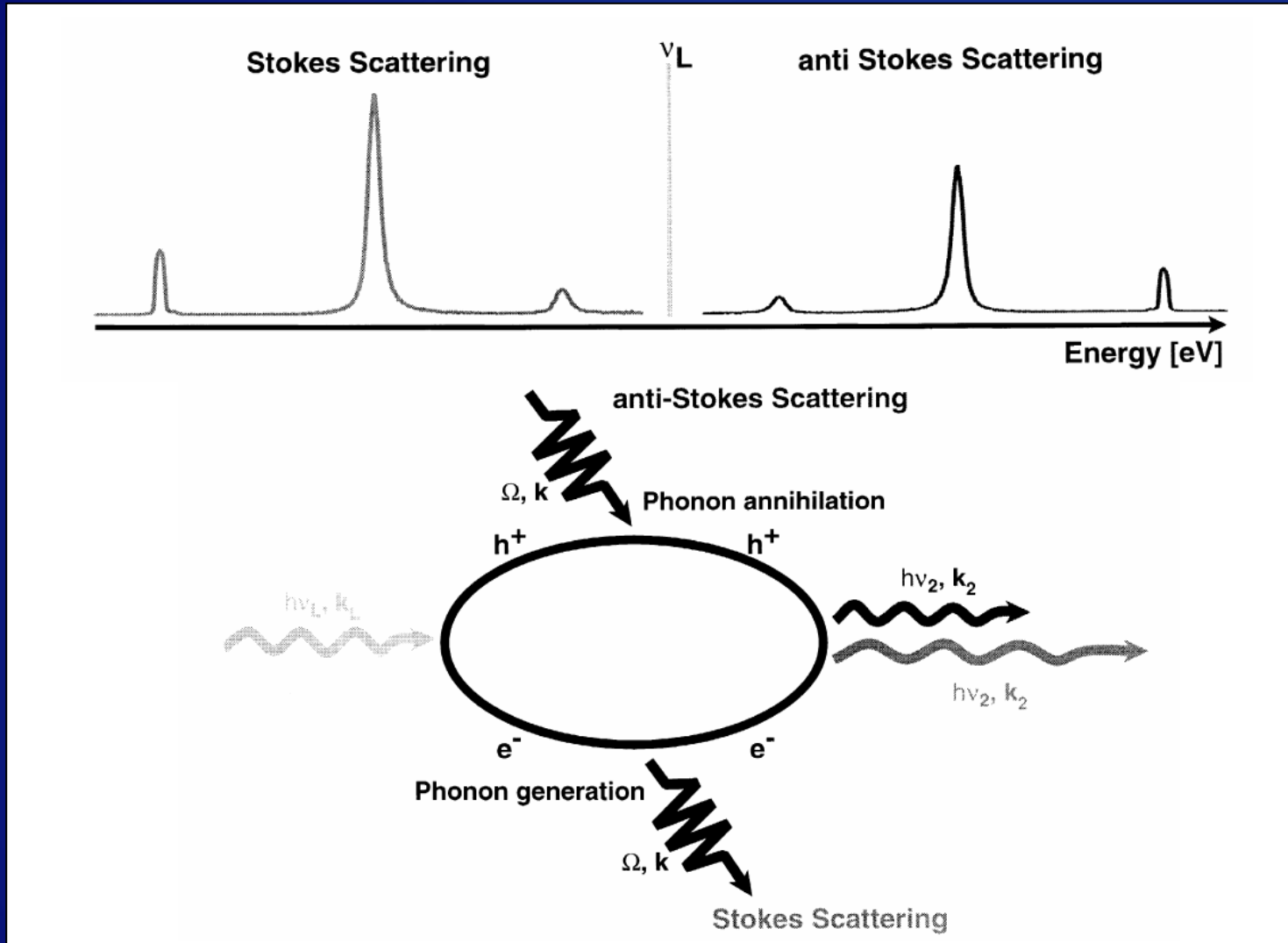
What method is better suited?



M. Bonn *et al.* J. Phys.: Condens. Mat. **17**, S201 (2005).

# Raman spectroscopy

## Basic aspects



# Raman spectroscopy

## Basic aspects



### Pro

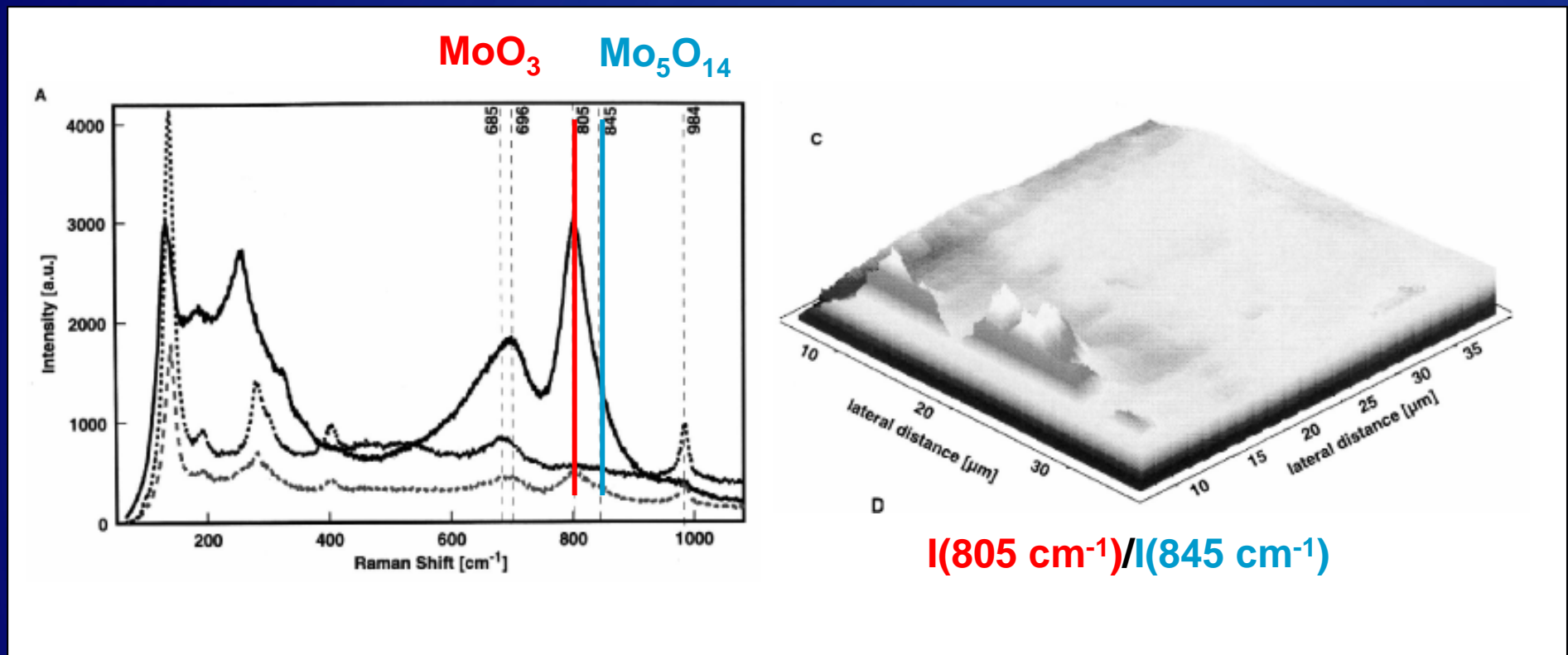
- wide spectral range 50 – 5000 cm<sup>-1</sup>
- negligible gas phase scattering
- quartz is a very weak Raman scatterer; cells/windows can be made out of quartz
- can be done also at high temperatures (e.g. 1000 °C) because of detection in the optical regime; no perturbation by blackbody radiation
- catalysis: typical oxide supports (silica, alumina) are weak scatterers

### Con

- low intrinsic cross section
- $(d\sigma/d\Omega)_{NRS} \approx 10^{-28} \text{ cm}^2 \text{ sr}^{-1}$  ( $I \propto v^4$ )
- susceptible to fluorescence (can be up to 10<sup>6</sup> higher; especially coke has a high fluorescence yield)
- heating due to intense lasers
- quantification of Raman intensities is very difficult (even with reference samples, because of possible electronic effects of the substrate)

# Raman spectroscopy

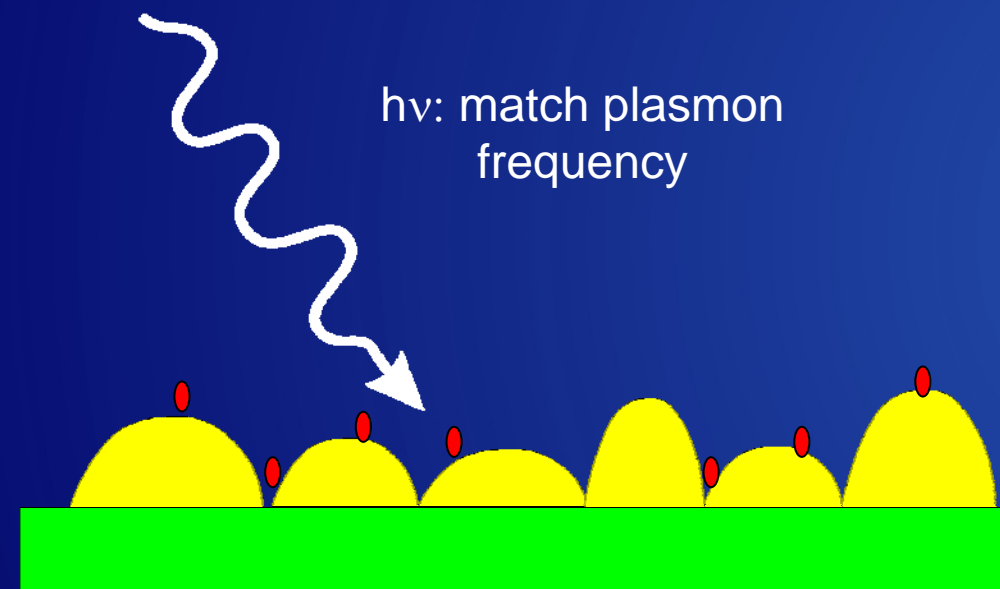
## Material characterization



G. Mestl, J. Mol. Catal. A 158, 45 (2000).

# Raman spectroscopy

## Surface enhancement, SERS



Works for rough surfaces of coinage metals (Cu, Ag, Au)

Idea: excitation of local surface plasmons

Field enhancement by plasmons in particular in between particles (gap states)

Enhancement: average effect approx  $10^7$  (gap mode may influence only a small number of molecules => local effects even much higher)

# Raman spectroscopy

## Surface enhancement, TERS



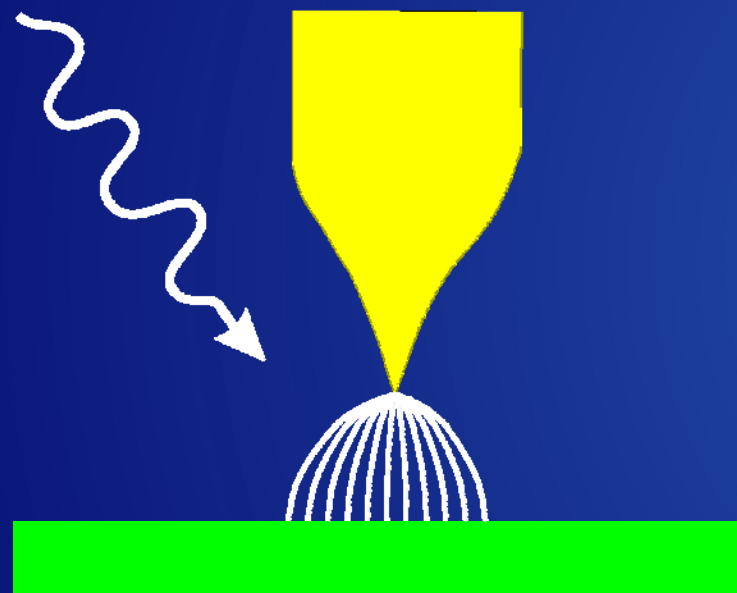
**Idea: using the enhancement due to gap modes and  
combine an STM with a Raman spectrometer**  
**(Tip Enhanced Raman Spectroscopy)**

# Raman spectroscopy

## Surface enhancement, TERS



Idea: using the enhancement due to gap modes and  
combine an STM with a Raman spectrometer  
(Tip Enhanced Raman Spectroscopy)



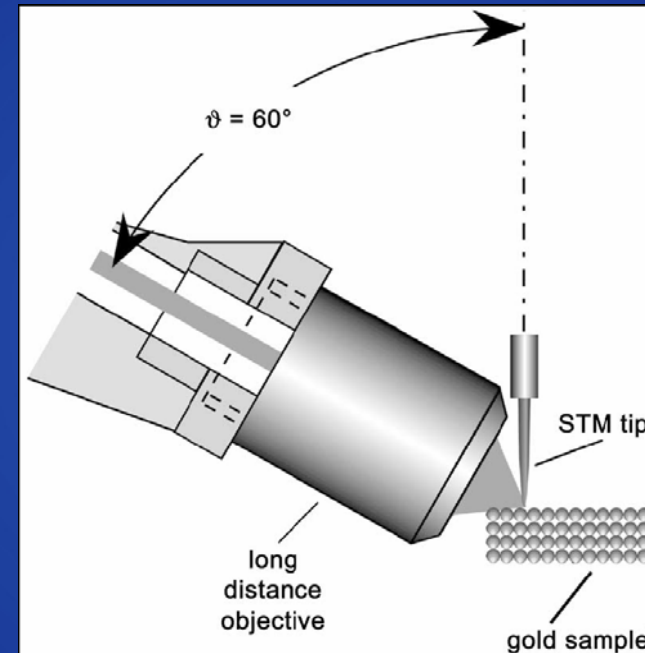
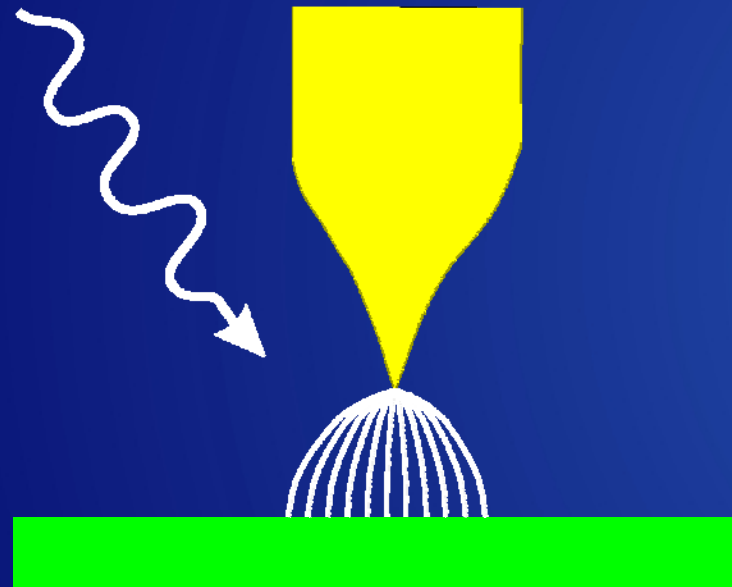
B. Pettinger et al.: Single Molec. 3, 285 (2002).

# Raman spectroscopy

## Surface enhancement, TERS



Idea: using the enhancement due to gap modes and  
combine an STM with a Raman spectrometer  
(Tip Enhanced Raman Spectroscopy)



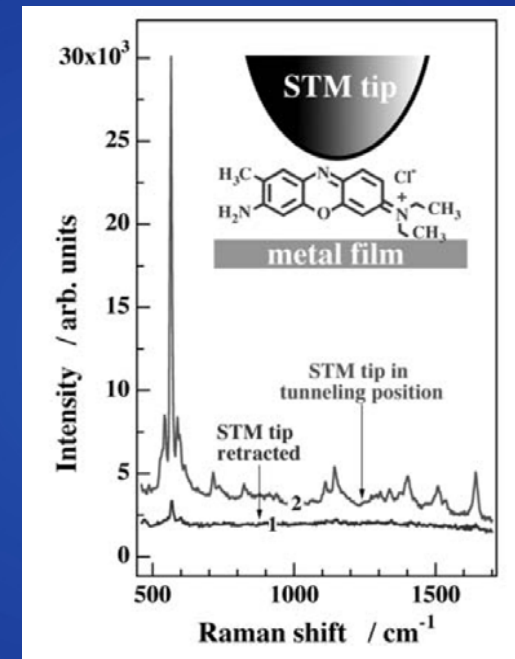
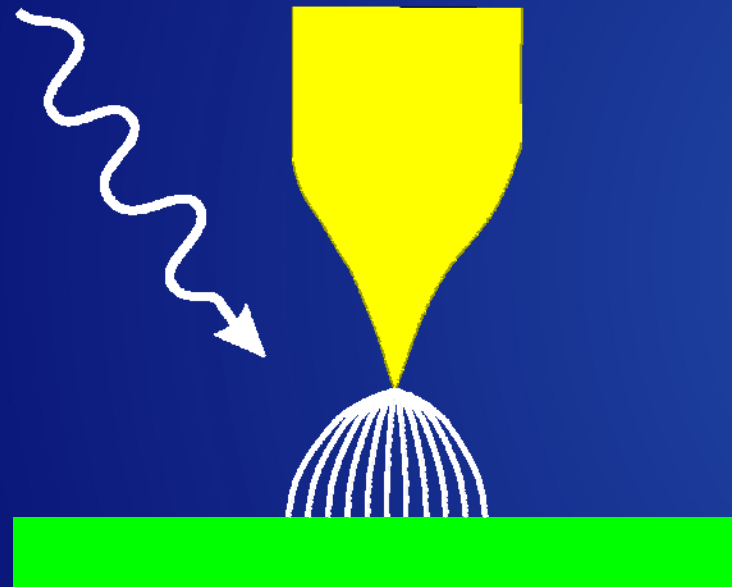
B. Pettinger et al. Phys. Rev. Lett. **92**, 096101 (2004).

# Raman spectroscopy

## Surface enhancement, TERS



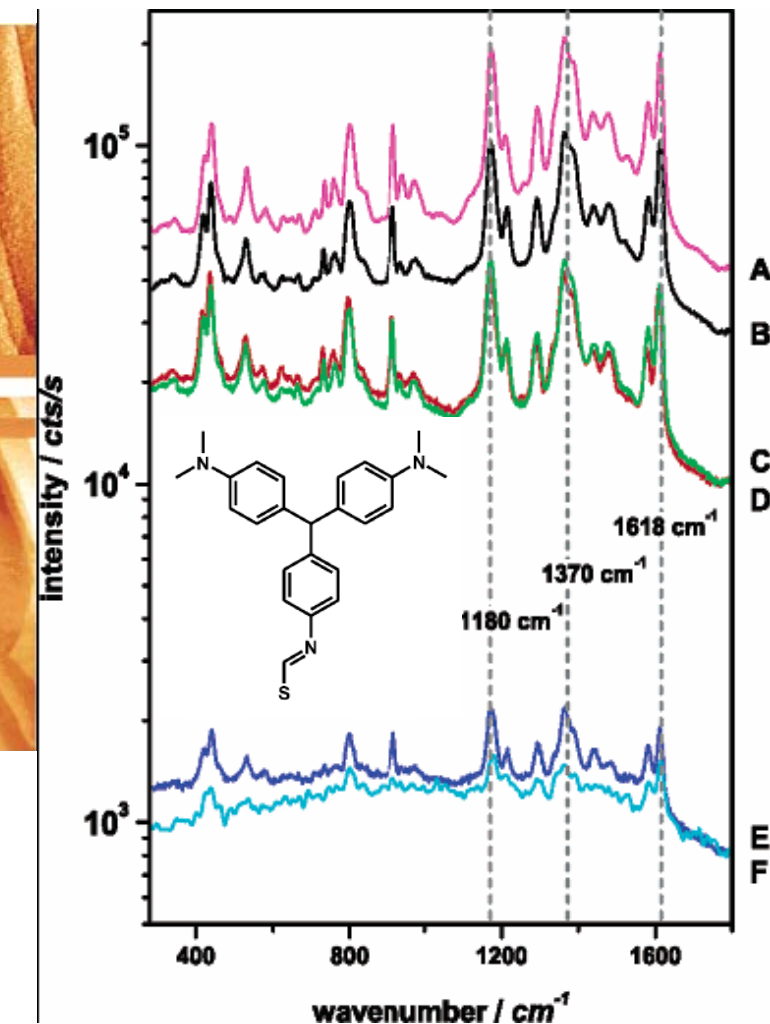
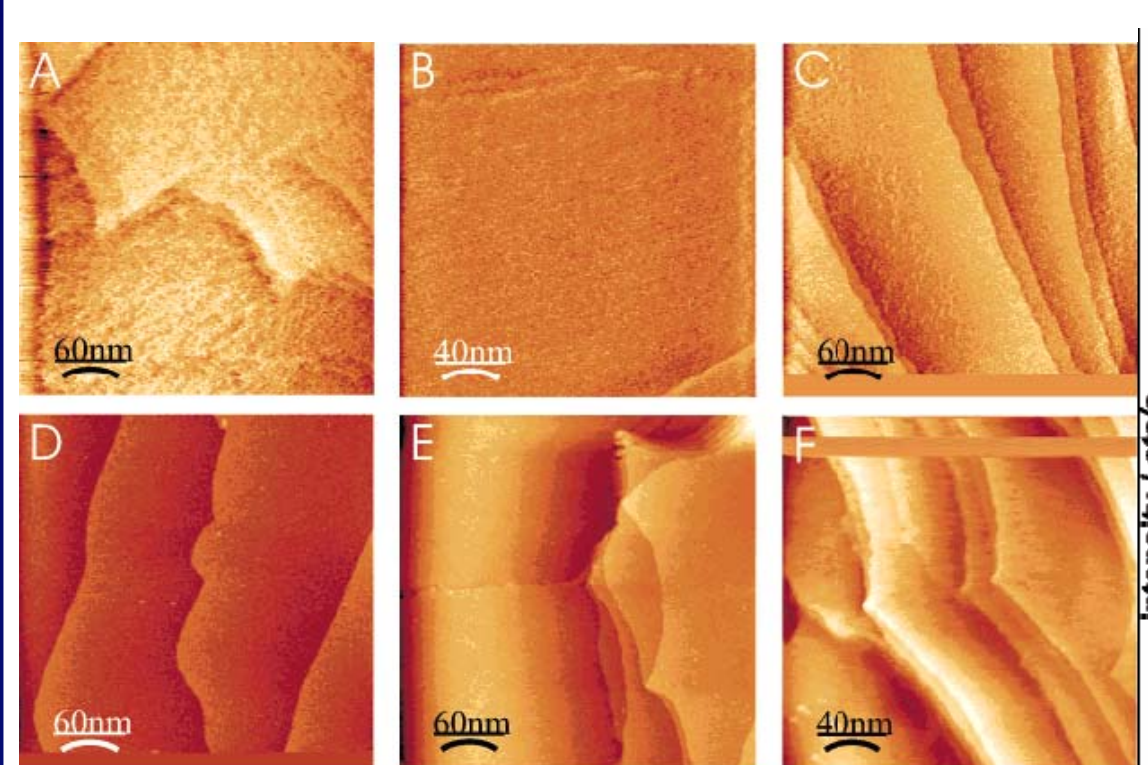
Idea: using the enhancement due to gap modes and  
combine an STM with a Raman spectrometer  
(Tip Enhanced Raman Spectroscopy)



B. Pettinger et al.: Single Molec. 3, 285 (2002).

# Raman spectroscopy

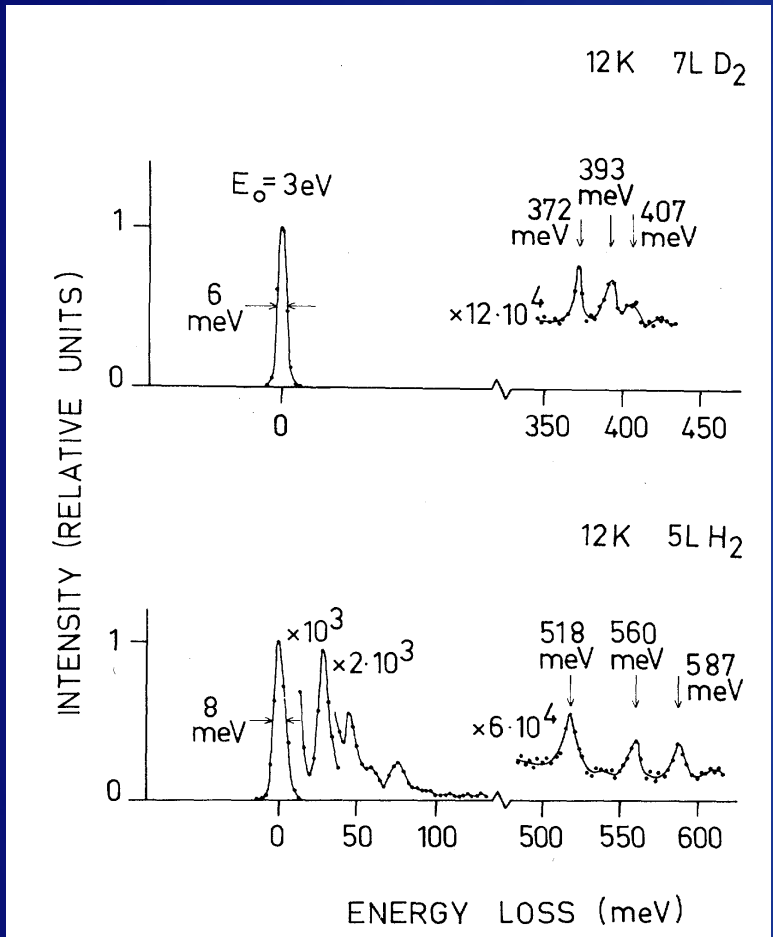
## Surface enhancement, TERS



K. F. Domke et al. J. Am. Chem. Soc. 128, 14721 (2006).

# EELS

## H<sub>2</sub> on Cu(100)



- D<sub>2</sub>-streich at 372 meV
- 21-23 meV is close to gas phase rotation form J(0->2)
- H<sub>2</sub>-streich at 518 meV
- 42 meV is close to gas phase rotation form J(0->2)
- 69 meV is close to gas phase rotation form J(1->3)

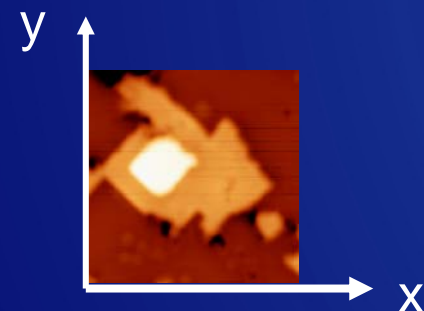
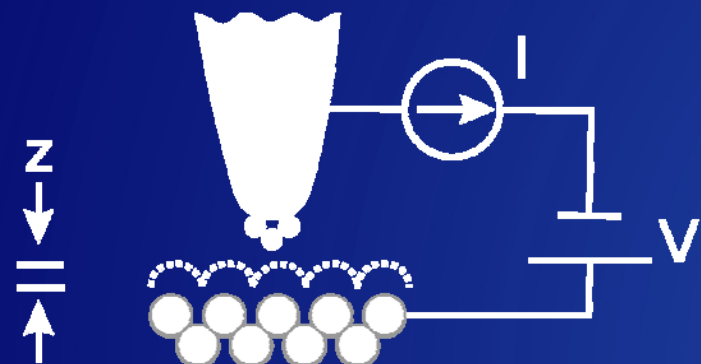
S. Andersson, J. Harris, Phys. Rev. Lett. 48, 545 (1982).

# STM/STS modes of operation



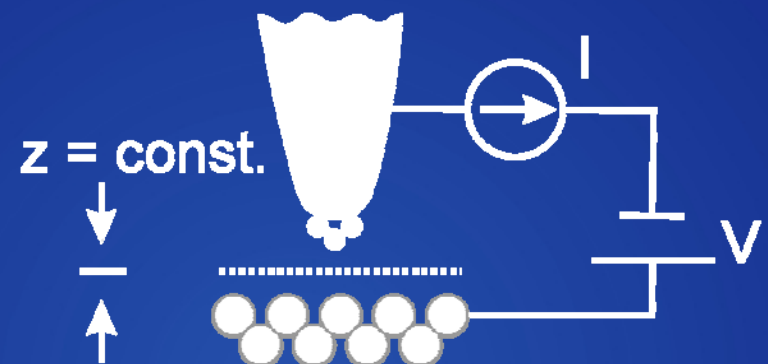
STM

constant current mode

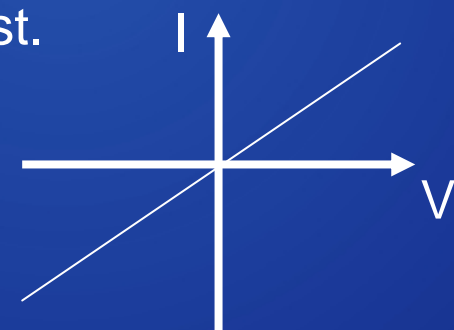


STS

constant height mode



x, y = const.

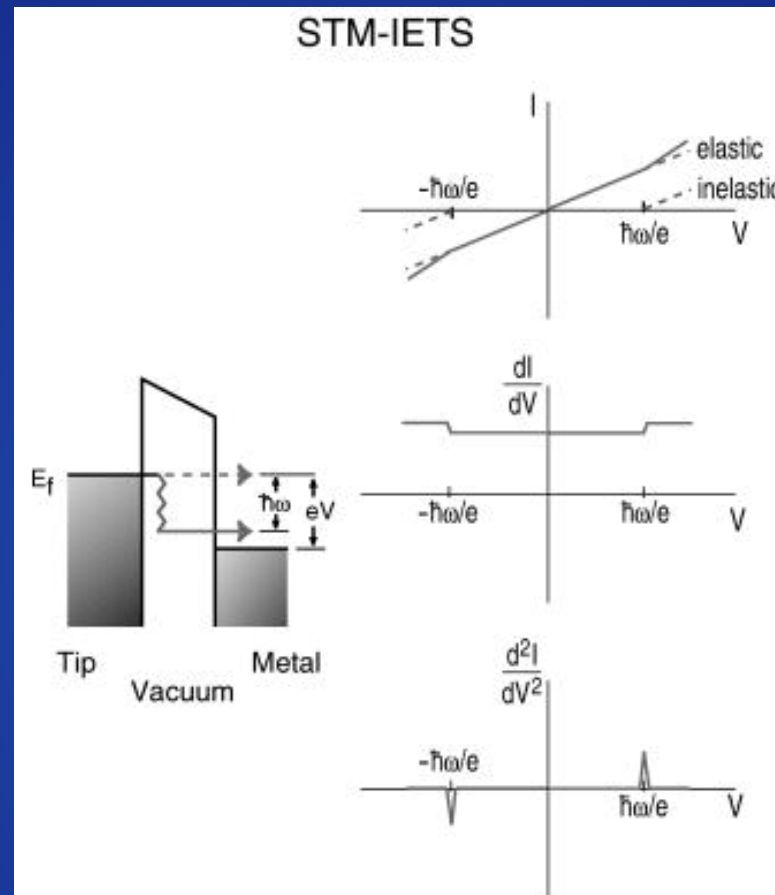


# STS

## inelastic tunneling processes



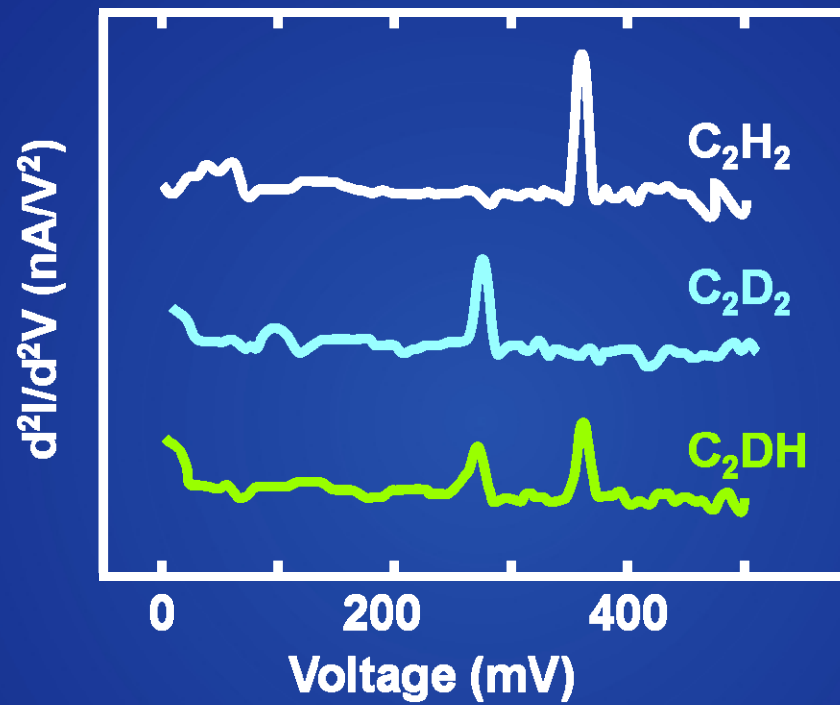
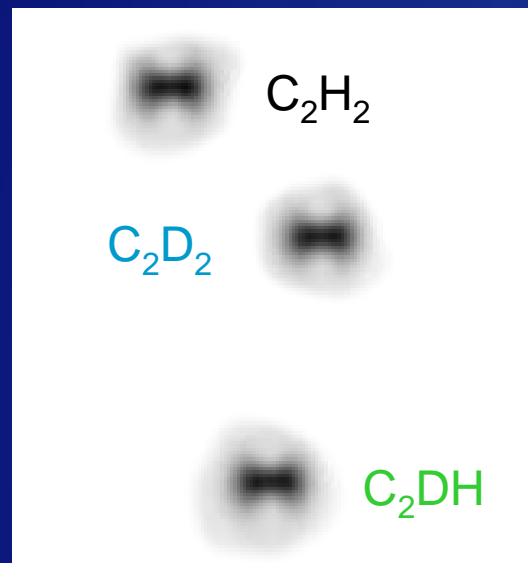
threshold spectroscopy



W. Ho J. Chem. Phys. 117, 11033 (2003).

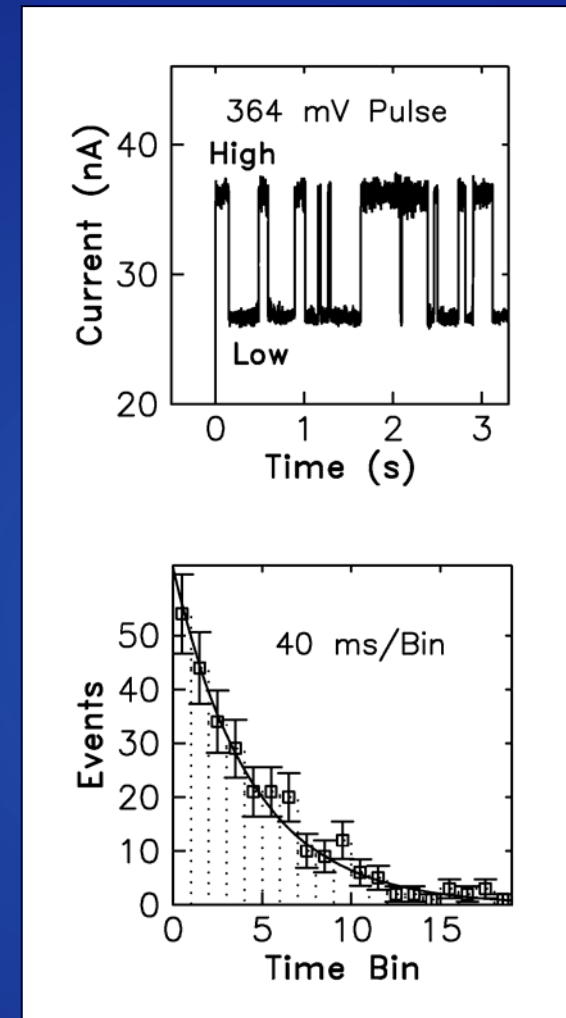
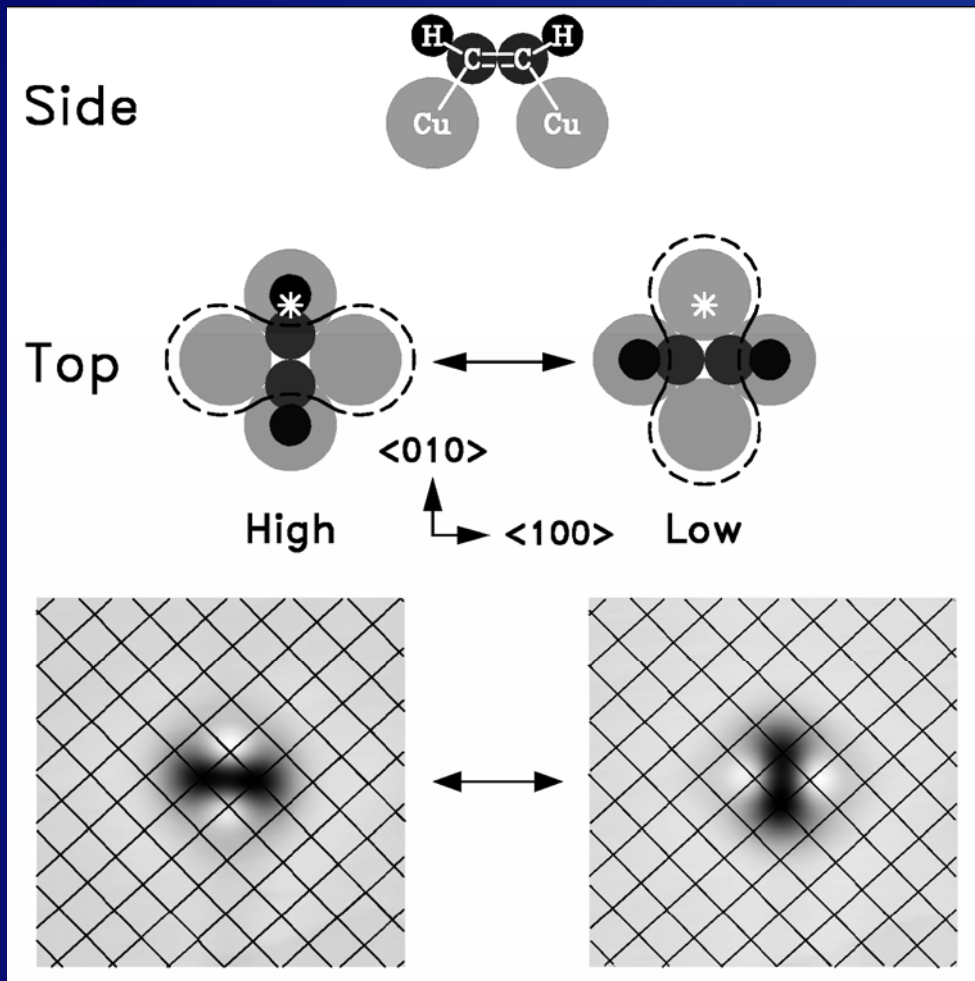
# STS

## acetylene/Cu(001)



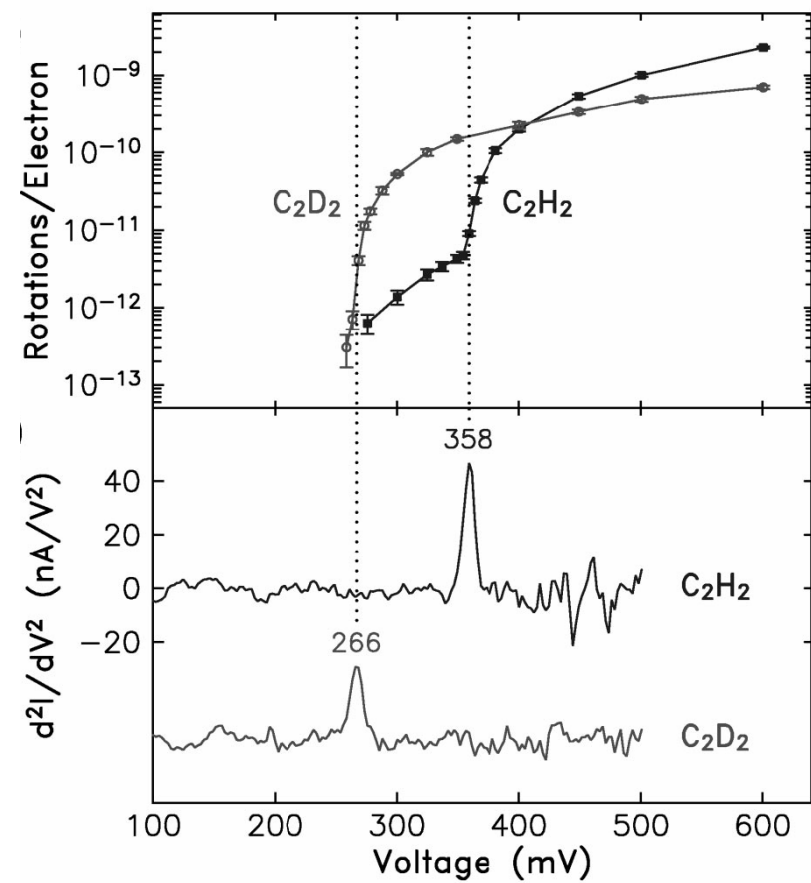
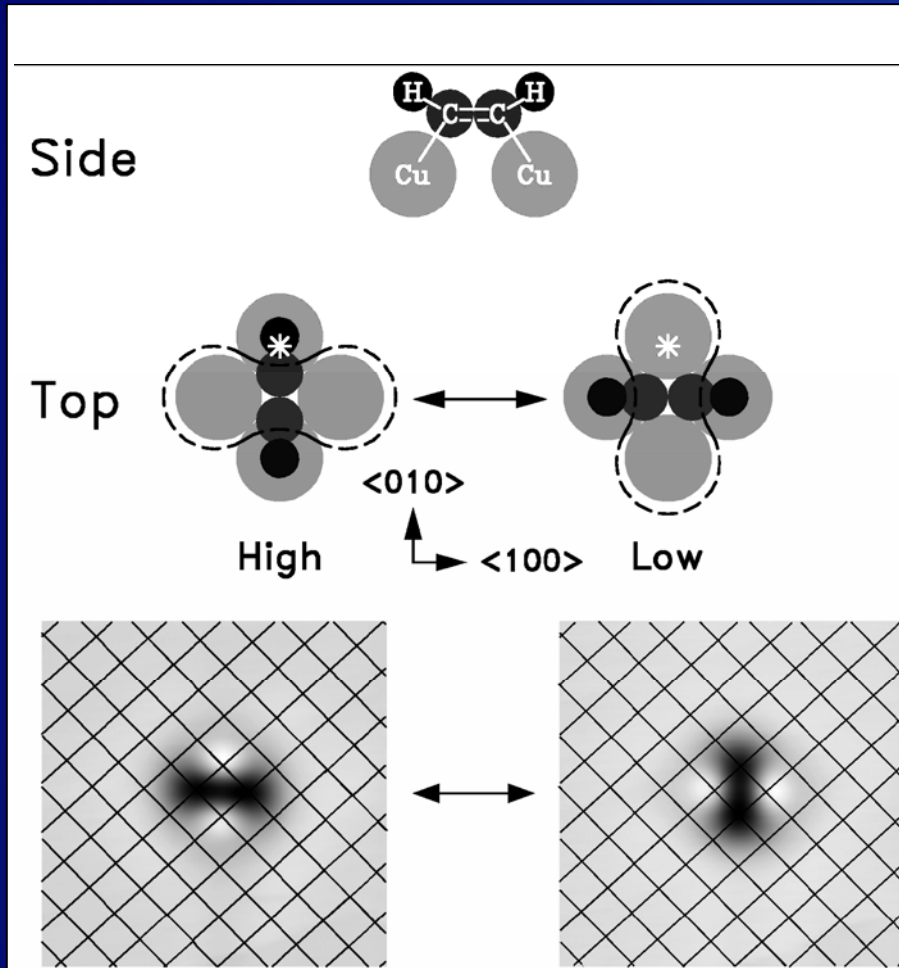
W. Ho J. Chem. Phys. 117, 11033 (2003).

# STS acetylene/Cu(001)



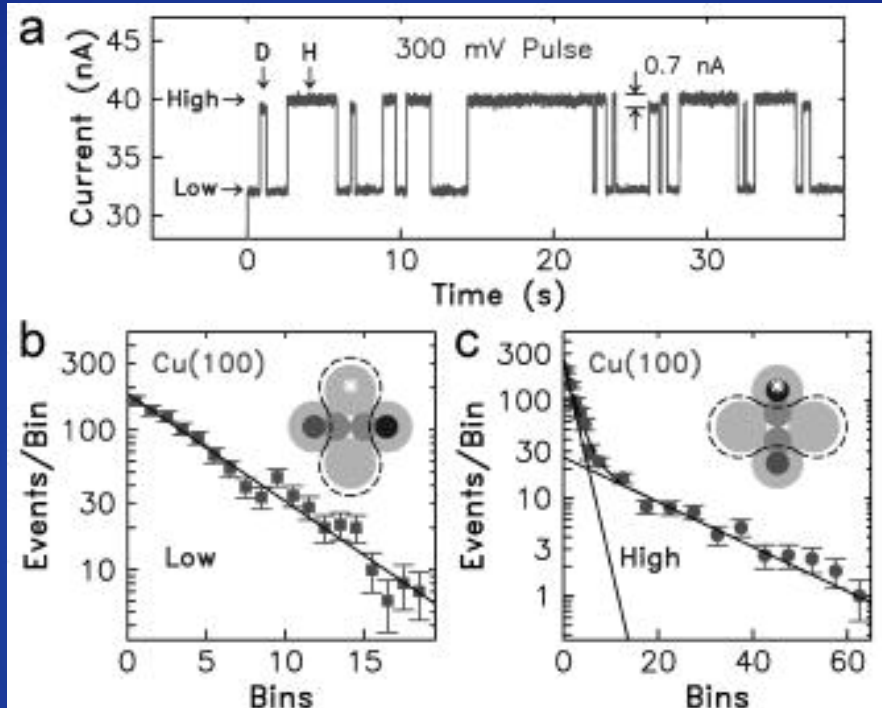
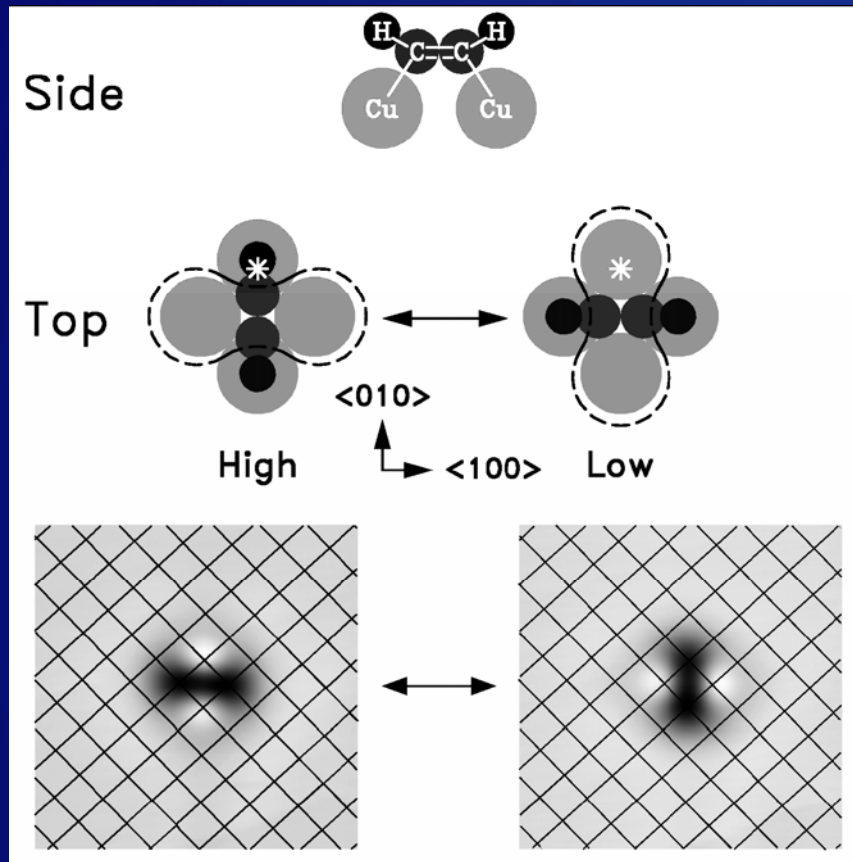
B.C. Stipe et al., Phys. Rev. Lett. 81, 1263 (1998)

# STS acetylene/Cu(001)



B.C. Stipe et al., Phys. Rev. Lett. 81, 1263 (1998)

# STS acetylene/Cu(001)



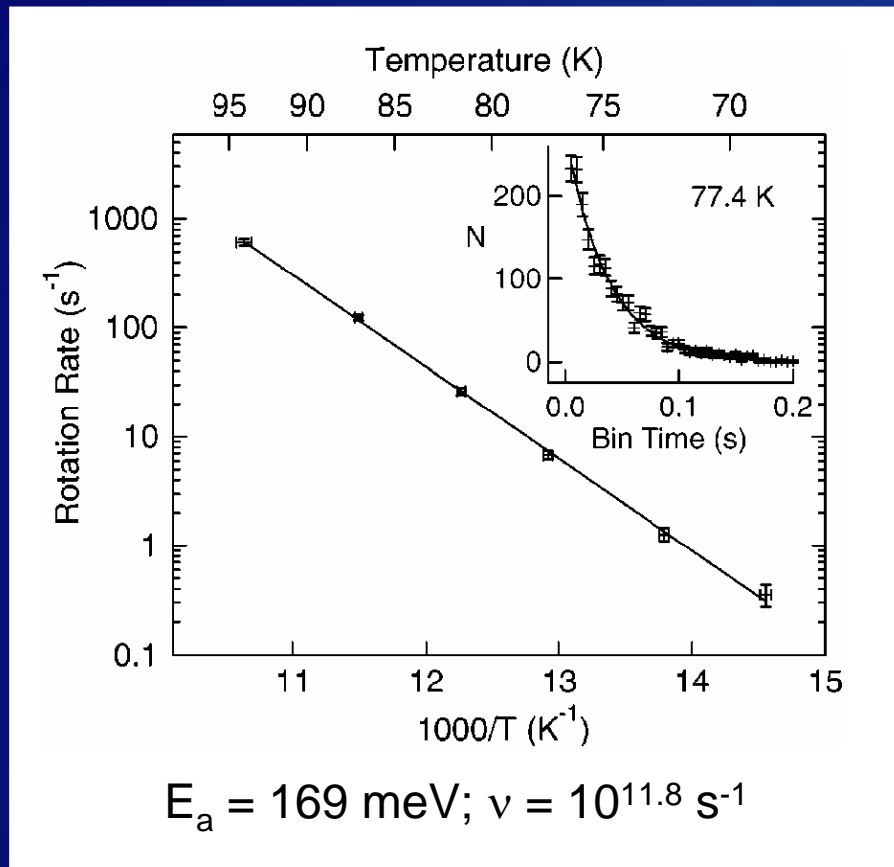
B.C. Stipe et al., Phys. Rev. Lett. 81, 1263 (1998)

# STS

## acetylene/Cu(001)



temperature induced rotation



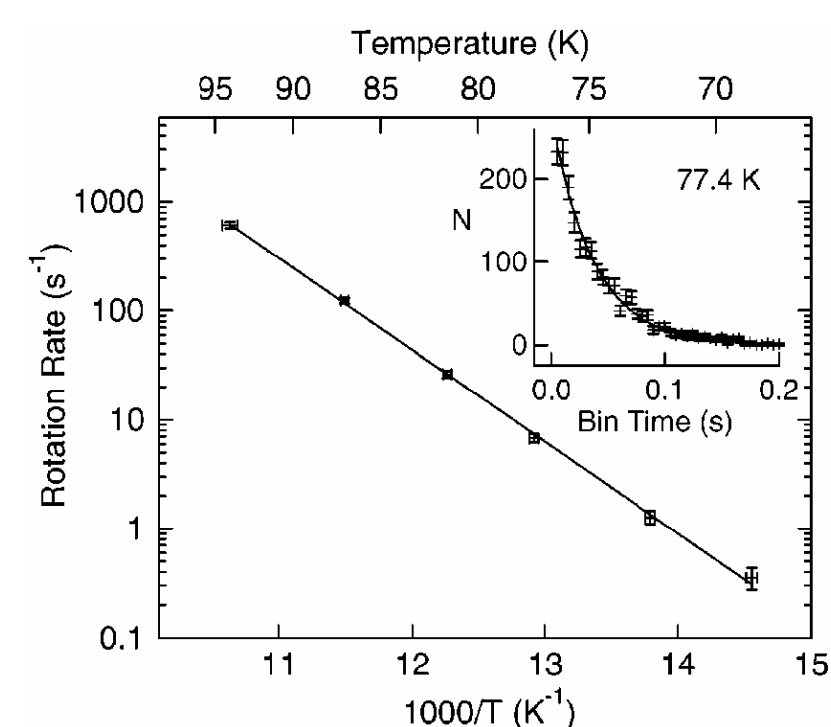
L. J. Lauhon and W. Ho, J. Chem. Phys. 111, 5633 (1999)

# STS

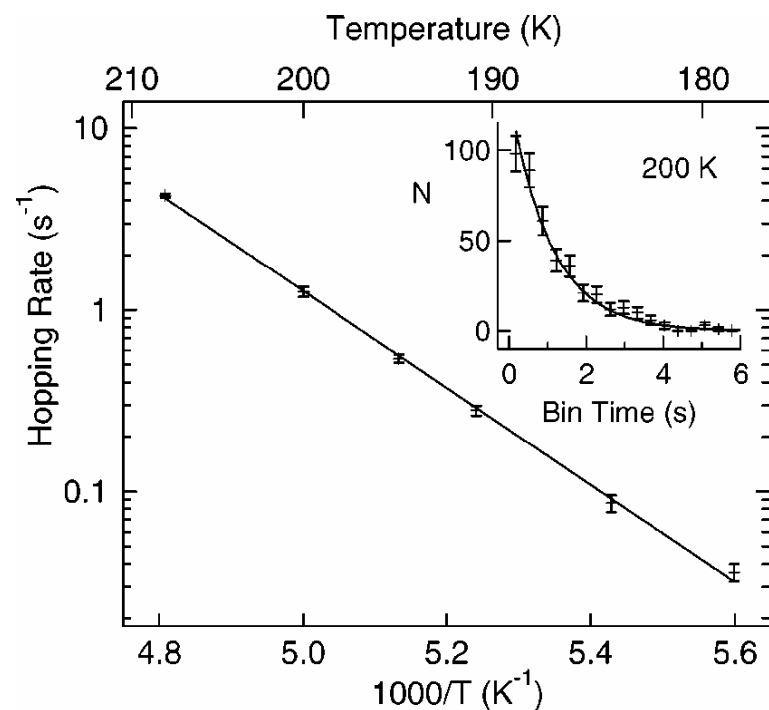
## acetylene/Cu(001)



temperature induced rotation



temperature induced translation



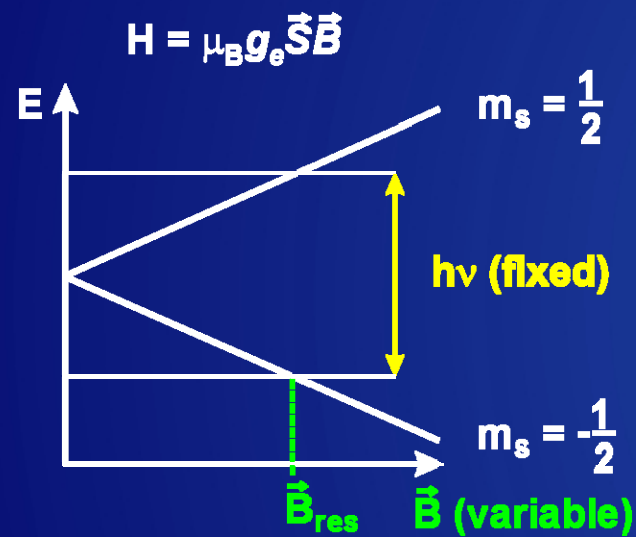
L. J. Lauhon and W. Ho, J. Chem. Phys. 111, 5633 (1999)

# EPR spectroscopy

## basic aspects



free electron

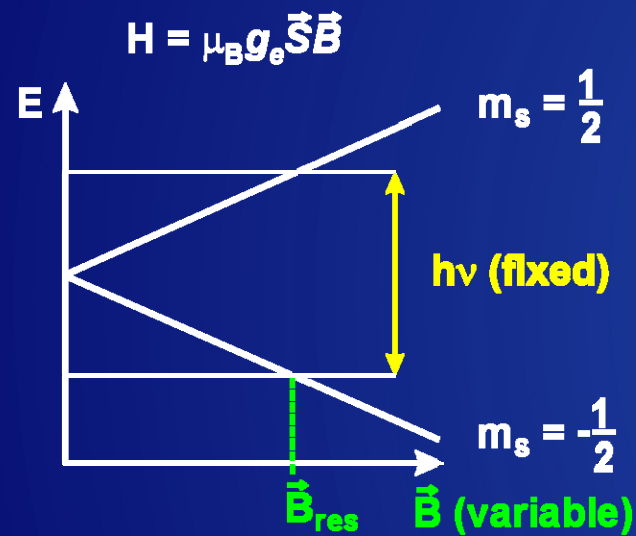


# EPR spectroscopy

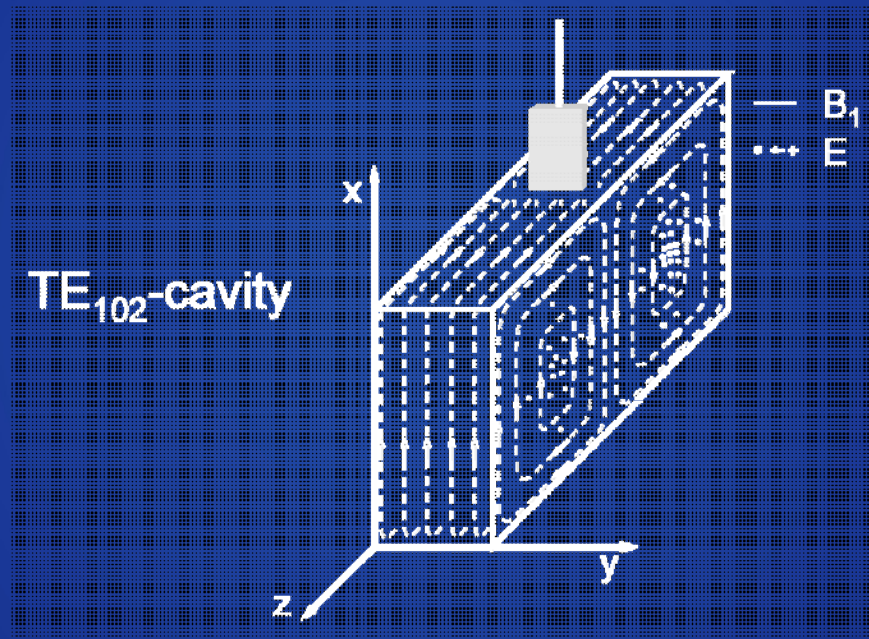
## basic aspects



free electron



field distribution in a microwave resonator

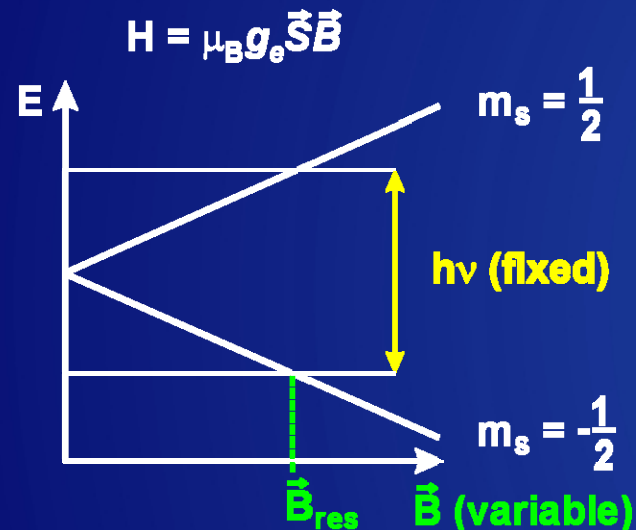


# EPR spectroscopy

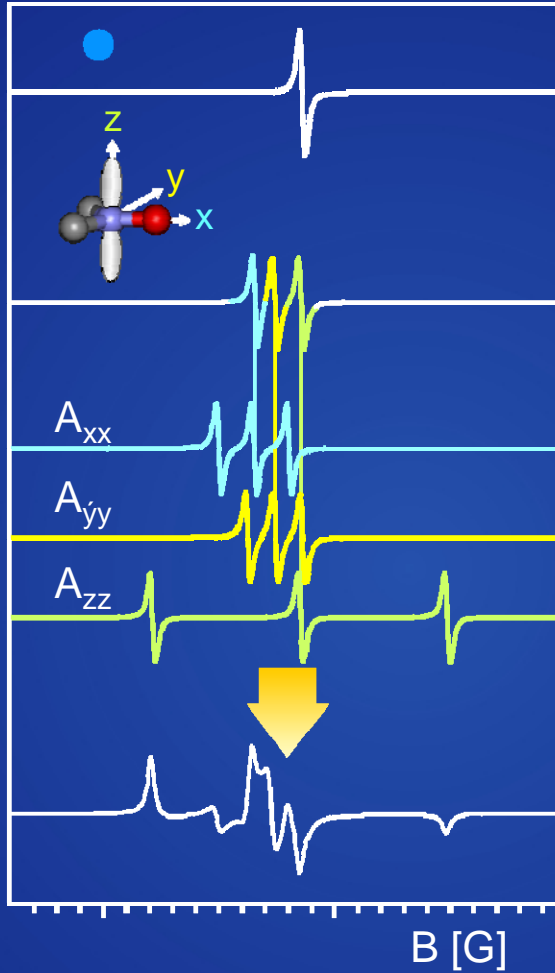
## basic aspects



free electron



rigid limit



free electron

g-tensor

$B \parallel x$

$B \parallel y$

$B \parallel z$

hyperfine  
interaction  
 $I(^{14}\text{N}) = 1$

powder  
spectrum

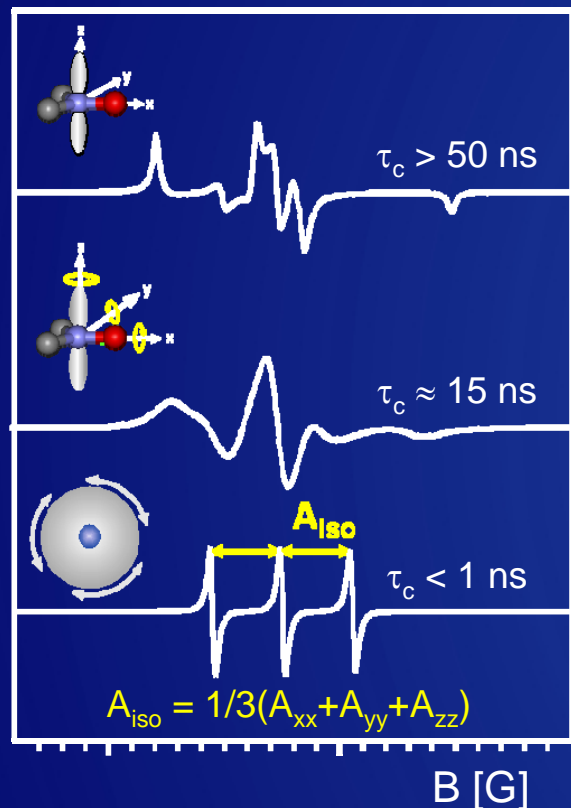
# EPR spectroscopy

## effect of rotational motion

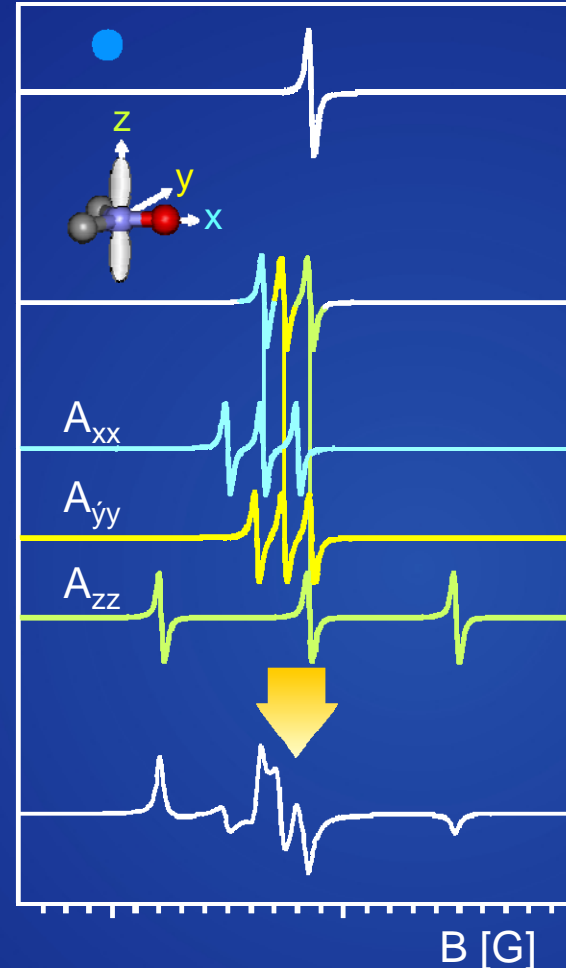


### rotational motion

isotropic rotation



### rigid limit

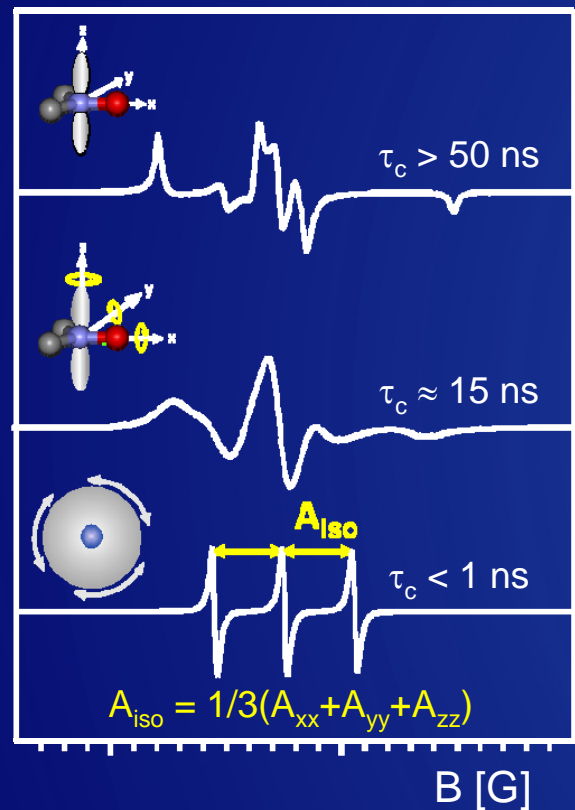


# EPR spectroscopy

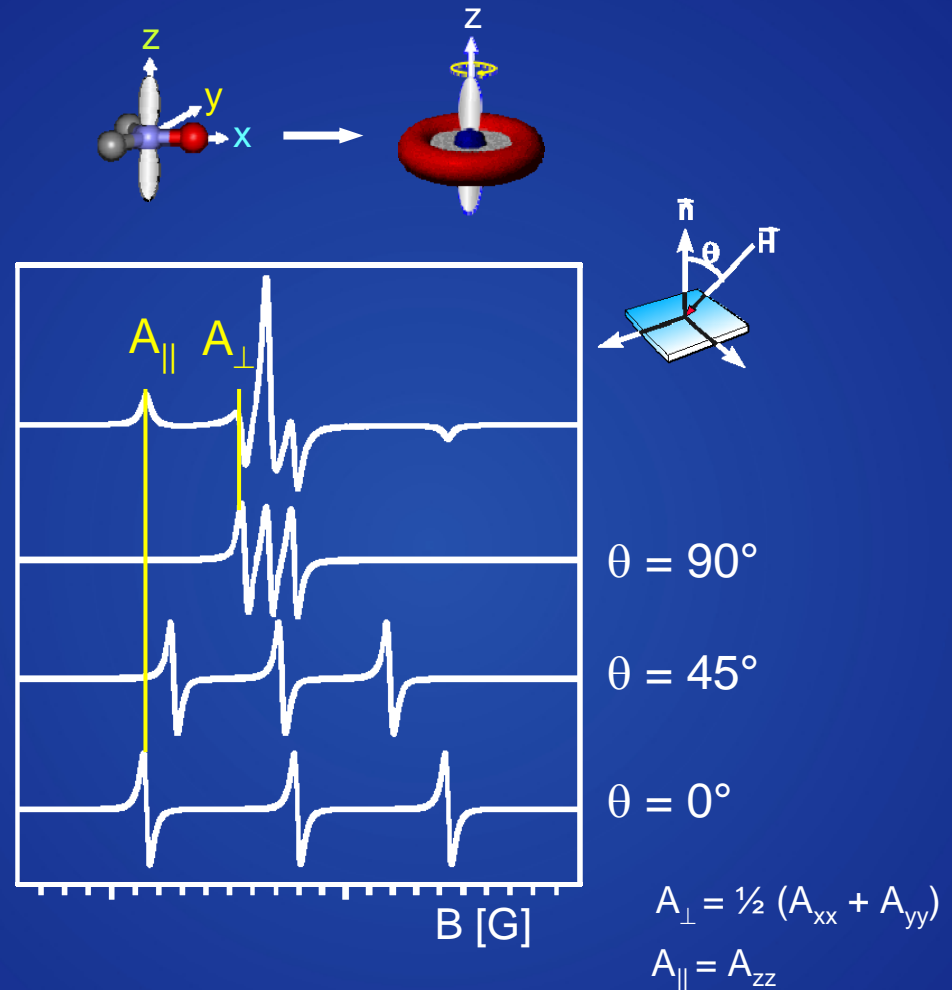
## effects of rotational motion



### isotropic rotation

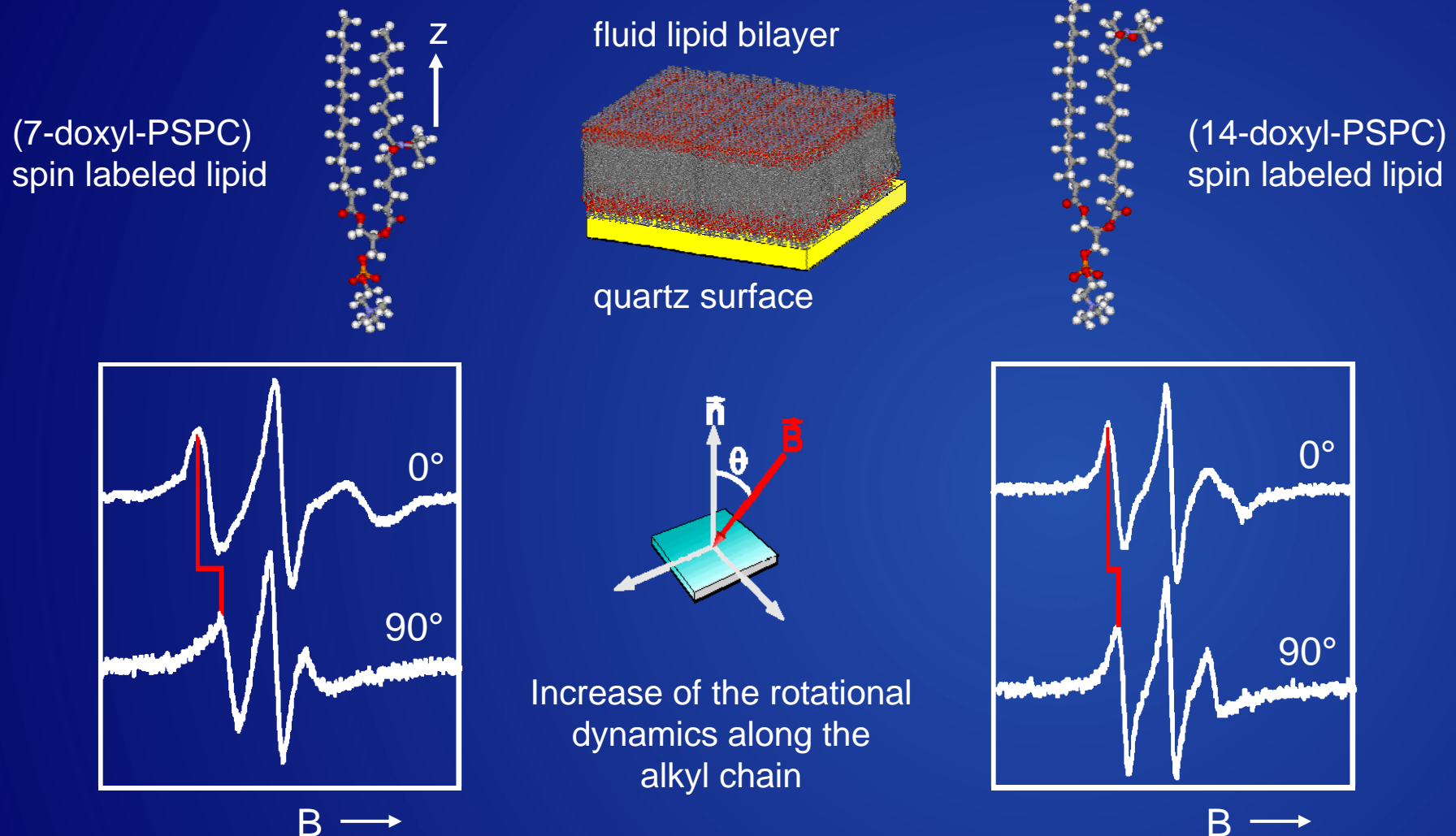


### fast motion around z-axis

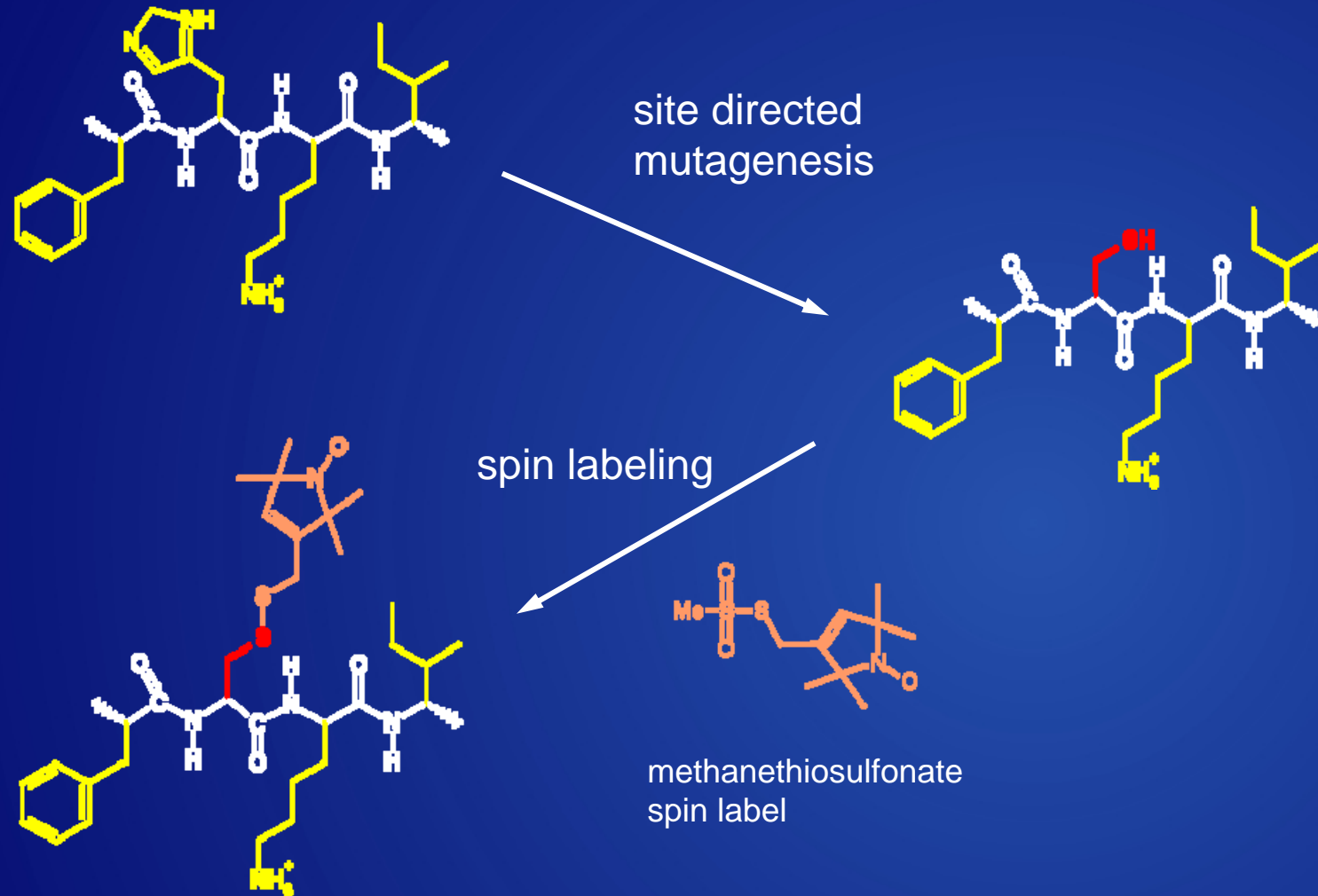


# Introduction

## Why ESR spectroscopy?

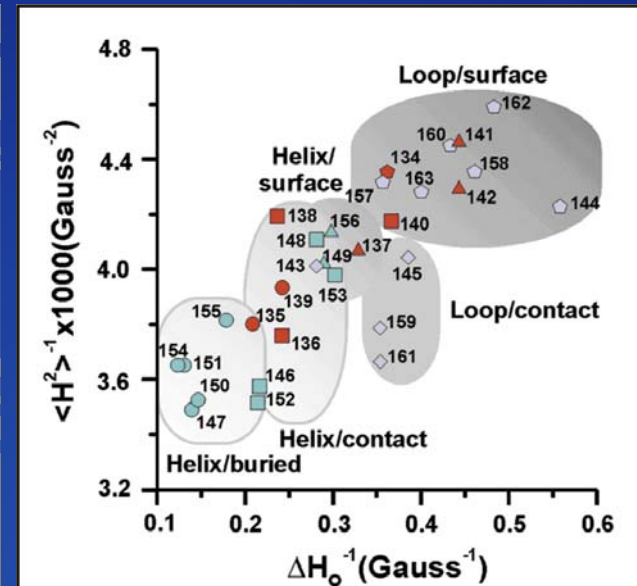
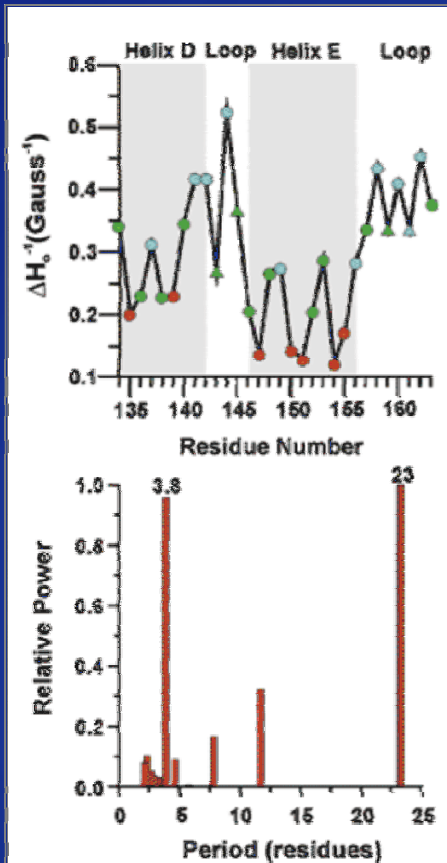
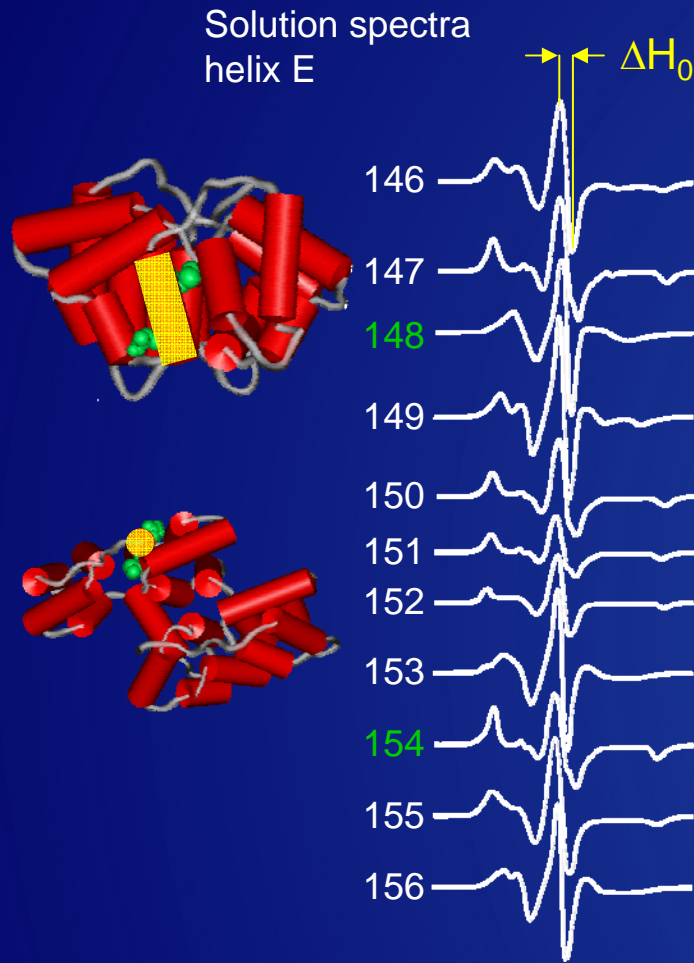


# Site Directed Spin Labeling (SDSL) strategy



# EPR Annexin 12

## secondary structure from line shape analysis



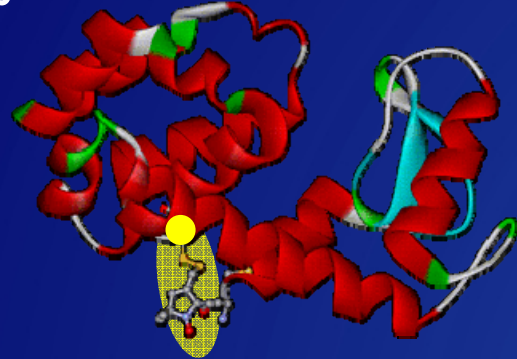
EPR data: Isas, J. M et al. Biochemistry **41**, 1464 (2002).

# EPR T4 Lysozyme on Surface

## Angular Dependence

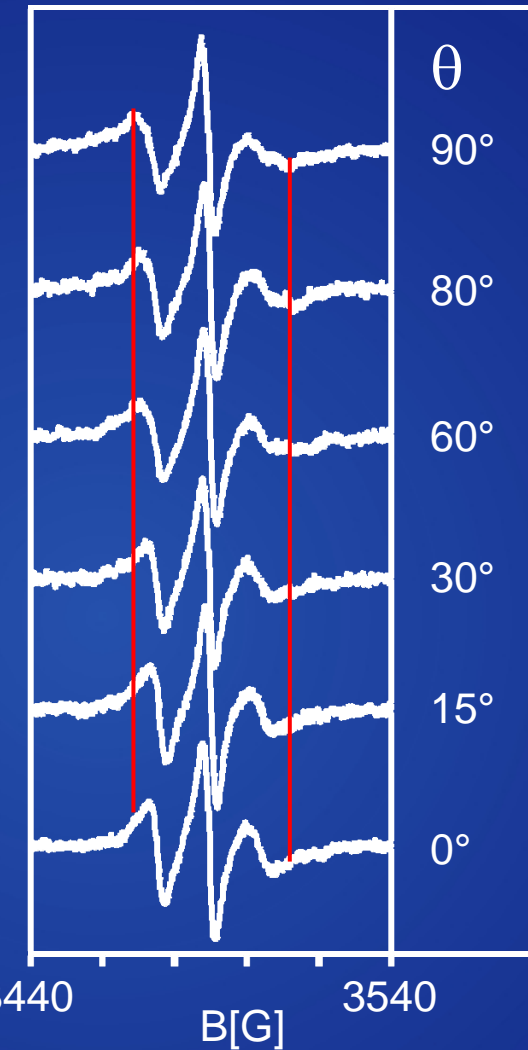
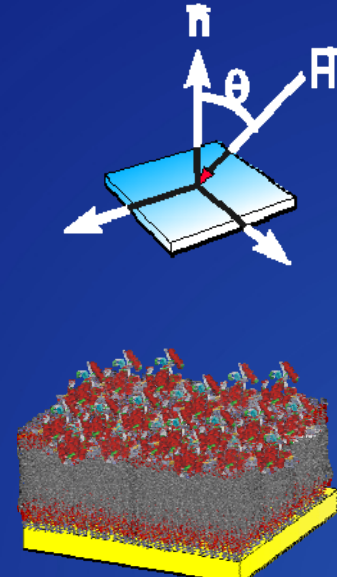
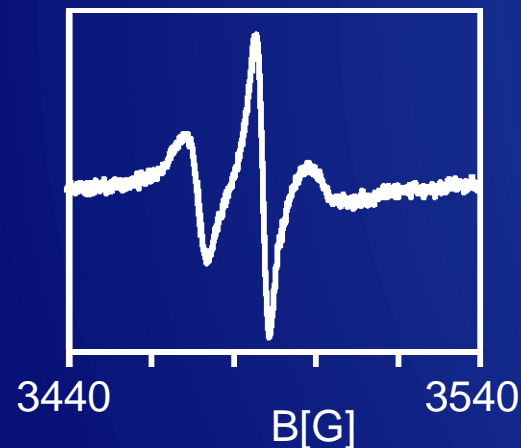


76 Cys



MTSSL

solution



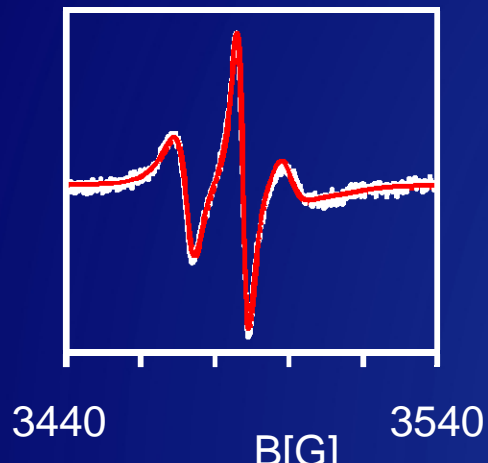
- Angular dependent EPR spectra
- Intensity correspond to 80% of a dense protein layer

# Simulations

Surface – Results: 76 Cys

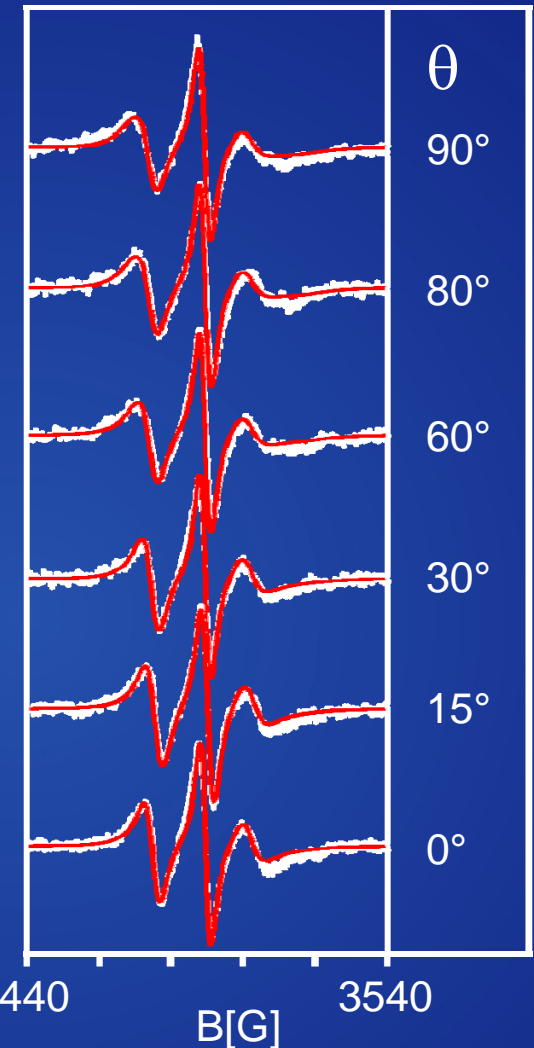
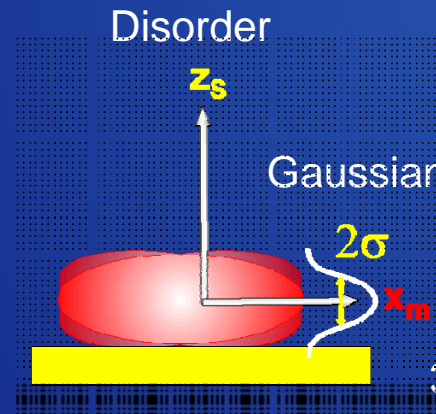
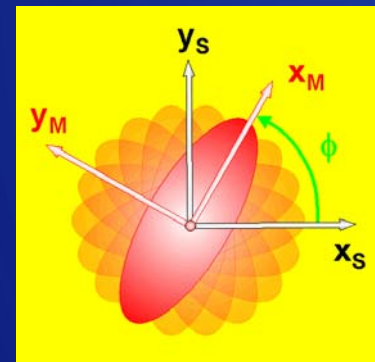
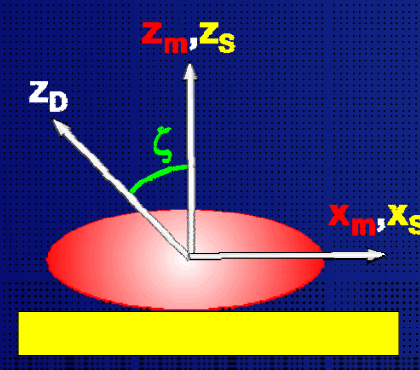


Dynamic model  
parameters from solution



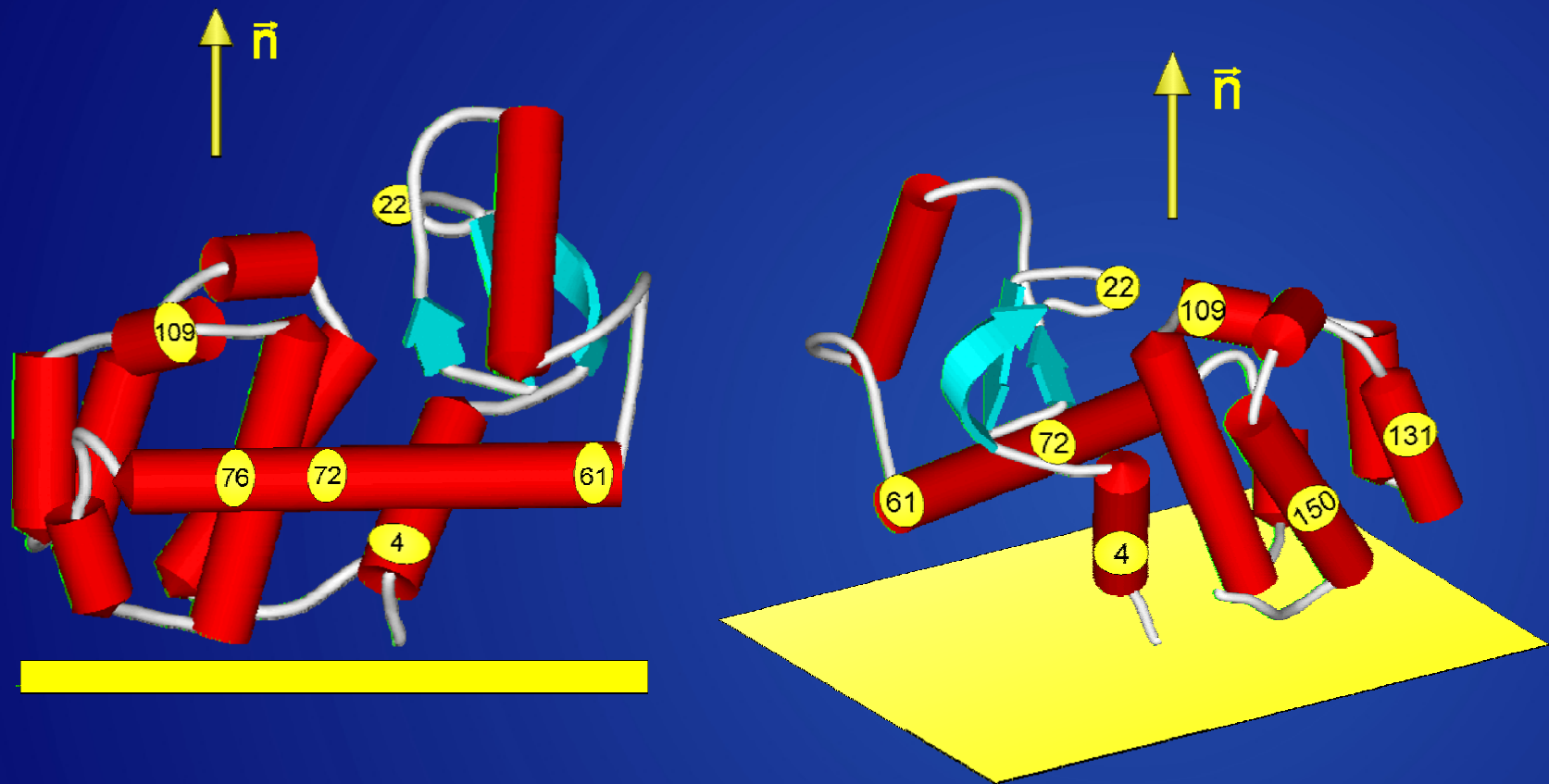
## Surface model

- tilt angle of director ( $\zeta$ )
  - azimuthal average ( $\phi$ )
  - Gaussian disorder profile ( $\sigma$ )
- Result of global fit T4L 76:
- $\zeta = 90^\circ$ ,  $\sigma = 15^\circ$



# T4Lysozyme on Model Surface

## orientation of the molecule on the surface



# Conclusions



## Vibrations

- IRAS  
optimal range from  $700 - 3500 \text{ cm}^{-1}$ ; restricted to dipole allowed excitations (metal surface selection rule)
- HAS  
powerful for low energy vibration such as frustrated translations or rotations  
energy resolution approx.  $0.1 - 0.5 \text{ cm}^{-1}$
- EELS  
complementary to IR; lower frequencies; non dipole transitions possible.
- Raman  
comparatively low sensitivity; wide spectral range ( $50 - 5000 \text{ cm}^{-1}$ ); enhanced surface sensitivity by plasmon excitation (combination with STM allows resolution down to a few nm)
- SFG  
intrinsic surface sensitive; background free detection; suitable for time resolution down to the fs-regime.

# Conclusions



## Rotations:

- EELS
  - does only work for very light molecules with large rotational quanta ( $H_2$ ,  $D_2$ )
- STM,STS
  - single molecule resolution; rotation (coupling to vibrations. Becomes complex for more complicated molecules.)
- EPR
  - can provide information on the rotational dynamics in the ns-regime; can be used e.g. to characterize large molecules.